CONTRACT NO. A932-050
FINAL REPORT
MAY 1993

Ozone and Particulate Matter Case Study Analyses for the Southern California Air Quality Study

CALIFORNIA ENVIRONMENTAL PROTECTION AGENCY

AIR RESOURCES BOARD
Research Division

OZONE AND PARTICULATE MATTER CASE STUDY ANALYSES FOR THE SOUTHERN CALIFORNIA AIR QUALITY STUDY

Final Report
Contract No. A932-050

Prepared for:

California Air Resources Board
Research Division
2020 L Street
Sacramento, CA 95814

Submitted by:

Sonoma Technology, Inc.
5510 Skylane Blvd., Suite 101
Santa Rosa, CA 95403-1083

Prepared by:

Paul T. Roberts
Hilary H. Main

Technical Contributions from:

Charles G. Lindsey
Marcelo E. Korc

MAY 1993

ABSTRACT

As part of the Southern California Air Quality Study (SCAQS), case study analyses of the surface and aloft air quality data for three SCAQS episodes were undertaken to improve our understanding of the evolution and sources of ozone and particulate matter (PM) concentrations in the South Coast Air Basin (SoCAB), the formation mechanisms of aloft pollutant layers, the importance of these aloft layers to surface concentrations, and to recommend how these phenomena and species distributions should be modeled. This report summarizes the data analyses performed for this project, the analysis results, and the conclusions and recommendations of the project.

The SCAQS episodes selected for analyses were June 24-25, 1987, July 13-15, 1987, and December 10-11, 1987. This report describes and displays the spatial and diurnal patterns of surface and three-dimensional air quality data and presents comparisons of aloft and surface data for these two summer and one fall episodes. Case study analyses of the June and July episodes provide a comprehensive look at two periods with high ozone concentrations; case study analyses of all three periods provide a comprehensive look at high PM concentrations during both summer and fall conditions.

High concentrations of ozone and other pollutants often existed in aloft layers covering much of the SoCAB. These layers were usually found at altitudes near the top of the daytime mixed layer (the boundary layer). Polluted layers aloft were generally horizontal in structure and existed at about the same height above mean sea level throughout most of the SoCAB. This means that terrain-following procedures, such as those used in most modeling efforts, are not consistent with the observed pollutant structure.

Model predictions of ozone did not agree with aloft ozone measurements. In the lower 200 meters above the ground (m agl) during the morning, ozone predictions were often significantly higher than measured concentrations, indicating that these model simulations did not produce enough ozone titration by fresh nitric oxide. Model predictions of ozone above about 200 m agl were about 50 to over 100 ppb lower than measured concentrations.

Future meteorological and photochemical model simulations need to properly represent the formation and transport of aloft polluted layers, including the characteristics described above. In this report, additional recommendations are made on the use of field data for model inputs and on other ways to evaluate and improve model performance during future programs.

ACKNOWLEDGEMENTS

The work described in this report was funded by the Motor Vehicle Manufacturers Association (MVMA), via the California Air Resources Board (ARB), as part of the Southern California Air Quality Study (SCAQS); Dr. Marcel Halberstadt, Director of the Environmental Department of the MVMA arranged for the funding. Mr. Bart Croes, ARB, managed this work; his comments and patience are greatly appreciated.

We would also like to thank the following individuals for their help during this project:

- Dr. Eric Fujita, ARB, for providing us with the results of his intercomparison of NO_2, nitric acid, and formaldehyde measurements; and for his comments and suggestions during the project.
- Mr. Bart Croes, ARB, for providing us with the SCAQS data base and for his comments and suggestions during the project.
- Mr. Neil Wheeler, ARB, for comments on the comparisons between model simulations and aloft measurements.
- Mr. Henry Hogo and Ms. Julia Lester, South Coast Air Quality Management District (SCAQMD), for providing us with wind fields, mixing heights, and air quality simulation output for various modelled episodes.
- Mr. Jerry A. Anderson and Mr. John C. Koos, STI, for collecting the STI aircraft data, for performing quality control on that data, and for preparing an excellent and usable data volume and report.
- Mr. Charles G. (Lin) Lindsey, STI, for performing the isentropic and aloft transport analysis for the July 13-14, 1987 episode.
- Dr. Marcelo E. Korc, STI, for processing the model simulation results and preparing the figures which compare the model and measurement results.
- Mr. Frederick W. Lurmann, STI, for many helpful discussions during the course of this project.
- Mr. Jeffrey D. Prouty and Ms. Corrine J. Cottle, STI, for processing the aircraft data and preparing files with altitude-averaged data.
- Dr. Ted B. Smith, T. B. Smith and Associates, for performing the analysis of mixing heights and for comments on the use of the lidar data to understand aloft layer formation and transport.
- Dr. Susanne V. Hering, Aerosol Dynamics, Inc., for answering numerous questions about the measurement methods and her data evaluation efforts.
- Ms. Sharon G. Douglas, Systems Applications International, for providing air parcel trajectories for our analyses.

- Dr. Jim McElroy, Environmental Protection Agency (EPA) Las Vegas, for providing the lidar data for specific times and locations on magnetic media.

- Ms. Susan Z. Hynek, STI, for preparing the text, figures, and tables for this report.

- All of the numerous investigators who collected and analyzed data during the SCAQS (for example, see tables and Appendix A in Hering and Blumenthal, 1989).

This report was submitted in fulfillment of ARB Contract A932-050 by Sonoma Technology Inc.

Without the support and financial commitments of the sponsors, the Southern California Air Quality Study would not have been possible. These sponsors were: the ARB, the EPA, the SCAQMD, the CRC, the Electric Power Research Institute, the Ford Motor Company, the General Motors Research Laboratories, the Motor Vehicle Manufacturers Association, Southern California Edison, and the Western States Petroleum Association.

DISCLAIMER

The statements and conclusions in this report are those of the contractor and not necessarily those of the California Air Resources Board or its employees. The mention of commercial products, their source, or their use in connection with material reported here is not to be construed as either an actual or implied endorsement of such products.

TABLE OF CONTENTS

TABLE OF CONTENTS (Continued)

TABLE OF CONTENTS (Continued)

LIST OF FIGURES

LIST OF FIGURES (CONTINUED)

Figure | Page

LIST OF FIGURES (CONTINUED)

LIST OF FIGURES (CONTINUED)

LIST OF FIGURES (CONTINUED)

Figure | Page

LIST OF FIGURES (CONTINUED)

Figure — Page

LIST OF FIGURES (CONTINUED)

Figure | Page

LIST OF FIGURES (CONTINUED)

LIST OF FIGURES (CONTINUED)

LIST OF FIGURES (CONTINUED)

Figure | Page

LIST OF TABLES

List of Abbreviations and Terminology

Abbreviation/Term	Definition
Measurement and Analysis:	
DNPH	2,4-dinitrophenylhydrazine
GC-FID	Gas chromatography - flame ionization detection
GC-MS	Gas chromatography - mass spectrometry
GC-ECD	Gas chromatography - electron capture detection
Lidar	LIght Detection And Ranging
DDM	Denuder Difference Method
DOAS	Long Pathlength Differential Optical Absorption Spectroscopy
TDLAS	Tunable Diode Laser Absorption Spectroscopy
L1 to L12	Leg numbers in the SCAQS sampler (Figure 2-2)
SOP	Standard Operating Procedures
QC	Quality Control
A- and B-sites:	
ANAH	Anaheim
BURK	Burbank
AZUS	Azusa
CLAR	Claremont
CELA	Downtown Los Angeles
HAWT	Hawthorne
LBCC	Long Beach City College
RIVR	Riverside - Rubidoux
SNI	San Nicolas Island
Aircraft Sample Locations:	
AMTRA	Airway Intersection 8 km W of El Monte Airport
BUR	Burbank
CAB	Cable Airport
DOYLE, TANDY	Airway Intersections about 20 km W of Palos Verdes
EMT	El Monte
FUL	Fullerton
GYB	Goodyear Blimp Site in Carson
HHR	Hawthorne
LGB	Long Beach
ONT	Ontario
MINOE	Airway Intersection 25 km SE of Long Beach
PADDR	Airway Intersection 15 km S of Long Beach
POMA	Pomona
RAL	Riverside Airport
Pollutants:	
VOC	Volatile organic compounds
NMHC	Nonmethane hydrocarbons
NMOC	Nonmethane organic compounds (NMHC + carbonyl compounds)
Carbonyl compounds	C1-C7 aldehydes and ketones
OC	Organic carbon
EC	Elemental carbon
PAN	Peroxyacetylnitrate
NO	Nitric oxide
NO_2	Nitrogen dioxide
NO_x	Oxides of nitrogen
CO	Carbon monoxide
CH_4	Methane
CO_2	Carbon dioxide
HNO_3	Nitric acid
NO_3	Nitrate radical
PM	Particulate matter

Abbreviation/Term	Definition
NO_3^-	Nitrate ion
HONO	Nitrous acid
HCHO	Formaldehyde
b_{scat}	Light scattering coefficient
b_{ext}	Extinction coefficient
NH_3	Ammonia
NH_4^+	Ammonium ion
PM_{10}	Particulate mass less than 10 μm
$PM_{2.5}$	Particulate mass less than 2.5 μm
SO_2	Sulfur dioxide
$SO_4^=$	Sulfate ion
Investigators:	
AIHL	Air and Industrial Hygiene Laboratory
ARB	California Air Resources Board
AV	AeroVironment
Cal Tech, CIT	California Institute of Technology
DGA	Daniel Grosjean & Associates.
EMSI	Environmental Monitoring Services, Inc.
ENSR	ENSR Corporation, formerly ERT
EPA	US Environmental Protection Agency
GMRL	General Motors Research Laboratories
OGI	Oregon Graduate Institute
SAI	Systems Applications International
SCAQMD	South Coast Air Quality Management District
SCE	Southern California Edison
STI	Sonoma Technology Inc.
T&B	Technical and Business Systems
UCR	University of California, Riverside
UW	University of Washington
Measurement Units:	
pphm	parts per hundred million
ppb	parts per billion
ppbC	parts per billion Carbon
Mm^{-1}	10^{-6} m^{-1}
mb	millibars
Miscellaneous:	
agl	above ground level
AQMP	Air Quality Management Plan (for South Coast Air Basin)
CBL	Convective Boundary Layer
D	Vector-averaged wind direction
DWM	Diagnostic Wind Model
L	Vector-averaged transport distance
LORAN	LOng RAnge Navigation
LT	Local Time
msl	mean sea level
PDT	Pacific Daylight Time
PST	Pacific Standard Time
R	Recirculation factor (L/Sw)
SFV	San Fernando Valley
Sw	Scalar wind run
SCAQS	Southern California Air Quality Study
SoCAB	South Coast Air Basin
UAM	Urban Airshed Model

EXECUTIVE SUMMARY

Concentrations of ozone and particulate matter regularly exceed the State and Federal standards at surface-based monitoring sites in the South Coast Air Basin (SoCAB). Knowledge of pollutant concentrations aloft is important for understanding the evolution and sources of ozone and particulate matter concentrations measured at surface-based monitoring sites in the SoCAB. The Southern California Air Quality Study (SCAQS) was conducted in the SoCAB during the summer and fall of 1987 to provide a comprehensive database for data analysis and modeling of ozone and particulate matter.

As part of the SCAQS, case studies of three specific pollutant episodes were performed to improve our understanding of the evolution and sources of ozone and particulate matter concentrations in the SoCAB, the formation mechanisms of aloft pollutant layers, the importance of these aloft layers to surface concentrations, and to recommend how these phenomena and species distributions should be modeled. The major features of the data, the results of the case study analyses, and the conclusions and recommendations of the project are summarized below.

Characteristics of diurnal profiles of pollutants at the surface and aloft during the June and July summer SCAQS episodes:

- At surface sites, diurnal profiles of primary species such as nitrogen oxide (NO) and elemental carbon (EC) were highest during the morning and afternoon rush hours, as expected for pollutants with motor vehicles as the major emissions source; this typically caused ozone concentrations to be zero at night. However, NO and EC concentrations at Anaheim were low all the time and ozone concentrations there were not titrated to zero at night.

- Early morning NO concentrations were often high near the surface and decreased significantly above about 300 m agl; NO concentrations were typically low (less than 5 ppb) from the surface to 1500 m agl during the midday and the afternoon. NO_x concentrations during the midday and the afternoon were highest in the mixed layer (typically 30-50 ppb) and low at higher altitudes.

- Diurnal profiles of ozone, nitric acid, peroxyactylnitrate (PAN), organic carbon (OC), and particulate mass were similar, with the highest concentrations during the midday and low concentrations overnight. This is consistent with the conceptual models of transport and chemistry.

- Diurnal profiles of ammonia and $PM_{2.5}$ ammonium ion were also similar to ozone with the highest concentrations during the midday and low concentrations overnight. This is consistent with the conceptual models of transport and chemistry. However, diurnal profiles of $PM_{2.5}$ nitrate concentrations often indicated two peaks, one during the midday and another at night.

- Diurnal profiles of acetic and formic acid at Claremont and Long Beach were also similar to ozone with the highest concentrations during the

midday and low concentrations overnight, except formic acid concentrations were high during the early morning of July 13 at Claremont. In addition, acetic and formic acid concentrations were low at Long Beach on June 24-25. Acetic acid concentrations were typically higher than formic acid concentrations.

- Concentrations of most pollutants aloft were also typically highest during the midday and lowest early in the morning. However, ozone concentrations were often still quite high (up to 200 ppb) above the nocturnal inversion in the early morning. This indicates that there is a significant amount of pollutant carryover from one day to the next. In fact, the thick layer of over 200 ppb ozone which existed over much of the SoCAB on the morning of June 24 (the first day of intensive SCAQS measurements) indicates that modeling of the June 24-25 episode started with dirty conditions. Ozone concentrations on July 13 (the beginning of the July 13-15 episode) were significantly cleaner.

Aloft layers of pollutants during the June and July summer SCAQS episodes:

- High concentrations of ozone and other pollutants often existed in aloft layers covering much of the SoCAB. These layers were usually found at altitudes near the top of the daytime mixed layer (the boundary layer).

- The principal mechanisms which form polluted layers aloft included sea-breeze undercutting of the mixed layer, slope-flows along the mountains and the resulting return flow out over the SoCAB, the formation of the nocturnal surface layer in the lower part of the boundary layer, and the transport of buoyant air parcels from the mixed layer into the inversion layer (convective debris). Injection of pollutants aloft by stationary source emissions and convergence zones was also observed during the SCAQS.

- Aloft layers were generally horizontal in structure and existed at about the same height above sea level (msl) throughout most of the SoCAB. In general, meteorological/wind modeling results do not produce this type of horizontal structure. This inconsistency between model results and observed pollutant structure may be due to a number of issues, including the following: a terrain-following system of layers in the model; layers in the model which remain at a constant thickness, even over the mountains surrounding the SoCAB; an inversion structure in the model which is not sufficiently influenced by synoptic-scale processes (which are, by nature, horizontal); and insufficient meteorological and pollutant data near the mountain slopes to identify the mixing and transport characteristics which are important there.

- Ozone concentrations in the midday and afternoon mixed layer were greater than ozone concentrations measured at nearby surface monitors by about 20-30 ppb. We have reviewed aircraft audits and calibrations and found that they were within reasonable bounds ($\pm$ 5%). Aircraft audits were performed at the surface when the aircraft was stationary. Details of audit results and corrections to data for pressure and temperature effects are provided in Anderson, et al. (1989). In addition, these differences did not depend on sampling date, time, or location. We

conclude that this difference between surface and aircraft concentrations might be due to ozone deposition at the surface and/or to titration by fresh NO near the surface.

- Midday and afternoon mixed-layer concentrations of most secondary pollutants, including ozone, carbonyls, nitric acid, PAN, and $PM_{2.5}$ OC were typically higher than pollutant concentrations at the surface. In contrast, surface concentrations of species dominated by primary sources, including NMHC, NO, NO_x, EC, and ammonia were higher than concentrations aloft in the mixed-layer. It seems that chemical and transport processes aloft combined to keep the aloft concentrations of these secondary pollutants high.

- Midday and afternoon surface concentrations of a few other secondary pollutants, including $PM_{2.5}$ mass and sulfate, nitrate, and ammonia ions were typically higher than concentrations aloft in the mixed-layer. This distribution must be strongly influenced by the ammonia distribution (ammonia source and highest concentrations at the surface).

Comparison of model predictions of ozone with ozone measurements aloft:

- Model predictions of ozone in the lower 200 m agl during the morning were often significantly higher than measured concentrations, indicating that these model simulations did not produce enough ozone titration by fresh NO.

- Model predictions of ozone above about 200 m agl were about 50 to over 100 ppb lower than measured concentrations.

Characteristics of NMOC distributions during the June and July summer SCAQS episodes:

- The spatial pattern of average NMOC concentrations showed moderate concentrations (200-400 ppbC) at the surface in the western and southern SoCAB (at Hawthorne, Long Beach, and Anaheim), high concentrations (400-800 ppbC) in the central SoCAB (at Los Angeles and Burbank), and moderate concentrations in the eastern SoCAB during the summer. On average, NMOC concentrations decreased with distance from a high concentration ridge between Los Angeles and Burbank in summer. The spatial pattern of the aloft data in the afternoon was consistent with the surface NMOC patterns.

- Surface NMOC concentrations were highest at 0700-0800 PDT because of a combination of high emission rates from morning traffic and low mixing heights. Concentrations decreased over the day because wind speeds and mixing heights increased during daylight.

- The summer aircraft NMOC data, which were collected between 500 and 800 m msl during orbits, showed NMOC levels that were mostly lower than surface concentrations and NMOC composition that was more aged than surface data. The carbonyl content aloft (about 35 percent of NMOC carbon) was more than twice that in the surface data, indicating the secondary nature of the aloft samples.

- The similarity of NMOC composition throughout the day suggested fresh NMOC emissions were continuously injected into the atmosphere in the SoCAB. While there was evidence of oxidation of the more reactive hydrocarbon species and formation of large amounts of carbonyl compounds, there were significant concentrations of species typical of fresh emissions (Lurmann and Main, 1992).

- The NMOC concentrations had significant day-to-day and seasonal variations, which were undoubtedly controlled by meteorology. In addition, the NMOC concentrations had significant spatial variation within the SoCAB due to the non-uniformity of emission rates and the effects of transport.

- Fresh emissions had a significant influence on NMOC concentrations everywhere in the SoCAB. This made it extremely difficult to estimate pollutant fluxes and to perform analyses which were designed to evaluate the formation of secondary species along a typical trajectory path. The ideal trajectory path for these analyses would transport pollutants from an upwind emissions area to a downwind receptor area; however, samples collected at most surface locations included significant contributions from local emissions which overwhelmed the secondary species.

Characteristics of particulate matter and carbon, nitrogen, and sulfur species during the June and July summer SCAQS episodes:

- Peak concentrations of pollutants with large secondary contributions such as $PM_{2.5}$ mass, carbonyl compounds, and organic carbon occurred at central and eastern SoCAB sites in the afternoon. This is consistent with the conceptual models of transport and chemistry.

- Surface ammonia and ammonium ion concentrations were highest, and nitric acid concentrations were lowest, at Rubidoux in the eastern SoCAB because of upwind sources of ammonia. $PM_{2.5}$ mass and nitrate ion concentrations were also high at Rubidoux. The nitrogen chemistry at Rubidoux was driven by fresh ammonia. In contrast to the surface, aloft ammonia and ammonium ion concentrations were relatively similar across the SoCAB.

- SO_2 and sulfate ion concentrations were generally low throughout the SoCAB, both at the surface and aloft. The sulfur contribution to the particulate mass was small as well.

Characteristics of pollutant concentrations during the December fall SCAQS episode:

- NO_2 concentrations were high (over 50 ppb) in layers within the daytime mixed layer (surface layer); concentrations were typically highest near the surface. The spatial and temporal variation of the pollutant profiles was much greater than in the summer.

- Mechanisms for the formation of aloft pollutant layers in the fall were similar to the summer: injection of stationary source emissions aloft, upslope flow, nocturnal boundary layer formation, and the transport of

buoyant air parcels from the mixed layer into the inversion layer (convective debris). Offshore flow and stagnation conditions were observed on all fall SCAQS days, so undercutting by the sea breeze did not contribute to the formation of layers.

- The aloft layers in the fall were generally horizontal in structure and existed at about the same height above sea level (msl) across the SoCAB.

- Fresh emissions were important contributors to the pollutant mix at all surface sampling sites in the SoCAB and within the mixed layer aloft.

- Afternoon mixed-layer concentrations of NO_2 and b_{scat} were similar to surface concentrations.

- Pollutant concentrations were generally highest at Hawthorne and Long Beach during the fall, reflecting the source distributions and the lack of transport. Mixing heights were often lower than during the summer and a strong sea breeze was not observed. These conditions, along with evidence of substantial pollutant carryover, contributed to pollutant build-up in the western and central SoCAB.

- Diurnal profiles of acetic and formic acid at Long Beach included the highest concentrations during the midday and low concentrations overnight. Formic acid concentrations were typically higher than acetic acid concentrations (the reverse of the summer data).

- The fall aircraft hydrocarbon data, which were collected between 30 and 900 m msl during spirals, showed NMHC levels that were mostly lower than surface concentrations and NMHC composition that was more aged than surface data. Sampling and analytical problems prevented a detailed comparison of total carbonyl concentrations at the surface and aloft.

- $PM_{2.5}$ mass, sulfate ion, and ammonium ion concentrations at all aloft altitudes were usually lower than concentrations at the surface. Organic and elemental carbon concentrations aloft within the mixed layer were equal to or greater than concentrations at the surface; while above the mixed layer, the OC and EC concentrations were lower than at the surface. Nitric acid and PAN concentrations aloft within the mixed layer were greater than the surface concentrations, while nitrate ion concentrations aloft were sometimes higher and sometimes lower than surface concentrations.

- In the fall, surface NMOC concentrations (on average) were similar in the western and central SoCAB and significantly lower in the eastern SoCAB. The highest NMOC concentrations occurred at Burbank in the fall. This is consistent with the conceptual models of transport and chemistry. Spatial trends of hydrocarbons aloft were difficult to assess because the spatial distribution of samples was limited.

- On average, surface NMOC concentrations were highest at 0700-0800 PST because of high emission rates and low mixing heights. Morning NMOC concentrations were about two times higher than in the summer. During the fall, NMOC concentrations declined between 0700 and 1200 as mixing

heights and wind speeds increased; and then increased between 1200 and 1600 PST, as mixing heights decreased with the formation of the nocturnal boundary layer.

- Fresh emissions had a significant influence on NMOC concentrations everywhere in the SoCAB; and NMOC concentrations were, in turn, a major component of all carbon species distributions. This made it extremely difficult to estimate pollutant fluxes and to perform analyses which were designed to evaluate the formation of secondary species along a typical trajectory path. The ideal trajectory path for these analyses would transport pollutants from an upwind emissions area to a downwind receptor area; however, samples collected at most locations included significant contributions from local emissions which overwhelmed the secondary species.

- SO_2 and sulfate ion concentrations were low (typically less than 5 $\mu g/m^3$) throughout the SoCAB, both at the surface and aloft. The sulfur contribution to particulate mass was also small (usually less than 5%). However, SO_2 and sulfate ion concentrations peaked at about 12 $\mu g/m^3$ during the afternoon of December 11 at most sites (except Rubidoux); an aloft layer with SO_2 concentrations of up to 25 ppb was also identified on this afternoon.

Recommendations for modeling in the SoCAB:

- The meteorological and photochemical models need to properly represent the formation and transport of aloft polluted layers including the following characteristics:

    - Clean boundary conditions aloft (above about 1500 m on most days).

    - The formation of layers aloft containing high concentrations of ozone, other chemical products, and precursors. Potential formation mechanisms include sea-breeze undercutting of the mixed layer, slope-flows along the mountains and the resulting return flow out over the SoCAB, the formation of the nocturnal surface layer, the injection of pollutants aloft by stationary source emissions and convergence zones, and the transport of buoyant air parcels from the mixed layer into the inversion layer (convective debris).

    - The mixing of many of these aloft polluted layers down to the surface during the midday and afternoon.

    - A pollutant and temperature structure aloft which is more horizontal than terrain-following (i.e. more msl than agl). In addition, the horizontal structure implies that aloft transport is generally horizontal as well.

    - Ozone concentrations in the midday and afternoon mixed layer are greater than ozone concentrations measured at nearby surface monitors by about 20-30 ppb. We conclude that this difference

between surface and aircraft concentrations might be due to ozone deposition at the surface and/or to titration by fresh NO near the surface. Additional analysis to support this conclusion is needed; if this conclusion is confirmed, then model evaluation procedures need to be revised.

- The meteorological and photochemical models need to properly represent the occurrence and altitudes of clean boundary conditions aloft (above about 1500 m on most days).

- Model simulations should start on mornings with clean conditions aloft and at the surface; and the model simulation should build up the spatial distribution of pollutants, rather than using dirty initial conditions to simulate that build up. Upper air meteorological and air quality data are needed on the starting day to document clean conditions. Many current model simulations started on the day prior to a SCAQS intensive day; maybe they should have been started two days prior to an intensive sampling day. Pollutant concentrations aloft were quite low on the morning of July 13, 1987; so the July 13-15, 1987 episode would be a good episode to model.

- The distribution of pollutants during SCAQS, even on clean days, was not spatially uniform; therefore, initial and boundary conditions should not be spatially uniform. In addition, concentrations at the top of the modeling domain were typically close to background; therefore, top boundary conditions which are significantly above background should not be used.

- Summer SCAQS aloft data show a progression of aloft ozone concentration characteristics over the course of an episode, for example: from clean on the morning of July 13, 1987; to high ozone concentrations over most of the SoCAB (including offshore) that afternoon; to moderate ozone concentrations the next morning; to high ozone concentrations again over most of the SoCAB on the afternoon of July 14; and to moderate concentrations on the next morning. Current model simulations do not seem to show this type of progression of aloft ozone concentration characteristics, but additional evaluation of simulation results should be performed. Model simulations might not properly represent aloft concentration history for a number of reasons; including improper specification of boundary conditions, initial conditions, emissions, winds aloft, and mixing height structure, or due to the starting time of the model simulation.

- It is difficult to adequately evaluate the performance of a meteorological model when all of the meteorological data has been used in the model. Potential approaches for additional work in this area include:

    - Performing additional particle trajectory studies with the meteorological model, with emphasis on the presence of particles in aloft layers and the history of these particles over a diurnal cycle. Questions to address might include: Are results from such studies similar to field results? Do particles occur in aloft

layers, mix down in the afternoon, and are they carried over to aloft layers on the following morning?

- Performing additional evaluation of the SCAQS inert tracer studies and comparison of aloft tracer data with model simulation results. Questions to address might include: Do aloft tracer results indicate the formation and transport of aloft pollutant layers in a manner similar to the aloft ozone data? Do model simulations of the tracer releases indicate similar results?

- As part of this project, we compared ozone concentrations measured aloft with ozone concentrations from model simulations using summer data. Because these comparisons were poor, we did not perform comparisons using aloft data for other species; such as NO, NO_x, PAN, or nitric acid, or for the fall data. However, once improved simulation results are available, these additional comparisons should be performed.

1. INTRODUCTION

Concentrations of ozone and particulate matter regularly exceed the State and Federal standards at monitoring sites in the South Coast Air Basin (SoCAB). The Southern California Air Quality Study (SCAQS) was conducted in the SoCAB during the summer and fall of 1987 to provide a comprehensive database for data analysis and modeling of ozone and particulate matter. Many separate data analysis and modeling projects have been performed using the SCAQS database. A broad-based and detailed case study of specific pollutant episodes can improve our understanding of the evolution and sources of ozone and particulate matter concentrations in the SoCAB by integrating techniques and results from the separate analysis and modeling efforts. This report summarizes the data analyses performed for the ozone and particulate matter case study analysis project, the analysis results, and the conclusions and recommendations of the project.

1.1 BACKGROUND

The scope of the SCAQS monitoring program was more comprehensive than any previous program in the SoCAB or in any other single urban area. The field study was conducted over eleven summer and six late fall days in 1987. Simultaneous measurements of both surface and upper-air air quality and meteorological parameters were performed. Data from existing monitoring networks were augmented by measurements made explicitly for the SCAQS. In addition, specialized state-of-the-art measurements for specific pollutants and processes were made by various participants.

The 1987 SCAQS has provided a unique data analysis opportunity because of the extensive and diverse data collected during the field program (see Blumenthal et al., 1987; Hering and Blumenthal, 1989; and Lawson, 1990 for a description of the data collected). Many separate data analysis and modeling projects have been performed using this database. Most of the data analysis projects have addressed specific issues, such as the spatial and temporal distribution of volatile organic compounds (VOC) (Lurmann and Main, 1992) and of other gaseous pollutants (Grosjean, 1990; Williams and Grosjean, 1990), the size and composition of aerosols (John et al., 1990; Cahill et al., 1990; Wolff et al., 1991), or the results of the various tracer experiments (Horrell, et al., 1991; Teuscher, 1989). Other analyses using SCAQS data have explored broader issues such as the general meteorology and air quality (Zeldin, et al., 1989) or the three-dimensional air quality (Roberts and Main, 1992; McElroy and Smith, 1992) during the SCAQS. Other investigators have developed model inputs using the SCAQS database and explored the performance of meteorological and air quality models (Harley et al., 1992; Cassmassi and Durkee, 1990; Cassmassi et al., 1990; Chico et al., 1990; SCAQMD, 1990, 1991; Roberts and Main, 1992; Wheeler, 1990, 1991a, 1991b). A broad-based and detailed case study approach can provide an opportunity to integrate techniques and results from these various analysis and modeling efforts into a comprehensive package.

1.2 OBJECTIVES

The specific objectives of the ozone and particulate matter (PM) case study analysis project were to:

- Describe in detail the three-dimensional (3-D) evolution of two ozone episodes in space and time, including the transport and transformation processes leading to the maximum ozone concentrations measured in the SoCAB;
- Describe in detail the 3-D evolution of three PM episodes in space and time, including the transport and transformation processes leading to the maximum PM concentrations measured in the SoCAB;
- Identify gaps in our understanding of the important processes; and
- Recommend ways to fill the gaps identified.

1.3 SELECTION OF EPISODES FOR THE CASE STUDIES

During the SCAQS, measurements were made during five episodes in the summer and three episodes in the fall. These periods of intensive measurements were one to three days in duration. In order to choose episodes for further analysis during this case study project, we reviewed the following information:

- The prioritized list of episodes for modeling applications developed by Zeldin et al. (1989), based on their review of the general meteorological and air quality characteristics of all of the SCAQS intensive days, compared to seasonal norm characteristics.
- Occurrences of high ozone concentrations and high PM_{10} concentrations.
- Availability of meteorological and air quality modeling results.
- Completeness of the 3-D data such as lidar, air quality aircraft, upper air meteorological, particle trajectory, and tracer data.
- Completeness of the surface data.
- Presence of important physical phenomena, including upslope flow, sea breeze intrusion, aloft pollutant layers with high concentrations, and flow out of the basin or offshore.

We chose the following episodes for analysis: June 24-25, July 13-15, and December 10-11, 1987. Case study analysis of the June and July episodes provides a comprehensive look at two periods with high ozone concentrations; case study analysis of all three periods provides a comprehensive look at high PM concentrations during both summer and fall conditions.

The June 24-24, 1987 episode was the highest ranked summer episode (Zeldin et al., 1989), exhibited widespread ozone exceedances and high PM_{10}

concentrations, had good 3-D and surface data completeness, and interesting (and representative) physical phenomena. This episode was modeled by the SCAQMD and thus, wind fields, mixing heights, and model results were available. The meteorology was very similar from one day to the next, facilitating modeling efforts. One of the problems with this episode was that high concentrations of ozone were already observed aloft on the morning of June 24, thus the buildup in pollutant concentrations from clean conditions was only measured with the routine network and not with the intensive SCAQS network.

The July 13-15, 1987 episode was ranked third by Zeldin et al. (1989). This episode was one of two three day intensive measurement periods during the summer, and surface and aloft air quality and meteorology measurements were extensive. One advantage of this episode was that the aloft ozone concentrations were very low on the morning of July 13, thus allowing the intensive measurements to observe the buildup in pollutant concentrations from clean conditions. Other interesting phenomena of this episode included: upslope flow, sea breeze intrusion, persistence of aloft pollutant layers with high concentrations, surface impact of aloft pollutants, and the presence of a thin layer of SO_2 aloft. A coastal eddy developed on the 15th and decreased ozone concentrations. This episode has not been modeled yet, primarily because pollutant concentrations were not as high as concentrations during the June and August episodes.

The December 10-11, 1987 episode was the highest ranked fall SCAQS episode (Zeldin et al., 1989). NO_2 concentrations were higher during this episode than any other SCAQS episode and PM_{10} concentrations were also high. Surface and aloft air quality and meteorological data are generally complete. This episode was modeled by the SCAQMD and thus, wind fields, mixing heights, and model results are available.

We did not choose June 19 and December 3 since these were single day episodes, and thus less useful for describing carryover from the previous day. While the August 27-29 episode had the highest ozone concentrations of any summer SCAQS day, and has been modeled by the SCAQMD and the ARB, the 3-D data were seriously incomplete: no lidar flights, and only three complete air quality aircraft flights out of a possible nine flights are available. The September 2-3 episode had somewhat unusual meteorology and thus was very interesting. However, lidar data were not collected and this episode has not been modeled. In addition, high ozone concentrations were not widespread in the basin. Finally, the November 11-13 episode was similar to the December episodes. However, Zeldin et al. (1989) ranked it lowest. While the air quality aircraft data are quite complete, lidar and tracer data, as well as model results, are lacking.

1.4 SUMMARY OF SCAQS DATA ANALYSES

Our case study analysis of the SCAQS data has used the results of other investigators as a foundation. Although a large number of data analysis and modeling projects have been completed, some projects are still in progress or have not been reported; and thus were not available for our use.

In addition to the numerous reports, the SCAQS was the focus of several sessions at the Air and Waste Management Association Annual Meeting in June 1989 (see Lawson, 1990 for a summary) and SCAQS data analysis and modeling results were presented at a three-day specialty conference in Los Angeles during July 1992 (proceedings will be available).

A brief description of many of the reports and analysis and modeling results which we used is provided below; additional details are available in the reports, which are included in the references in Section 8.

Meteorology: Zeldin et al. (1989) provided an overview of the surface meteorological and air quality conditions which occurred during the SCAQS. SCAQMD (1990) and Douglas et al. (1991) described aloft wind flows during various SCAQS episodes.

Emissions Inventory: Fujita et al. (1992) compared the ambient SCAQS hydrocarbon and carbonyl compound data with data from the emissions inventory. The focus of this work was primarily on the NMOC/NO_x and CO/NO_x ratios; ambient CO/NO_x and NMOC/NO_x ratios were significantly higher than corresponding emission inventory ratios. Lurmann and Main (1992) explored the species composition, as well as the ratios, and found significant discrepancies between the ambient and emissions inventory compositions. Differences between the reactivities of the emissions inventory and ambient data were identified by Harley et al. (1992) and Lurmann and Main (1992). Numerous other studies have explored the SCAQS tunnel data, emission factors, emission inventory uncertainties, in-use vehicle emissions, and driving cycles.

Model Performance: During various model simulations using the SCAQS data, a number of model components have been identified as important to model performance, including mixing heights, wind fields, initial and boundary conditions, and the emissions inventory.

- Many previous investigators have shown that mixing height is a critical parameter in the "Urban Airshed Model" (UAM). The sensitivity of the model to mixing height was investigated by Cassmassi and Durkee (1990) and Wheeler (1990).

- Wind fields were generated by diagnostic, prognostic, and hybrid techniques. In general, the wind fields generated for use in the various UAM applications in the SoCAB showed good agreement with measured winds in areas with an abundance of observed data (SCAQMD, 1990; Wheeler, 1992). However, Wheeler (1991a) showed there could be a number of errors in the wind fields, and that these errors could produce significant biases in predicted ozone concentrations (Wheeler, 1991b). Wheeler (1991a) found that in some areas, observational data showed that sites in adjacent grid squares were significantly different and these measurements can introduce artificial divergence, and that interpolation of data from nearby sites could create unrealistic wind fields or reduce predicted wind speeds. In addition, some sites are not representative of the surrounding area (such as a site located in a canyon). Cassmassi et al. (1990) investigated three types of wind-field generation methods and illustrated similarities and differences between the resulting wind

fields. Chico et al. (1990) assessed wind model performance using the tracer data and found that general transport paths and stagnation in eastern SoCAB were well-modeled, but that transport was, in general, too slow. Some features which were not well modeled included flow out of the SoCAB via Cajon Pass, flow offshore overnight, and transport along the base of the San Gabriel Mountains. Horrell et al. (1991) identified important wind-flow characteristics using the wind and tracer data.

- In general, sensitivity tests to initial conditions show that the model simulation results are relatively insensitive by the second or third model day (SCAQMD, 1990). However, if boundary conditions are set significantly higher than clean background conditions, model results are affected. Harley et al. (1992) found that higher initial and boundary conditions produced better agreement between model output and observed ozone concentrations in the eastern basin.

- Harley et al. (1992) showed better agreement between predicted and observed ozone concentrations at many sites when the mass of the running (hot-stabilized) exhaust emissions of CO and ROG were increased to three times baseline values, as suggested by Ingalls (1989) and Fujita et al. (1992).

- Roberts and Main (1992) found that model predictions of aloft ozone concentrations did not match very well with ozone concentrations measured by aircraft during two SCAQS episodes, June 24-25 and August 27-29. The June 24-25 comparisons are discussed in Section 3 of this report.

VOC Spatial and Temporal Variability: Lurmann and Main (1992) described the spatial and temporal patterns of ambient total nonmethane organic compound (NMOC) concentrations, individual organic compound concentrations, and NMOC/NO_x ratios in the SoCAB using the SCAQS data. Using receptor modeling, Gertler et al. (1992) found that nearly 90% of the NMOC at all sites an all times of day were attributed to motor vehicle exhaust.

3-D Air Quality Analysis and S, N, and C Species Mass Balance: A detailed analysis of the SCAQS 3-dimensional air quality data was undertaken to develop an improved understanding of aloft concentrations and processes in the SoCAB (Roberts and Main, 1992). In addition, sulfur, nitrogen, and carbon species distributions were prepared for selected periods and locations during the SCAQS. Aloft layers containing high concentrations of pollutants frequently occur in the SoCAB and influence ozone concentrations at surface monitoring sites. Maximum ozone concentrations aloft were often higher than ozone concentrations at surface monitoring sites. Vertical profiles of pollutants varied more temporally than spatially.

Aerosol Composition: Hering (1990a, 1990b, 1992) explored the fine and coarse aerosol composition and gaseous pollutant concentrations measured at the SCAQS surface monitoring sites using the SCAQS sampler. Huntzicker and Turpin (1991) identified episodes of high secondary organic carbon formation, including June 22-28, July 11-13, July 25-27, August 25-31, and November 17-19. Watson et al. (1992) applied the chemical mass balance receptor model to chemically-speciated aerosol samples; dust was a major contributor during the

summertime, while ammonium nitrate concentrations were high in the winter. Primary motor vehicle exhaust contributions peaked during the morning rush hour, as expected.

Tracer Studies: The results of an atmospheric tracer study conducted by Southern California Edison showed that there were no differences between ground and elevated sources on total impacts in the SoCAB. However, there were different impacts in downwind areas from the two types of releases (England and Marsh, 1992). The Los Angeles/Glendale divergence zone was investigated using SF_6 tracer (Horrell, 1992).

1.5 ORGANIZATION OF THE REPORT

This report is organized into seven sections. Section 2 provides a summary of the SCAQS data which were used in this report. Important quality control and selection procedures are also discussed. Sections 3, 4, and 5 focus on each of the three episodes selected for case study analysis: June 24-25; July 13-15; and December 10-11, 1987. The text, figures, and tables in each of these sections describe the 3-D evolution of pollutant concentrations during the episodes. The June and July episodes emphasize both ozone and PM, while the December episode is primarily a PM episode. Section 6 summarizes the results and provides the conclusions and recommendations of the study. Because of the large number of illustrations used in this report, figures and tables are provided in numerical order after the text in each section. Section 7 provides a list of references for the report. Appendix A provides information on measurements and site locations. Appendix B provides comparisons of ozone concentrations from model simulations and aircraft measurements for June 24-25, 1987.

2. SUMMARY OF DATA USED FOR THIS REPORT

The data available from the SCAQS are extensive. The SCAQS intensive periods of sampling occurred on eleven summer days during 1987: June 19, June 24-25, July 13-15, August 27-29, and September 2-3, and on six fall days during 1987: November 11-13, December 3, and December 10-11. The field study included extensive surface and aloft measurements of air quality and meteorological parameters. The data collected during the SCAQS were submitted to ENSR, the California Air Resources Board, and STI for archiving, validation, and management (Croes and Collins, 1989; Lawson, 1990). For this project, we focused on the data collected during surface and aloft sampling during three SCAQS episodes: June 24-15, July 13-15, and December 10-11, 1987.

This section summarizes the database which was available for our analyses; additional details are available in Blumenthal et al. (1987), Hering and Blumenthal (1989), and numerous other SCAQS publications. The following subsections summarize surface and aloft measurements made during the SCAQS, including sampling durations and locations; differences between data from multiple measurements of a single parameter and our selection of the measurement data which we used in our analyses; special supplemental data from the SCAQS which were used in our analyses; and major gaps in the database.

2.1 SURFACE MEASUREMENTS

2.1.1 SCAQS Sampling Locations

The surface data for SCAQS were obtained from the routine hourly measurements at existing sites, plus supplemental measurements made at a subset of the existing sites. The general types of measurements made at the various sites are summarized below:

- Surface air quality and meteorological measurements were made at the existing network of monitoring stations (called C-sites). Site locations are shown in Figure 2-1. Measured parameters included ozone, NO, NO_x, CO, SO_2, light scattering (b_{scat}), temperature, dew point, wind speed and wind direction. The South Coast Air Quality Management District (SCAQMD) operated these sites.

- Surface measurements of reactive gases, aerosol size distribution and chemistry, and toxic air contaminants were made at a selected subset of the C-sites (called B-sites). These locations are shown in Figure 2-1 with site names spelled out. The basic B-site measurements were made using a specially-designed sampler, the SCAQS sampler, which provided samples integrated over five periods on each intensive sampling day. The periods ranged from four to seven hours.

- Specialized measurements by universities and research institutions were performed at new sites installed at Claremont and Long Beach (called A-sites, see Figure 2-1). During the summer, measurements were taken at both the Claremont and Long Beach sites; during the fall, measurements

were taken only at Long Beach. A complete list of all A-, B-, and C-site locations and elevations is provided in Appendix A, Table A-1. Lists of principal investigators and measurements are provided by Hering and Blumenthal (1989).

Many of the measurement and analytical methods used during the SCAQS were developed for and tested in the Carbonaceous Species Methods Comparison Study (CSMCS) held in August 1986 (Lawson and Hering, 1990) and in the Nitrogenous Species Methods Comparison Study held in 1985 (Hering et al., 1988).

2.1.2 SCAQS Aerosol Sampler

Aerosol samples were collected at B-sites using the SCAQS sampler, developed for the SCAQS (Fitz and Zwicker, 1988). The sampler schematic is shown in Figure 2-2. The sampler consisted of twelve different sampling lines, with various substrates for the measurement of aerosol chemistry in two particle size fractions: aerodynamic particle diameters less than 2.5 μm ($PM_{2.5}$) and less than 10 μm (PM_{10}). The sampler also provided measurements of fine particle absorption, nitric acid, ammonia, and SO_2. Aerosol samples were analyzed for mass, elemental composition, inorganic ions, and organic and elemental carbon (Countess, 1989; Fitz et al., 1989). The sampler also provided measurements of fine particle absorption, nitric acid, ammonia, and SO_2. The media in the SCAQS sampler were changed at 0600, 1000, 1400, and 1800 local time (PDT in the summer, PST in the fall) and midnight standard time (0100 PDT in the summer, 2400 PST in the fall).

2.1.3 Air Quality Data Selection

A large portion of the SCAQS data archive was used in this study. Some species were measured using more than one analytical technique or using the same technique but employing different laboratories for analyses. Quality assurance audits were performed during the SCAQS to determine whether the quality control procedures were adequate and whether the tolerances for accuracy and precision were being achieved. The results of these audits are described by Hering and Blumenthal (1989) and Collins and Fujita (1990). In addition, the data from the SCAQS sampler were evaluated by Hering (1990a and 1990b).

For cases in which we had to choose between two or more sources of data, we based our choice on the consistency of the analytical method, data availability, comparability with data at other locations and times, accuracy and precision of the analyses, and recommendations from past methods intercomparisons and from SCAQS measurement method intercomparison results. Table 2-1 lists the data which were obtained from the ARB. The sample averaging times, detection limits, and SCAQS audit results are provided in the table (if readily available). The following paragraphs summarize the multiple measurements of a single parameter, the rationale for selecting the measurements for use in our analyses, and important caveats concerning these selections.

NO, NO_2, NO_x - Hourly average NO and NO_x, with NO_2 determined by difference, were reported at routine monitoring stations in pphm units (rounded off in

10 ppb increments). The following NO, NO_2, and NO_x data were available at Claremont, where more comprehensive measurements were made: NO and NO_x were measured by both GMRL and EPA using chemiluminescence, with NO_2 by difference; UCR measured NO_2 using differential optical absorption spectroscopy (DOAS) (Winer and Biermann, 1989; Winer, et al., 1989); and Unisearch measured NO_x and NO_2 using the Luminox technology (Drummond et al., 1989). The SCAQMD, GMRL, and EPA NO_x measurement methods may also include positive interferences from organic and inorganic nitrates (such as PAN and nitric acid) which can comprise a significant portion of the NO_x signal (up to 40%, according to Grosjean, 1983). DOAS provides a direct measure of NO_2. Tests by the Luminox developers showed that interferences from other forms of oxidized nitrogen that have been identified as interferences for other commercial NO_x monitors are not a problem with the Luminox method (Drummond et al., 1989).

An evaluation of these three measurements was made to select the best data for use in our analyses. During data evaluation, Eric Fujita (ARB) recommended choosing the mean value of the GMRL and EPA NO and NO_2 data. In addition, he invalidated the GMRL and EPA data for June 24-25. A time series plot of the Claremont NO and NO_2 measurements is shown in Figure 2-3. The diurnal variations of the data were very similar, however, the magnitude of the measurements varied considerably. EPA reported the highest, and Unisearch reported the lowest, NO and NO_2 concentrations. The average GMRL and EPA NO values correlated well ($r^2 > 0.95$) with the Unisearch data. The average GMRL and EPA NO_2 data also correlated well with the Unisearch ($r^2 = 0.93$) and UCR ($r^2 = 0.78$) NO_2 data. For both NO and NO_2, the GMRL and EPA average concentrations were usually higher than the Unisearch and UCR measurements.

The difference in concentrations between these measurements may be due to interference from other organic or inorganic nitrates. To test this hypothesis, we determined the period-average nitric acid and PAN concentrations which corresponded to the average GMRL and EPA NO_2 values. The sum of PAN and nitric acid was subtracted from the NO_2 and the linear regressions with the UCR and Unisearch data were recalculated. The adjusted data did not correlate as well with the Unisearch and UCR data ($r^2 = 0.82$ and 0.56, respectively) as the unadjusted values although the correlations were still reasonable. To be consistent with other investigators (e.g. Fujita et al., 1992), we have used the average GMRL and EPA NO values. In addition, UCR NO_2 data were used when available; otherwise, the average GMRL and EPA NO_2 values (unadjusted for possible nitric acid and PAN interferences) were used. Note that the unadjusted NO_2 value could contain considerable interference. In most discussions of the summer data, we have used NO and NO_x.

During the fall, more comprehensive measurements were made at Long Beach than at other sites. In addition to the routine NO_x measurements, the following NO, NO_2, and NO_x data were available: NO and NO_x were measured by both the ARB and GMRL using chemiluminescence, UCR measured NO_2 using DOAS, and Unisearch measured NO_x and NO_2 using the Luminox technology. During data evaluation, Eric Fujita (ARB) recommended choosing the mean value of the GMRL and ARB NO and NO_2 data. The diurnal variations of the three measurements were in excellent agreement; however, the magnitude of the measurements varied considerably. ARB reported the highest, and Unisearch reported the lowest, NO and NO_2 concentrations. Figure 2-4 shows the diurnal profiles of the NO and NO_2 data. The average GMRL and ARB NO data correlated well ($r^2 = 0.95$) with

the Unisearch data. The average GMRL and ARB NO_2 data also correlated well with the UCR (r^2 = 0.92) and Unisearch (r^2 = 0.90) data. The average GMRL and ARB concentrations were higher than the Unisearch measurements. The UCR NO_2 concentrations were typically the same or slightly higher than the average GMRL and ARB measurements. We have used the UCR NO_2 value, when available; otherwise we have used the average GMRL and ARB NO and NO_2 values.

Note that in presenting the fall data, we have shown NO and NO_2 data. In contrast to the summer, nitric acid and PAN comprise a smaller percentage of the total NO_x measured. Not only are fall NO and NO_2 concentrations much higher than the summer, nitric acid and PAN concentrations are lower.

Nitric Acid - Nitric acid was measured at B-sites using the SCAQS sampler by the denuder difference method (DDM) with an AIHL cyclone precut of 2.5 μm, MgO denuder tubes and Teflon-Nylasorb filter sandwich. At Claremont, nitric acid was also measured by the ARB using a separate denuder difference set-up and by Unisearch using a tunable diode laser absorption spectrometer (TDLAS) system which provides a direct measure of nitric acid (Drummond et al., 1989). The Unisearch data were only available for June.

To compare these measurements, a diurnal plot of the filter-interval-averaged data is shown in Figure 2-5. The diurnal profiles of the measurements were very similar, however, the concentrations differed. The ARB and SCAQS sampler data agreed well (r^2 = 0.85) except for the peak values on July 14 and August 28 which differed by more than 10 ppb. On average, the SCAQS sampler concentrations were greater than the ARB values by about 18%. The SCAQS sampler and Unisearch data also correlated very well (r^2 = 0.97). Overall, the data correlated excellently considering the uncertainties in the denuder difference method. Eric Fujita calculated the measurement uncertainty (which includes flow rate and analytical precision, standard deviation of blanks, and propagation of error) in the DDM nitric acid values and plotted the uncertainty as a function of the wt% of nitric acid in the total nitrate (Figure 2-6). The total uncertainty (expressed as the standard deviation divided by the mean) was more than 50% for samples in which the nitric acid comprised less than 40 wt% of the total nitrate. For our analyses, we used the SCAQS sampler data set since it was the most complete. However, for low nitric acid fractions of the total nitrate, there may be significant uncertainty in the values.

Data invalidated by other investigators in early data quality control reviews were not used. In some cases, these investigators had invalidated one or both of the measurements used in the DDM (Leg 3, L3 and Leg 4, L4) but had not invalidated the corresponding nitric acid value. We invalidated the nitric acid data in these cases.

Peroxyacetylnitrate - PAN was measured at the B-sites by DGA using gas chromatography with electron capture detection (GC-ECD). In addition, the EPA measured PAN at Claremont during the summer using the same measurement method but a different calibration technique. A diurnal plot of EPA and DGA PAN data is shown in Figure 2-7 for the summer. During June, the data correlated poorly (r^2 = 0.27) and the peak PAN concentrations measured by the EPA were up to 16 ppb higher than the DGA concentrations. After June, the correlation

improved significantly (r^2 = 0.70) although there was still a significant bias in concentration.

In addition to the measurement discrepancies at Claremont, much of the DGA PAN data in the database we received from the ARB were suspect. At all sites, some concentrations were reported as 22 or 25 ppb at night when we would not expect these high concentrations. Furthermore, the hours before and after these high concentrations typically showed concentrations of 0 ppb. In comparing the database to tables and plots in Williams and Grosjean (1990), it was clear that these anomalous high values had been invalidated. Unfortunately, alternate PAN measurements were available only at Claremont. For most analyses, the EPA PAN data were used for Claremont. The PAN data at the other sites should be viewed with caution, particularly data collected in June.

Nitrate Ion - Nitrate ion concentration data were obtained from the SCAQS sampler at B-sites. Fine particle nitrate was measured in Leg 3 (L3) of the sampler from a denuded teflon-nylon filter sandwich following an AIHL cyclone. The Leg 3 (L3) and Leg 4 (L4) nitrate concentrations were used to provide nitric acid (using the denuder difference method). Nitrate measured on Leg 9 (L9) was subject to losses (or gains) and was not used in our analyses (Hering, 1990a). Data which were invalidated by other investigators in early data quality control reviews also were not used.

Ammonium Ion, Ammonia - Ammonium ion and ammonia concentrations were obtained from the SCAQS sampler at B-sites. Leg 5 (L5) of the sampler provided a measure of the fine particle ammonium ion from a denuded oxalic acid-impregnated filter. Ammonia (as ammonium ion) was recovered from an oxalic acid denuder also in L5. Ammonium ion from L9 was subject to volatilization and was not used in our analyses. The PM_{10} ammonium ion data collected in Leg 12 were not used as the volatilization artifact was also significant for this leg (Wolff et al., 1991; Hering, 1990a). Data which were invalidated by other investigators in early data quality control reviews also were not used.

Sulfur Dioxide - SO_2 was measured continuously at routine monitoring sites and reported in pphm units. The routine data showed SO_2 concentrations were typically 0 to 1 pphm. At B-sites, SO_2 was also measured using the SCAQS sampler by passing ambient air through a carbonate-impregnated filter below a Teflon filter. These data indicated SO_2 was typically below 10 ppb. When available, the filter chemistry data were used in our analysis because the detection limits for SO_2 were much lower than the detection limit for routine measurements. For sites at which the SCAQS sampler was not operated, routine data were generally used qualitatively rather than quantitatively in our analyses.

Organic Carbon - At B-sites, the SCAQS sampler was used to collect particulate organic carbon samples. Organic carbon measurements were corrected for vapor adsorption by subtracting the organic carbon from the quartz backup filter (Hering, 1990a); this correction had been made before we received the database and could not be evaluated. Another measurement of organic carbon, using a carbon analyzer, provided fine particle organic and elemental carbon data with two-hour time resolution at Claremont in the summer and Long Beach in the fall (Turpin and Huntzicker, 1991). A detailed comparison of these data to the

SCAQS sampler was beyond the scope of this project. However, a cursory comparison showed that the two data sets had similar diurnal patterns and peak concentrations. The SCAQS sampler data were used in our analyses.

Hydrocarbon and Carbonyl Data - The one-hour hydrocarbon samples were collected in initially-evacuated six-liter stainless steel canisters. The C2-C12 hydrocarbon analyses were performed by Len Stockburger of the U.S. EPA's Atmospheric Sciences Research Laboratory using gas chromatography - flame ionization detection (GC-FID) (Stockburger et al., 1989). Most of sample canisters were also analyzed for the C2-C4 hydrocarbons by Rei Rasmussen of the Oregon Graduate Institute (OGI). A subset of the samples were reanalyzed by William Lonneman of the EPA by GC-FID (Lonneman et al., 1989) and by Stockburger and Rasmussen using gas chromatography-mass spectrometry (GC-MS). Carbonyl compounds were collected using cartridges impregnated with DNPH. Aldehydes and ketones react with DNPH to form hydrazones which are measured by high performance liquid chromatography. Analyses were performed by ENSR (Fung, 1989).

The species for which multiple laboratories supplied data were handled as follows: Rasmussen's C2-C3 hydrocarbon data were used instead of Stockburger's C2-C3 data, Stockburger's C4 hydrocarbons were used instead of Rasmussen's C4s, and Fung's acetone was used instead of Stockburger's acetone data. Rasmussen's C2-C3 data were selected because his analytical system provided better separation of the C2-C3 peaks. Stockburger's C2-C3 data were used only for the cases where the OGI C2-C3 data were missing and then, because of the uncertainty in Stockburger's individual C2 peaks, only the total C2s were included in the database. The C4 hydrocarbon concentrations measured by Stockburger and Rasmussen agreed well and Stockburger's data were selected. The two sets of acetone data were very different and Fung's data were selected because the DNPH method was considered more reliable than GC-FID for acetone at ambient levels. Further details concerning sampling, analysis, data selection, and data validation are discussed by Lurmann and Main (1992).

Carbon Monoxide - Carbon monoxide was routinely measured at several sites in the SoCAB using CO monitors. These data were limited in their usefulness because they were reported in ppm units, with a detection limit of 500 ppb. However, OGI used GC-FID to quantify CO in all the hydrocarbon canister samples (detection limit 20 ppb). These data showed CO concentrations ranged from 220 to 5100 ppb, with a median value of 1300 ppb in the afternoon (summer). In the fall, CO ranged from 392 to 16,400 ppb. The OGI data were used in our analysis whenever available. For cases in which GC-FID CO data were not available, routine data were generally used qualitatively rather than quantitatively in our analyses.

Light Scattering - Light scattering (b_{scat}) was measured using nephelometers at the B-sites during SCAQS. Two nephelometers were operated at Claremont during the summer by AV and GMRL. While these two data sets agreed relatively well ($r^2 = 0.59$) both diurnally and in magnitude, the Claremont data were a factor of three or more lower than measurements made nearby at Upland (see Figure 2-8). Since the Claremont and Upland sites are less than 6 km apart, we would expect data from the two sites to agree. Although b_{scat} for the two nephelometers at Claremont agreed fairly well, the data from the GMRL nephelometer was better correlated with the Upland data ($r^2 = 0.80$) than the

AV data (r^2 = 0.54). Figure 2-9 shows the time series b_{scat} data for Claremont and Upland, plus the extinction coefficient (b_{ext}) data measured along a sight path from Claremont to Cable Airport during the daytime by Richards et al. (1988). The magniture of the b_{ext} data matches the Upland b_{scat} data better than the Claremont data.

Additional work is needed to understand these differences. However, since the aircraft b_{scat} data also agreed with the Upland data, we have used the Upland data, not the Claremont data, in our analyses.

Particulate Mass - The SCAQS sampler provided measurements of both PM_{10} and $PM_{2.5}$ mass. These measurements were subject to losses and gains of nitrate and ammonium ions and nitric acid from the Teflon filters. Wolff et al. (1991) applied a correction factor to the 12-hr GMRL data to account for this phenomenon. We also corrected the SCAQS surface mass data. Table 2-2 shows the average precent correction for the GMRL data and for the SCAQS data. In general, the intensive four to seven hour SCAQS data showed smaller mass corrections than did the 12-hr GMRL data taken on intensive and non-intensive sampling days. Both data sets show smaller mass corrections for PM_{10} than for $PM_{2.5}$. The percent corrections for the SCAQS data set were very similar across all sites. Surface particulate mass data shown in this report were corrected. All of the L1 nitrate data for December at Burbank were invalid. We used an average factor, based on the November Burbank data, to correct the December Burbank PM_{10} mass.

2.2 MEASUREMENTS ALOFT

Table 2-3 summarizes the data which were used in this study to characterize the structure of pollutants and meteorology aloft. Sample averaging times, sampling locations, and SCAQS audit results are provided in the table (if available). In general, it was desirable for our analyses to have different parameters measured at the same locations and time; however, this was not always possible. The following sections describe the different types of measurements and the ways we addressed differences in the data and data gaps.

2.2.1 Upper Air Meteorological Measurements

Vertical profiles of winds, pressure, temperature and humidity were obtained primarily using rawinsondes and Airsondes, which are small, radio-equipped weather balloons. The rawinsondes used a LORAN tracking system for deriving winds and reported data up to about 3300 meters above ground level (m agl) or higher. The Airsondes measured temperature and humidity to the same altitudes, but because the wind data are derived by visual tracking, the vertical range for winds was sometimes limited by cloud cover and visibility. Soundings were performed six times per day at approximately 0500, 0800, 1100, 1400, 1700, and 2200 LT at eight summer and six fall sites. A Doppler acoustic sounder and aircraft measurements supplemented the weather balloon data. Additional details are provided by Hering and Blumenthal (1989) and Lehrman et al. (1988).

2.2.2 Air Quality Aircraft Measurements

Three aircraft were operated during the SCAQS. Two of the aircraft made real-time measurements of air quality and meteorological parameters while the third aircraft, operated by the EPA, used lidar for the vertical mapping of aerosol backscatter. The air quality aircraft were operated by the University of Washington (Hegg and Hobbs, 1988) and STI (Anderson et al., 1989).

The SCAQS aircraft flew spirals, orbits and traverses to document the vertical and horizontal pollutant gradients. Spirals were flown over a fixed location on the ground. In a spiral, the aircraft descended or ascended at a rate of about 150 meters/minute in a turn with about a 2 km diameter. Spirals were usually made from about 1500 meters mean sea level (m msl) down to within about 30 m of the surface. Orbits were circular or elliptical paths flown at a constant altitude above a fixed point on the ground. Orbit diameters were about 5 km, about the size of one modeling grid cell. During an orbit, the aircraft flew repeatedly (about six or seven times) over the same path to provide sufficient time (typically about 30 minutes) for collection of integrated samples for chemical analysis. Typical orbit altitudes ranged from 300 to 750 m msl. Traverses are straight paths flown between predetermined points. The lidar aircraft flew traverses at a constant altitude.

The air quality aircraft flew three flights daily during the summer: early morning, midday, and afternoon. In the fall, the aircraft only flew in the morning and the afternoon. Continuous measurements of ozone, NO, NO_x, SO_2, light scattering, temperature, dew point, and turbulence were made by the air quality aircraft during both spirals and orbits. Grab samples of hydrocarbons were made at preplanned locations and altitudes during orbits and some spirals. Integrated aerosol and trace gas samples were made during orbits using a modified version of the SCAQS sampler. These samples were later analyzed for nitric acid, SO_2, PAN, carbonyls, and particulate sulfur, carbon, and nitrogen species. Spiral and orbit locations are shown in Figure 2-10. Additional details on the air quality aircraft instrumentation, flight plans and measurement audits are provided by Hering and Blumenthal (1989), Anderson et al. (1989), and Hegg and Hobbs (1988).

The lidar aircraft flight pattern was designed to map the 3-D aerosol distribution throughout the SoCAB and at the boundaries. The aircraft typically flew at 3000 m msl, with the lidar mapping the aerosol distribution from the aircraft to the ground. The flights included traverses across the SoCAB, offshore, over the northern mountains and into the Coachella Valley. The lidar aircraft flew once or twice per day, with one flight in the early morning and the other flight in the afternoon. Flight times approximately overlapped those of the air quality aircraft. Additional details are provided by Hering and Blumenthal (1989) and McElroy et al. (1988).

During the first half of the summer, the STI aircraft flew the spirals, while the UW aircraft flew the orbits. In general, complete data sets for all measured parameters were available and used in our analyses. During the second half of the summer study (August and September) and during the fall study, the STI aircraft collected all of the aloft air quality data. Note that the STI aircraft was the only aircraft which provided vertical profiles of ozone and NO, NO_x. The UW aircraft reported NO, NO_x, b_{scat}, and ozone every

second. Much, and in some cases, all, of the NO and NO_x data during an orbit were flagged as 'bad' by UW. Consequently, the orbit-average NO and NO_x data that were available from UW were questionable since the average could consist of only a few minutes of data. For most of the orbits, the STI aircraft flew spirals near the same locations within two hours of the orbit. To evaluate the comparability of the UW orbit data and the STI spiral data, the air quality parameters for the UW orbit were matched to the same parameters from the nearest STI spiral location and altitude. Scatter plots were made and linear regressions were performed. Ozone and b_{scat} correlated fairly well considering the time differences (r^2 = 0.58 and 0.52, respectively). The NO and NO_2 data did not correlate well, which was not surprising due to the lack of valid UW NO_x data. Where the data matched within about one hour, we used the STI NO, NO_x data. For ozone or b_{scat} concentrations which corresponded to filter samples, the UW data were used.

Vertical profiles of light scattering were measured by the lidar aircraft and STI. The different measures of light scattering compared well and a detailed discussion of these data is given in Section 3.3.5. The STI b_{scat} data were used in most of our analyses, since these data were collected simultaneously with ozone and NO, NO_x data.

The particulate mass samples collected aloft were subject to some problems. First, the modified SCAQS sampler collection of $PM_{2.5}$ mass provided no way to estimate losses or gains. Thus, the aloft $PM_{2.5}$ mass values were not corrected. Second, most of the $PM_{2.5}$ mass samples collected by the UW aircraft (all June and July orbit samples) were marked invalid or suspect by the analytical laboratory because the filters looked "oily". We did not use any of the UW orbit mass data.

During the summer, most of the aircraft VOC samples were collected during orbits flown during the mornings and afternoons of the SCAQS intensive days. Hydrocarbon samples were collected in 3.2-liter stainless steel canisters, similar to the canisters used at the surface. However, unlike the surface samples which filled slowly over an hour, the aircraft samples were grab samples that were filled within one to two minutes. The two-minute fill time corresponds to approximately 7% of an orbit or 20% of a spiral. The aircraft canisters were analyzed using the same procedures as used for the surface canisters. Carbonyl compounds were collected during orbits using DNPH cartridges. Air was sampled through the cartridges at one liter per minute for 20 to 35 minutes. A few hydrocarbon samples were collected in spirals for which there were no matching carbonyl data. Samples were collected both on- and off-shore.

During the fall, the aircraft VOC samples were collected during spirals typically above and below the mixed layer at several spiral locations during the morning and afternoon flights. However, the carbonyl compounds were collected at only one altitude at two orbit locations during each flight. Because of the differences in altitude and location between the VOC and carbonyl samples, these data were not merged together.

Both the fall and summer VOC and carbonyl data were subjected to the same quality control (QC) procedures as the surface data. These procedures and the results for the summer data are described in Lurmann and Main (1992).

For the fall, VOC and carbonyl data were considered separately; only one carbonyl and six hydrocarbon samples were eliminated during QC. These samples are listed in Appendix A, Table A-2. All of the acetone data in the aloft fall samples were invalid because of contamination in the analytical laboratory.

2.3 DIFFERENCES BETWEEN ALOFT AND SURFACE MEASUREMENTS

The principal differences between the aloft and surface pollutant measurements were the following:

- Grab samples of C1-C12 VOC were collected in one to two minutes aloft, while surface samples were integrated over an hour. Thus, the aloft samples taken during spirals represent an average over about 300 m; an altitude range about comparable to the height of one modeling grid cell. On the other hand, the samples taken during orbits represent an average over about one-half of a circuit, out of a total of six to seven circuits per 30-minute orbit; this distance is comparable to the horizontal size of one modeling grid cell. But the aloft samples are all more of a 'snapshot' of the pollutant concentrations, rather than an integrated one-hour average for both the surface measurements and the model predictions.

- PAN and carbonyl species samples were collected over a 30-minute period aloft during orbits. At the surface, both PAN and carbonyls were averaged over one-hour periods. The same sampling and analysis methods were used for both the aloft and surface carbonyl samples; but a filter method was used for the collection of aloft PAN samples, while a gas chromatograph with electron capture detection was used for the surface samples. Since the time scales of the samples were similar, and orbits were performed in an area about the size of one modeling grid cell, aloft and surface PAN and carbonyl results are comparable.

- Only the fine aerosol particles, ≤ 2.5 μm, were collected aloft during orbits and samples were integrated over 30 minutes. Surface samples included both $PM_{2.5}$ and PM_{10} and were collected over four- to five-hour periods. Both aloft and surface particle mass measurements were subject to losses and gains of nitrogen-containing species: We were able to correct the surface samples, but not the aloft samples. Again, the aloft samples are more of a 'snapshot' than the surface samples.

- NO, NO_x, and ozone concentrations were reported in ppb units aloft and in pphm units at the surface. When concentrations are low (less than 25 ppb, for example), surface NO and NO_x concentrations are uncertain by as much as 50% just due to round-off; this could cause a significant difference between reported aloft and surface concentrations, even when no difference existed. This is less of a problem with ozone concentrations, since ozone concentrations are seldom less than 25 ppb.

2.4 SUPPLEMENTAL DATA AND INFORMATION

Table 2-4 lists the data, reports and papers which were used extensively in our analyses. Most of the supplemental data are available from the ARB or are in the open literature. Some of the data were prepared at our request; the following paragraphs briefly discuss these supplemental data.

Lidar Vertical Profiles - We reviewed the flight maps of each aircraft and identified the locations and times at which the lidar aircraft flew a traverse near an air quality aircraft spiral location. We then requested lidar data from Jim McElroy (EPA) if the flights were within ±2 hours and within ±20 km of each other. Additionally, we requested lidar data for times and locations for which there were no air quality aircraft data. In all, 78 lidar profiles were requested. Of these, 40 lidar profiles met the matching criteria, 32 summer and eight fall profiles. The lidar data were provided in 30 m bin averages, averaged from the surface (agl). Each lidar profile covered 1 km horizontally. These data are discussed in Section 3.3.5 and elsewhere in the report.

Forward and Backward Particle Trajectories - Douglas et al. (1991) analyzed wind data using the SAI Diagnostic Wind Model (DWM). One of the products of their analyses was the calculation of forward and backward particle trajectories to examine pollutant transport. At the request of the ARB, particle trajectories were determined five times per day for each intensive day for selected locations and altitudes. SAI calculated additional trajectories at our request based on our identification of aloft pollutant layers at various altitudes and locations in the SoCAB.

Hourly Wind Fields - Henry Hogo and his staff (SCAQMD) provided us with gridded hourly wind field output by the UAM for days during three SCAQS episodes: June 23-25, August 26-28, and December 9-11. Wind fields were available at 10, 100, 300, 600, and 1000 m agl. Douglas et al. (1991) also reported gridded wind field output by the DWM for four periods on each SCAQS day, at 10, 300, and 1000 m agl. These wind fields were used to estimate pollutant transport and to observe trends in the winds.

Mixing Height Estimates - SCAQMD provided the gridded hourly mixing heights from the UAM for the three SCAQS episodes listed above. In addition, Ted Smith (T.B. Smith and Associates) analyzed the aircraft and upper air soundings and provided estimates of mixing heights for each sounding (Appendix B). The mixing heights from the soundings are used throughout the report.

UAM Air Quality Output - SCAQMD provided the UAM output for ozone, NO, NO_x, and PAN for the June and August episodes. Aloft data for grid cells which matched air quality aircraft spirals were extracted for comparison with the air quality aircraft data (see Section 5).

2.5 MAJOR GAPS IN THE DATABASE

In general, the above discussion has focused on the data that are available for analyses. This discussion has demonstrated that the data collected during the SCAQS were extensive. However, there were some major

gaps in the database. Perhaps the most significant missing data were the lack of air quality aircraft data on the following dates and times:

July 15 midday and afternoon: all spirals;
August 27 morning: all spirals and orbits except Cable, El Monte, and AMTRA;
August 28 morning: spiral at Riverside;
August 28 midday and afternoon: all spirals and orbits;
August 29 morning, midday and afternoon: all spirals; and
September 3 afternoon: all spirals and orbits.

In addition, the lidar aircraft did not fly on the following SCAQS intensive days:

June 19 morning,
June 24,
August 27-29,
September 2-3,
November 11-12, and
December 11.

Finally, most of the $PM_{2.5}$ mass data collected by the UW aircraft were reported as either suspect or invalid.

Other gaps in the data are summarized in Table 2-5. Most of the data gaps were due to either equipment malfunction or the data being invalidated later during data review.

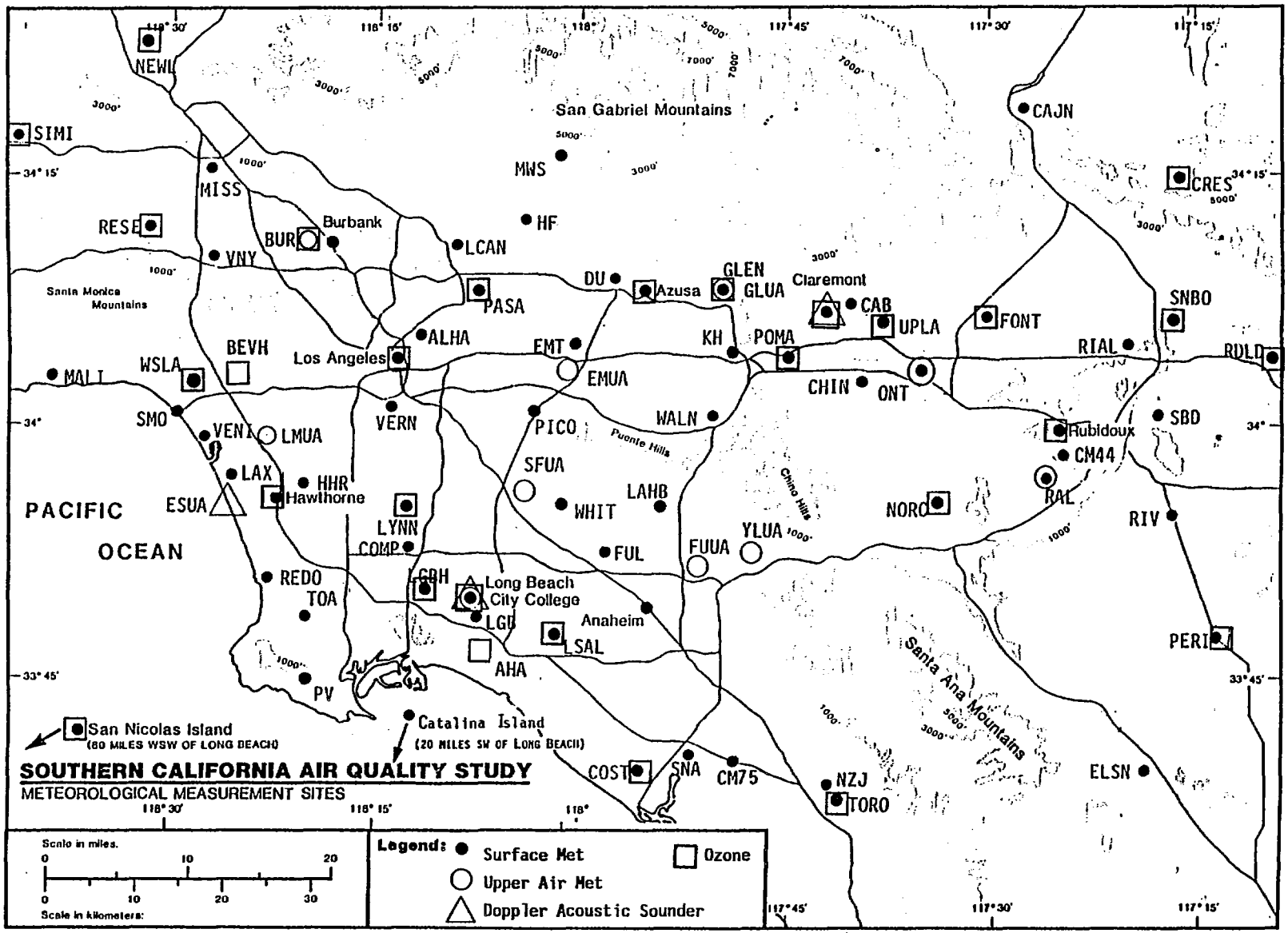

Figure 2-1. SCAQS Surface and Upper Air Meteorological and Surface Air Quality Measurement Locations. B-site names are spelled out. All sites are listed in Appendix A. (From Hering and Blumenthal, 1989.)

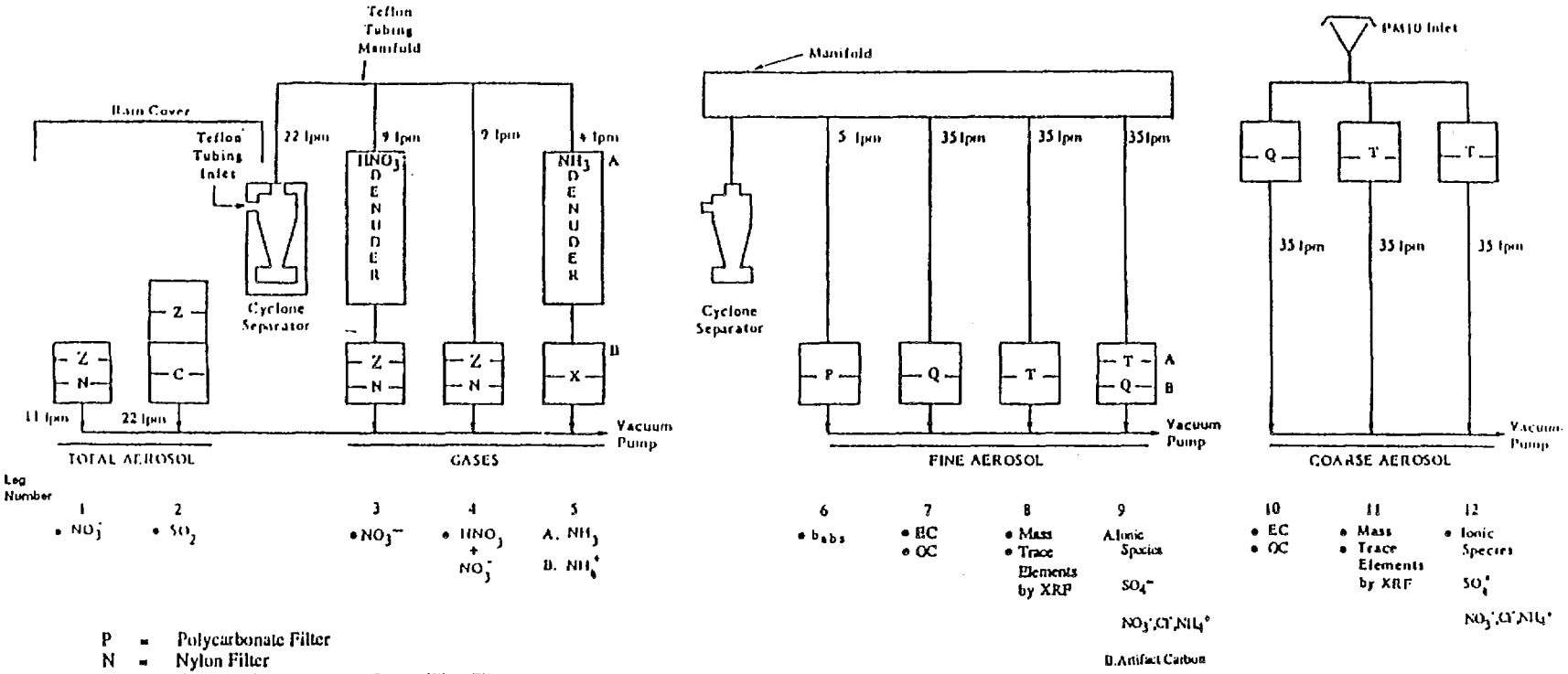

P = Polycarbonate Filter
N = Nylon Filter
X = Oxalic Acid Impregnated Quartz Fiber Filter
Q = Quartz Fiber Filter
T = (Teflo) Teflon Filter
C = Carbonate Impregnated Cellulose Filter
Z = (Zefluor) Teflon Filter

Figure 2-2. SCAQS Sampler Flow Diagram.

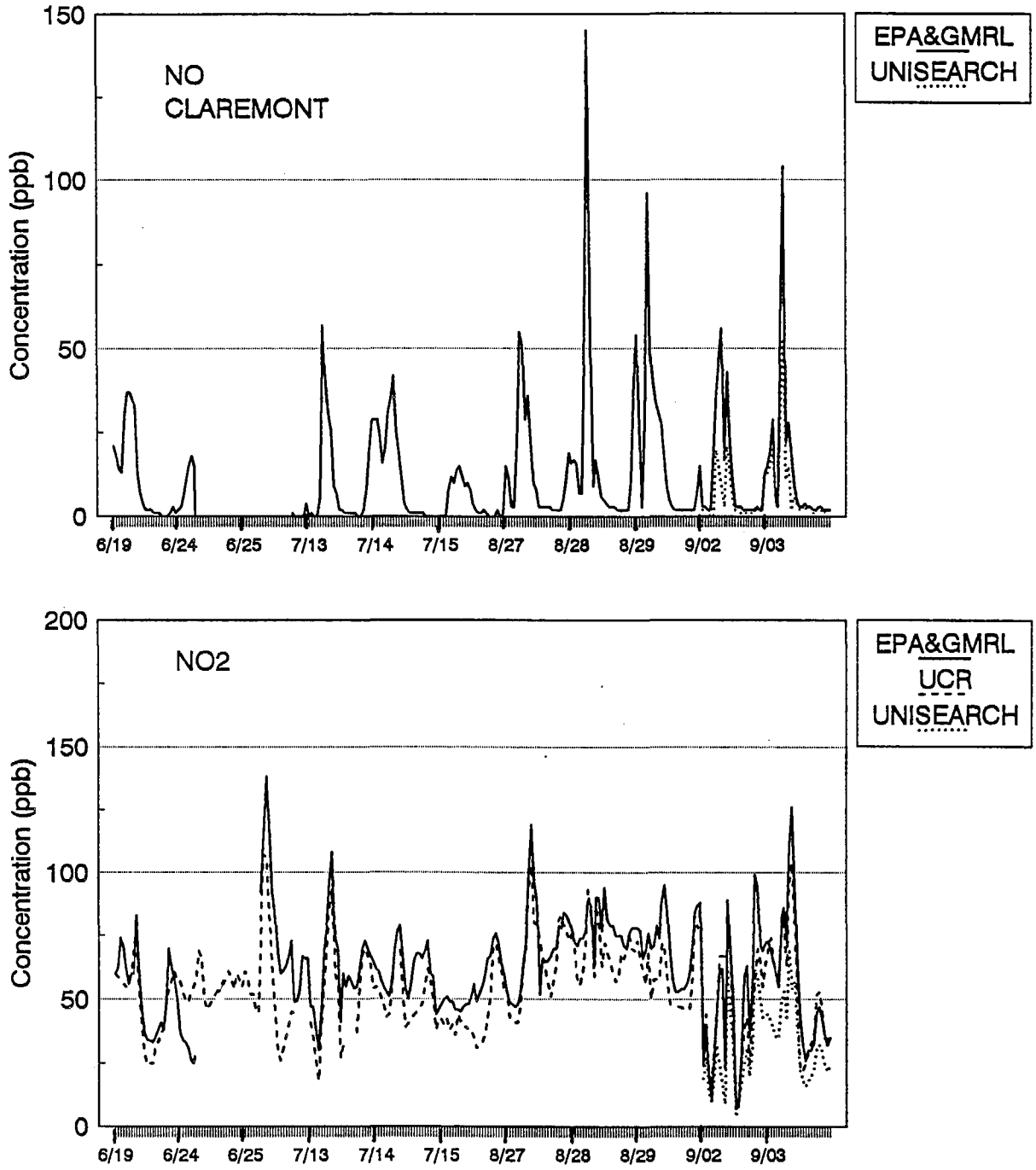

Figure 2-3. NO and NO_2 Measurements Made at Claremont During the Summer SCAQS by Different Investigators. Note Unisearch NO and NO_x data were only available in September.

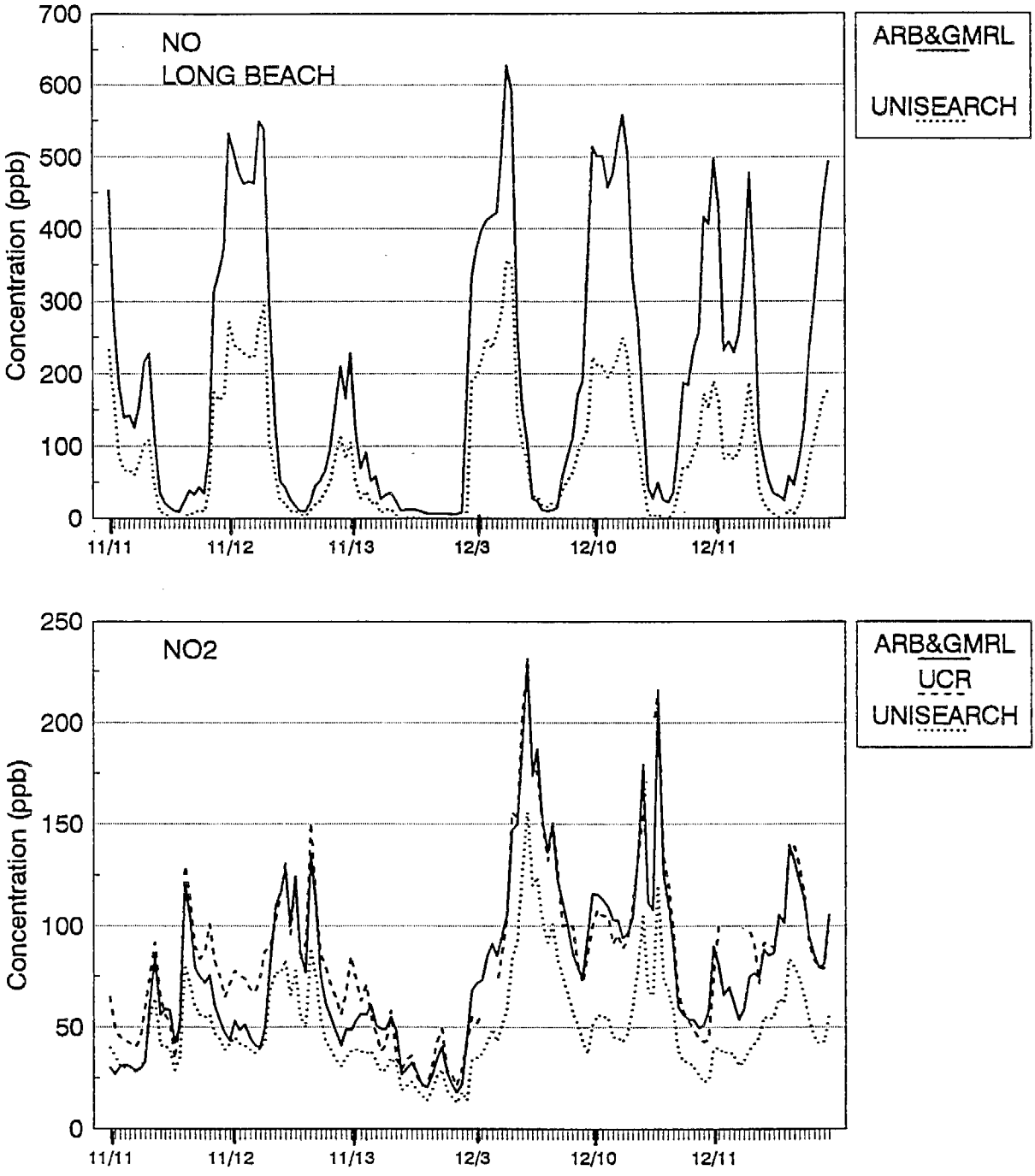

Figure 2-4. NO and NO_2 Measurements Made at Long Beach During the Fall SCAQS by Different Investigators.

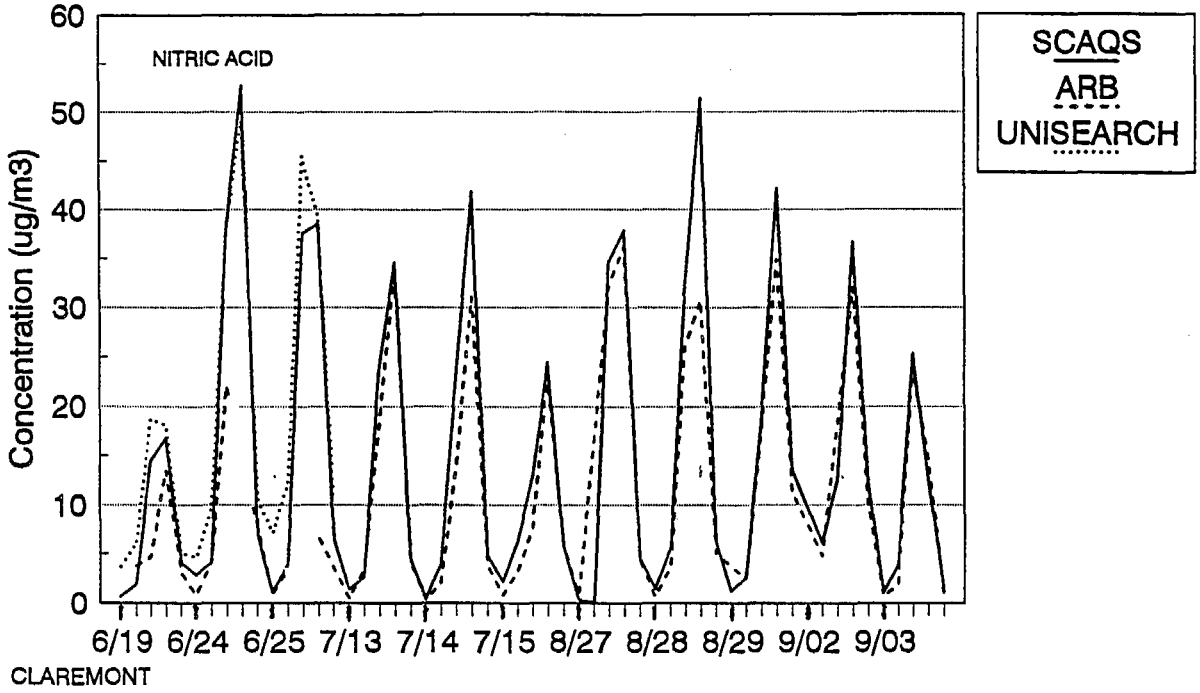

Figure 2-5. Nitric Acid Measurements Made at Claremont During the Summer SCAQS by Different Investigators. Note Unisearch nitric acid data were only available for June.

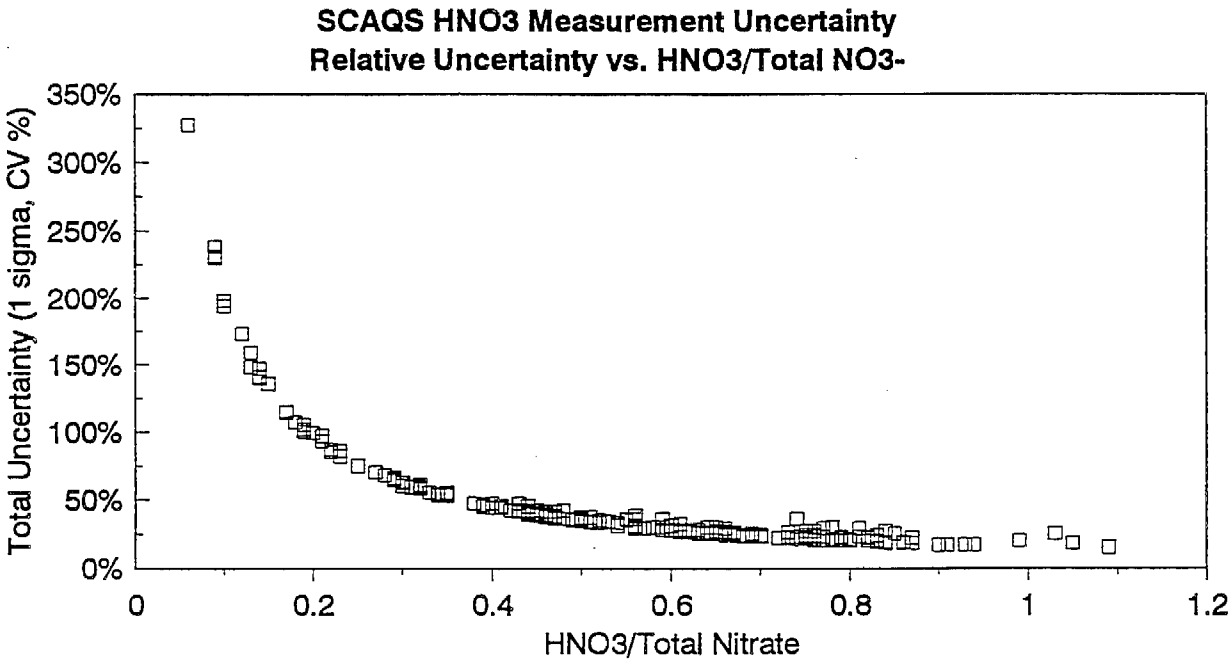

Figure 2-6. Measurement Uncertainty in SCAQS Nitric Acid Data Derived Using the Denuder Difference Method (from Fujita, 1992).

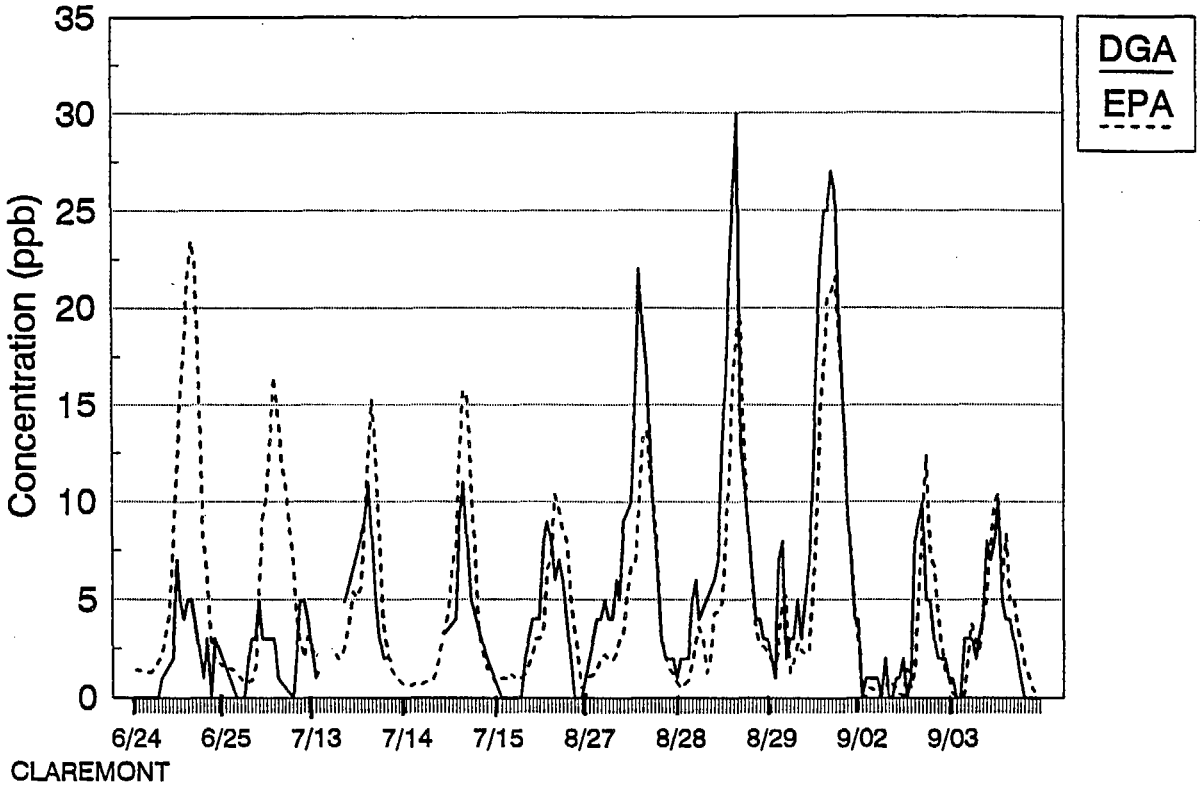

Figure 2-7. Comparison of PAN Concentrations Measured by the EPA and DGA at Claremont During the Summer SCAQS.

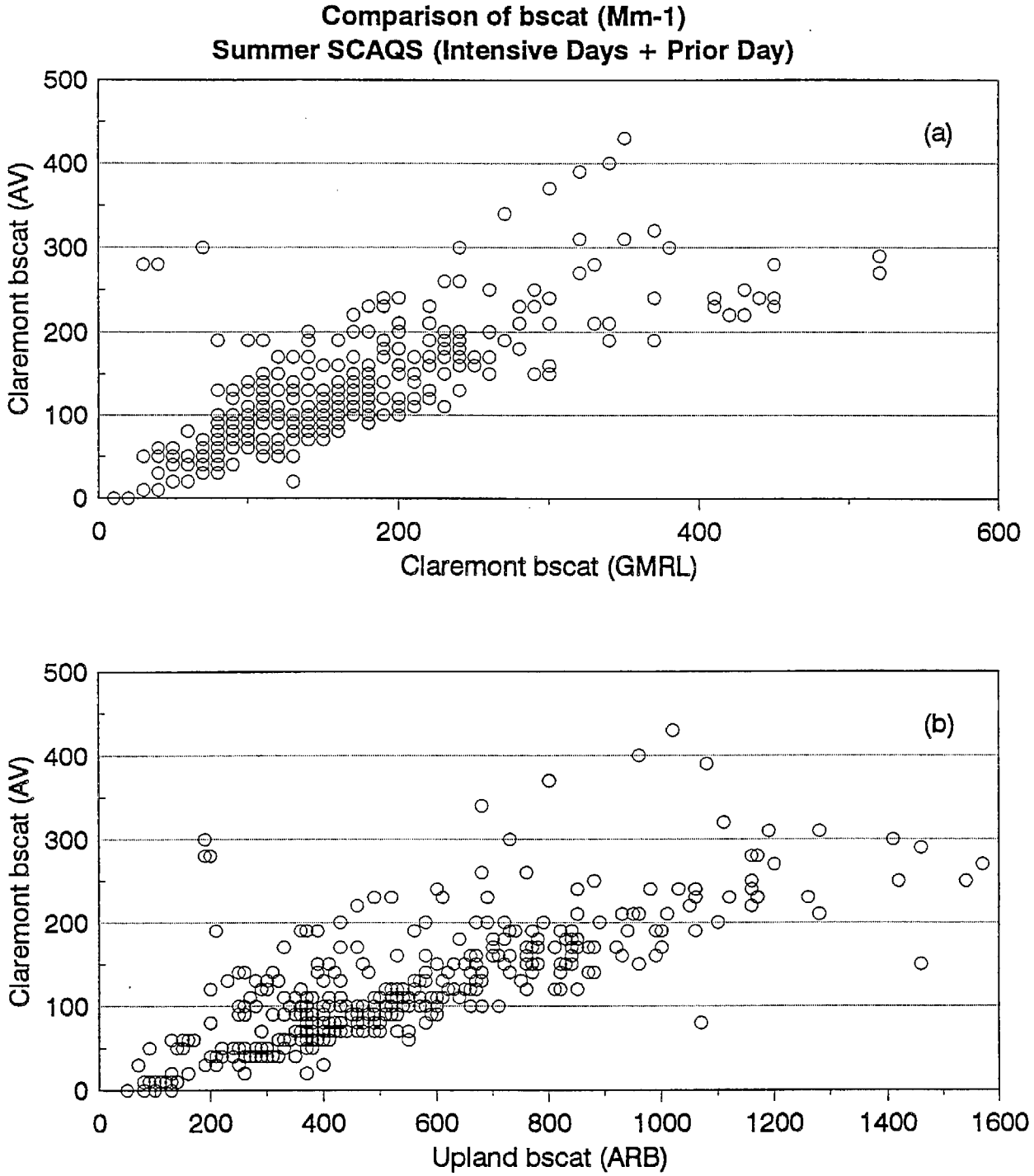

Figure 2-8. Comparison of Upland and Claremont b_{scat} During Summer SCAQS. a) Claremont AV and GMRL data (r^2=0.59), b) Claremont AV (r^2=0.54), and c) Claremont GMRL (r^2=0.80) and Upland data.

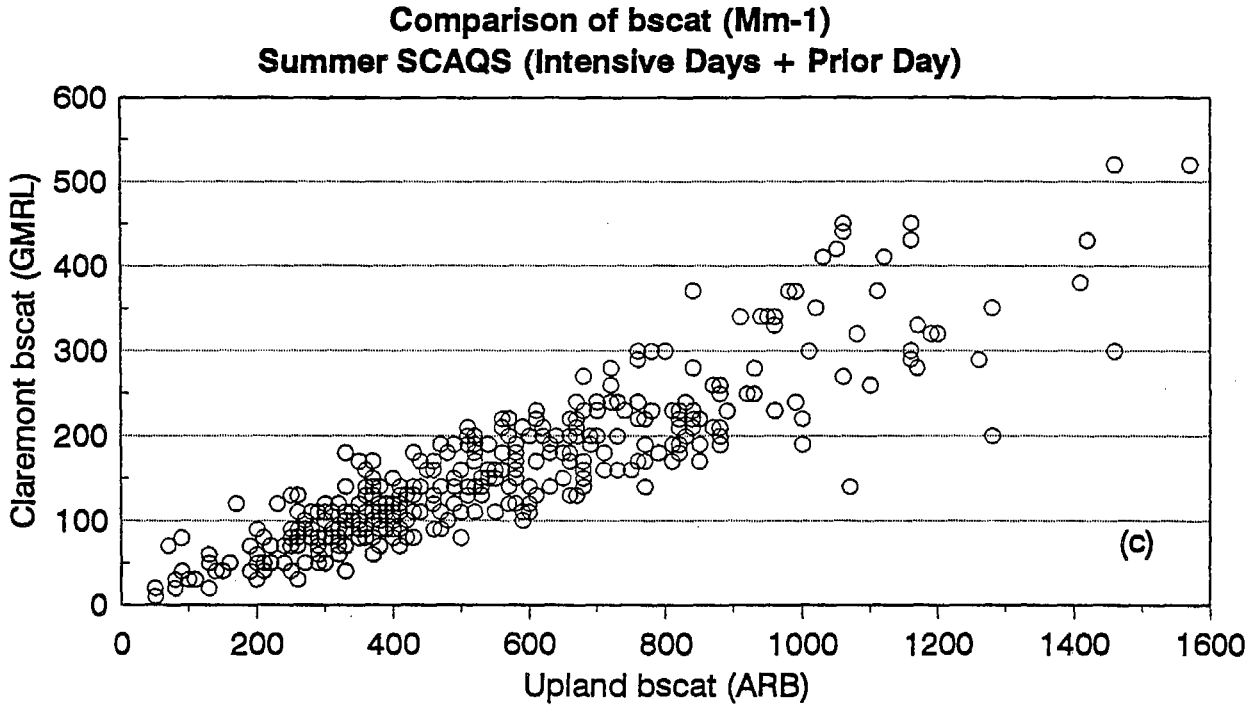

Figure 2-8. Comparison of Upland and Claremont b_{scat} During Summer SCAQS. a) Claremont AV and GMRL data (r^2=0.59), b) Claremont AV (r^2=0.54), and c) Claremont GMRL (r^2=0.80) and Upland data.

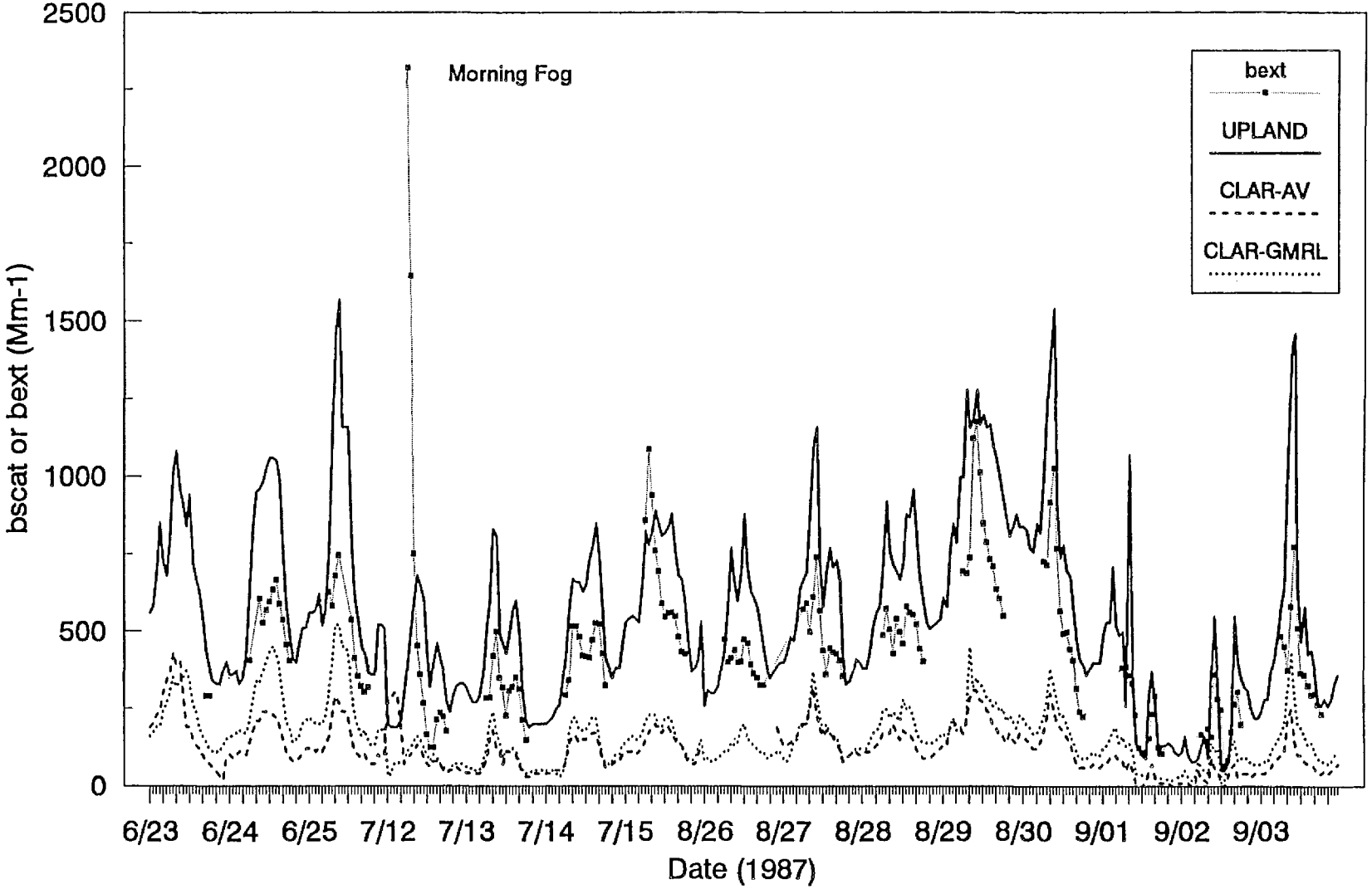

Figure 2-9. Time Series of b_{scat} and b_{ext} at Claremont and Upland During SCAQS.

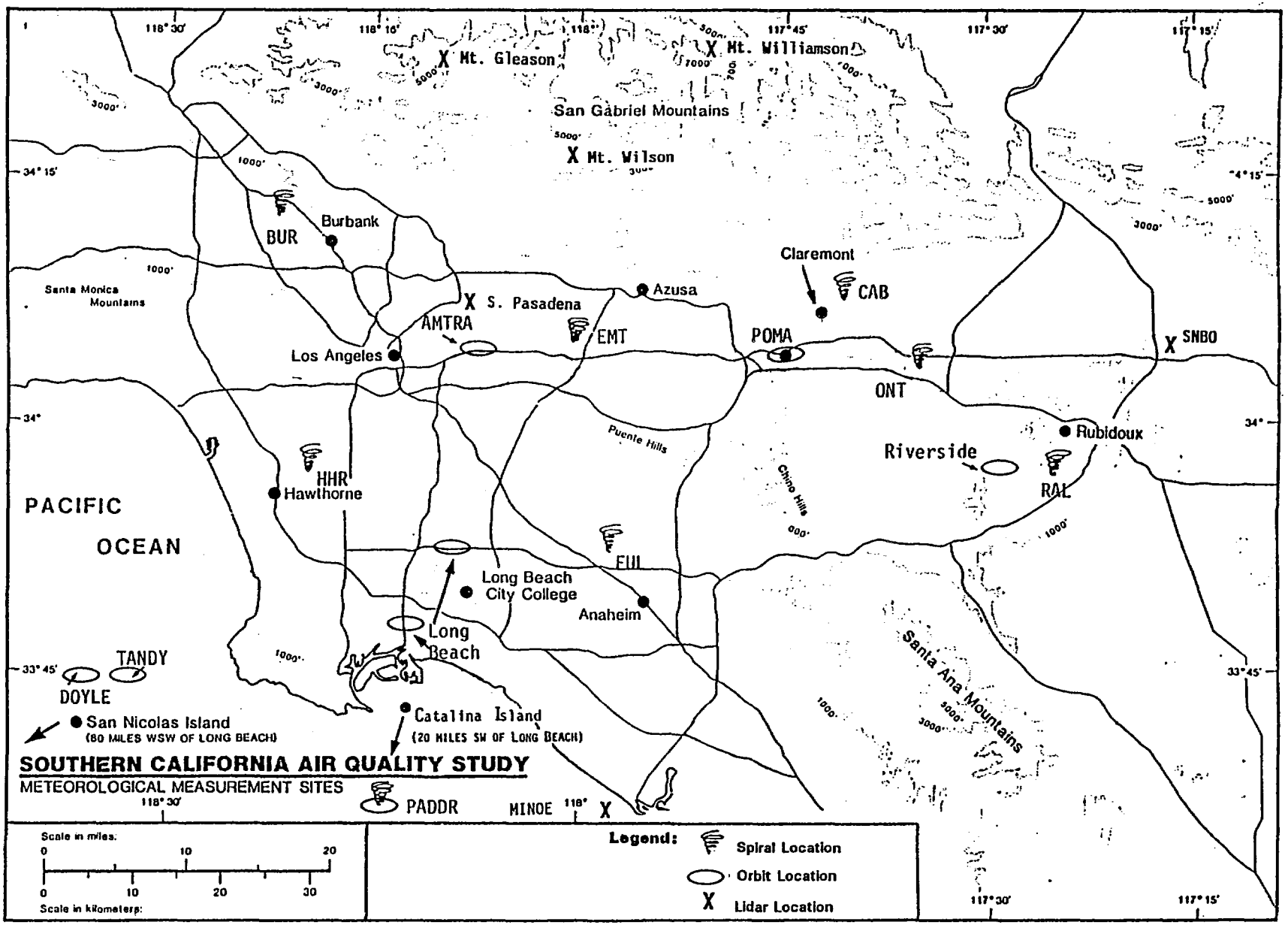

Figure 2-10. SCAQS Air Quality Aircraft Spiral and Orbit Points and Selected Lidar Traverse End Point Locations. (Site codes are listed in the List of Abbreviations and Terminology, p. xxiii) From Hering and Blumenthal (1989).

Table 2-1. Data Collected at the Surface During the SCAQS and Obtained From the California Air Resources Board for this Project. (See Hering and Blumenthal (1989) for additional details.)

Parameter(s)	Source	Units	Averaging Time	Samples per day	Reported Detection Limit	Notes (see Table 1-1 for abbrev.) (See Figure 2-2 for description of sampling legs L1 to L12)	Reported accuracy and precision or SCAQS Audit results
Ozone	SCAQMD	pphm	1-hr	24	10 ppb	Rounded to nearest whole pphm	Met SOP audit criteria. Criteria not given
Ozone	GMRL	ppb	1-hr	24	10 ppb	Compared to routine monitor data	Met SOP audit criteria. Criteria not given
bscat	SCAQMD	1/m	1-hr	24		Missing data from some sites	Met SOP audit criteria. Criteria not given
bscat	GMRL	1/m	1-hr	24		Used for comparison	
NO, NOx, NO2	SCAQMD	pphm	1-hr	24	10 ppb	Rounded to nearest whole pphm	15% precision, -6% audit
NO, NOx, NO2	GMRL (CLAR)	ppb	1-hr	24		Averaged with EPA or ARB Data	15% precision; NO2 low (up to 41%)
NO, NOx, NO2	EPA (CLAR)	ppb	1-hr	24	10 ppb	Averaged with GMRL Data	5% precision
NO, NOx, NO2	ARB (LBCC)	ppb	1-hr	24	10 ppb	Averaged with GMRL Data	
NO2	UCR	ppb	1-hr	24	4 ppb	Used when available	10% accuracy
NO2, NOx	Unisearch	ppb	1-hr	24	5 ppt	Luminox - used for comparison	
NO3-	EMSI	ug/m3	4-to6-hr	5	0.4 ug	Fine PM L3 denuded filter	Met SOP audit criteria. Criteria not given
NO3-	EMSI	ug/m3	4-to6-hr	5	0.4 ug	Coarse PM L1-L4 denuded filter	Met SOP audit criteria. Criteria not given
HNO3	SCAQS/EMSI	ppb	4-to6-hr	5		DDM (L4 - L3)	System losses <5%; large meas. uncertainty
HNO3	ARB	ppb	4-to6-hr	5		DDM	
HNO3	Unisearch	ppb	1-hr	24	0.15 ppb	TDLAS	
NH4+	EMSI	ug/m3	4-to6-hr	5	0.1 ug	Fine PM L5 denuded filter	System losses negligible, within 10% of reference
NH4+	EMSI	ug/m3	4-to6-hr	5	0.1 ug	Coarse PM L12 denuded filter	System losses negligible, within 10% of reference
NH3	EMSI	ppb	4-to6-hr	5	0.1 ug	Denuder (L5)	System losses negligible, within 10% of reference
PAN	DGA	ppb	1-hr	24		Poor quality June data	22% higher than EPA, +-50% @ 1ppb, 12% @ 10ppb
PAN	EPA (CLAR)	ppb	1-hr	24			Met SOP audit criteria. Criteria not given
HONO	UCR	ppb	1-hr	24	0.8 ppb	1-3 ppb summer, up to 15 ppb fall	30% accuracy
NMHC	EPA/OGI	ppbC	1-hr	3 to 6	0.2 ppb	See Lurmann and Main (1992)	Accuracy 10% > 5 ppb
Carbonyls	ENSR	ppb	1-hr	3 to 6	1-2 ppb	Summer LBCC carbonyls invalid	Accuracy 10%, precision 6%
OC	EMSI	ug/m3	4-to6-hr	5		Fine L7 corrected for organic vapor	
OC	EMSI	ug/m3	4-to6-hr	5		Coarse L10	
EC	EMSI	ug/m3	4-to6-hr	5		Fine L7	
EC	EMSI	ug/m3	4-to6-hr	5		Coarse L10	
Formic acid	DGA	ppb	4-to6-hr	5	0.4 ppb	Only LBCC, CLAR	Precision 5%, 0-25% accuracy
Acetic acid	DGA	ppb	4-to6-hr	5	0.6 ppb	Only LBCC, CLAR	Precision 5%, 0-25% accuracy
CO, CH4	OGI	ppb	1-hr	3 to 6	20 ppb	GC-FID	None
CO	SCAQMD	ppm	1-hr	24	500 ppb	Poor resolution (+-500 ppb)	Met SOP audit criteria. Criteria not given
Mass	EMSI	ug/m3	4-to6-hr	5		Fine (L8), Coarse (L11)	Met SOP audit criteria. Criteria not given
SO2	EMSI	ppb	4-to6-hr	5		L2	Within 4 - 10% of reference
SO2	SCAQMD	pphm	1-hr	24	10 ppb	Data rounded to nearest pphm	Met SOP audit criteria. Criteria not given
SO4=	EMSI	ug/m3	4-to6-hr	5	0.3 ug	Fine L9	Within 10% of reference
SO4=	EMSI	ug/m3	4-to6-hr	5	0.3 ug	Coarse L12	Within 10% of reference
temperature	SCAQMD	C	1-hr	24			Met SOP audit criteria. Criteria not given
wind speed	SCAQMD	m/s	1-hr	24			Met SOP audit criteria. Criteria not given
wind direction	SCAQMD	degrees	1-hr	24			Met SOP audit criteria. Criteria not given

SCAQS sampler sampling periods: 0000 PST, 0600, 1000, 1400, 1800 LT

Table 2-2. Average Net Loss of $PM_{2.5}$ and PM_{10} Mass Due to Volatilization and Absorption of Nitrogen-Containing Species

	Average Percent Loss to $PM_{2.5}$ Mass	Average Percent Loss to PM_{10} Mass
Summer		
GMRL Claremont	17	12
SCAQS Claremont	13	4
SCAQS All Sites	12	6
Fall		
GMRL Long Beach	8	6
SCAQS Long Beach	5	9
SCAQS All Sites	5	3

Table 2-3. Data Collected Aloft During the SCAQS Which Were Obtained From the California Air Resources Board for Use in This Study.

Parameter(s)	Source	Units	Where Collected	Notes (see Table 1-1 for abbrev.)	Reported accuracy and precision or SCAQS Audit results
Ozone	STI	ppb	Spirals, Orbits		Met SOP audit criteria. Criteria not given
Ozone	UW	ppb	Orbits		Incorrectly calibrated generator
NO, NOx, NO2	STI	ppb	Spirals, Orbits	For orbits, used closest spiral	Met SOP audit criteria. Criteria not given
NO, NOx, NO2	UW	ppb	Orbits	Used where necessary	Most data were invalidated by UW
Nitrate	EMSI	ug/m3	Orbits	Fine PM denuded filter	Met SOP audit criteria. Criteria not given
HNO3	EMSI	ppb	Orbits	Denuder Difference Method	System losses <=5%; large meas. uncertainty
NH4+	EMSI	ug/m3	Orbits	Fine PM denuded filter	System losses negligible, within 10% of reference
NH3	EMSI	ppb	Orbits	Denuder	System losses negligible, within 10% of reference
PAN	DGA	ppb	Orbits		
NMHC	EPA/OGI	ppbC	Spirals, Orbits	See Lurmann and Main (1992)	Accuracy 10% > 5 ppb
Carbonyls	ENSR	ppb	Spirals, Orbits	Fall acetone data invalid	Accuracy 10%, precision 6%
CO, CH4	OGI	ppb	Spirals, Orbits	See Lurmann and Main (1992)	
CO2	OGI	ppm	Spirals, Orbits	See Lurmann and Main (1992)	
OC	EMSI	ug/m3	Orbits	Fine PM	Met SOP audit criteria. Criteria not given
EC	EMSI	ug/m3	Orbits	Fine PM	Met SOP audit criteria. Criteria not given
Mass	EMSI	ug/m3	Orgbits	Fine; most UW data invalid	Met SOP audit criteria. Criteria not given
SO2	EMSI	ppb	Orbits		Within 4 - 10% of reference
SO2	STI	ppb	Spirals, Orbits		Met SOP audit criteria. Criteria not given
SO4=	EMSI	ug/m3	Orbits	Fine PM	Within 10% of reference
Turbulence	STI		Spirals, Orbits		Met SOP audit criteria. Criteria not given
Temperature	STI	C	Spirals, Orbits		Met SOP audit criteria. Criteria not given
Temp., dp	T&B	C	Upper Air Sites		Not available
Wind Speed	T&B	m/s	Upper Air Sites		Not available
Wind Direction	T&B	degrees	Upper Air Sites		Not available
Pressure	T&B	mb	Upper Air Sites		Not available

Table 2-4. Supplemental Data, Papers, and Reports Used in Three-Dimensional Analysis

Data	Source	Author(s)
Lidar gray-scale plots along flight transects	USEPA[1]	McElroy
Lidar data for selected portions of flights (magnetic media)	USEPA	McElroy
Forward and backward parcel trajectories for selected sites and times on SCAQS intensive days (plots and magnetic media)	SAI	Douglas
Hourly gridded wind fields for June 23-25, August 26-28, and December 9-11. UAM output for 10, 100, 300, 600, and 1000 m agl.	SCAQMD	Hogo
Hourly gridded mixing heights - UAM output.	SCAQMD	Hogo
Gridded emissions inventories	SCAQMD/ARB	Hogo/Technical Services
UAM air quality output	SCAQMD	Hogo
Air quality aircraft soundings (data volume and magnetic media)	STI[1]	Anderson
Upper air soundings (data volume plots)	T&B	Lehrman
Upper air soundings (magnetic media)	T&B[1]	Lehrman
UW aircraft air quality (magnetic media)	UW[1]	Hegg and Hobbs
QC'd VOC data (surface and aloft)	STI[1]	Lurmann and Main (1992)

Reports	Source	Author(s)
Gridded wind fields four hours per day, all SCAQS intensive days, 10, 300, and 1000 m agl.	SAI[1]	Douglas et al. (1991)
STI air quality aircraft final report	STI[1]	Anderson et al. (1989)
Atmospheric tracer data analysis final report	Cal Tech[1]	Horrell et al. (1989, 1991)
UW air quality aircraft final report	UW[1]	Hegg and Hobbs (1988)
Aerosol Data Management final report	STI[1]	Hering (1990b)
SCAQS Sampler Data Plots	STI[1]	Hering (1990a)
VOC analysis final report	STI[1]	Lurmann and Main (1992)
SCE Tracer Study	Tracer Tech[1]	Teuscher (1989)
Photochemical Modeling	SCAQMD, ARB	
Mixing Height Analysis	SCE	Smith et al. (1990)

Papers	Source	Author(s)
Carbonyl observations	ENSR	Fung (1989)
Formic and Acetic Acid Measurements	DGA	Grosjean (1990)
Peroxyacetylnitrate (PAN)	DGA	Williams and Grosjean (1990)
Differential Optical Absorption Spectroscopy Measurements of Gaseous Pollutants	UCR	Winer et al. (1989)
PM_{10} Species Analysis	GMRL	Wolff et al. (1991)
Tunable Diode Laser Absorption Spectroscopy and Luminox Technology for gaseous pollutants	Unisearch	Drummond et al. (1989)
Meteorological and Photochemical Modeling	SCAQMD, ARB	Wheeler (1990, 1991a, 1991b)
Ozone layers aloft		McElroy and Smith (1992)
Tracers-of-Opportunity		Bastable et al. (1990)

[1] Available from the California Air Resources Board

Table 2-5. Surface and Aloft Meteorological and Air Quality Data Which Were Missing or Invalid

Upper Air Soundings - Temperature, Dew Point and Winds (LT)[a]:		
	June 19	El Monte (1100), Long Beach (0500, 1100)
	June 25	Long Beach (1100, 1400)
	August 28	El Monte (1100), Ontario (1100), Riverside (1400)
	August 29	Loyola (1400)
	September 3	El Monte (0500)
	December 3	Long Beach (0500)
Air Quality Aircraft[b]:		
Ozone:		
	June 24	Midday Cable spiral
	August 27	Afternoon all spirals except Cable
	November 11	Morning Ontario spiral
b_{scat}:		
	June 24	Midday Cable spiral
	August 27	Morning all spirals
NO/NO_x:		
	June 24	Morning all spirals
	June, July	Orbit data collected by UW was invalidated.
	August 27	Morning all spirals
Orbit Filters:	June 19	All morning
	June 24	All afternoon
	July 13	All afternoon
	August 27	Morning and afternoon AMTRA orbits
$PM_{2.5}$ mass:		
	June 19	Afternoon Long Beach, Pomona, Riverside orbits
	June 24	Morning AMTRA, PADDR, orbits
	June 25	All morning orbits
		Afternoon Long Beach, Pomona, Riverside orbits
	July 13	Morning AMTRA, DOYLE, PADDR orbits
	July 14	Morning AMTRA, DOYLE, Long Beach orbits
		All afternoon orbits
	July 15	Morning DOYLE orbit
		Afternoon AMTRA, Long Beach, Pomona Orbits
	August 27	Morning and afternoon AMTRA orbit
	November 13	Morning Seal Beach orbit

[a] Site locations shown in Figure 2-1.

[b] Site locations shown in Figure 2-2.

Table 2-5. Surface and Aloft Meteorological and Air Quality Data Which Were Missing or Invalid

PAN:

July 14	Morning Doyle orbit

SO_2:

June 24	Midday Cable spiral
August 27	Afternoon Fullerton spiral
September 2	Afternoon all spirals
November 12	Midday all spirals
June 24	Morning orbits
June 25	Afternoon orbits

Surface b_{scat} (entire day missing or invalid)[a]:

June, July & August	Azusa
Summer & Fall	Rubidoux and Burbank
December 3	Upland

Surface PAN data (entire day missing or invalid)[a]:

June 19	Burbank, Claremont, Los Angeles, Long Beach, Rubidoux
July 13-15	Los Angeles
June 24	Long Beach
All Summer	Hawthorne
All Fall	Rubidoux

Surface Winds (entire day missing)[a]:

June 19	El Rio, Henniger Flats, Kellogg Hill, Walnut
June 24	Walnut, Temescal, Tanbark
June 25	Walnut
July 13-15	Piru
August 27-29	Piru, Kellogg Hill, Blythe, Anacapa
September 2-3	Anacapa, Barstow, Blythe, Piru
November 11	El Rio, Blythe, Warm Springs
November 12	El Rio, Blythe, Warm Springs
November 13	El Rio, Blythe, Anacapa
December 3	El Rio, Barstow
December 10-11	El Rio

Surface Ozone (entire day missing)[a]:

Summer & Fall	Beverly Hills
August 27, 28	Los Alamitos
August 29	Barstow
September 2	Banning

[a] Site locations shown in Figure 2-1.

[b] Site locations shown in Figure 2-2.

Table 2-5. Surface and Aloft Meteorological and Air Quality Data Which Were Missing or Invalid

Surface NO,NO_x (entire day missing)[a]:

June 25	Claremont
September 2-3	Glendora

Surface SCAQS Sampler (missing 3 or more periods)[a]:

Nitric Acid:		
	December 3	Anaheim, Rubidoux
PM_{10} mass:		
	July 15	San Nicolas Island
	August 27	Hawthorne
	September 2	Azusa, Rubidoux
$PM_{2.5}$ mass:		
	July 14-15	San Nicolas Island
	August 27	Hawthorne
	September 2-3	San Nicolas Island
Ammonia:		
	July 14-15	San Nicolas Island
	August 27	Azusa
Fine NH_4^+:		
	July 14-15	San Nicolas Island
	August 28	San Nicolas Island
	September 3	San Nicolas Island
	August 27	Los Angeles
Fine NO_3^-		
	June 19	Azusa, Los Angeles
	July 15	San Nicolas Island
SO_2:		
	July 14	San Nicolas Island
	November 11	Hawthorne
	November 12	Hawthorne, Los Angeles
	November 13	Los Angeles
	December 3	Burbank, Los Angeles, Hawthorne
	December 10	Hawthorne, Los Angeles
	December 11	Los Angeles

[a] Site locations shown in Figure 2-1.

[b] Site locations shown in Figure 2-2.

3. CASE STUDY: JUNE 24 - 25, 1987

Ozone concentrations on June 24-25, 1987 exceeded the State standard at 22 and 17 sites, respectively; high PM_{10} concentrations were also measured at many sites. This episode has been widely studied, partly because it consisted of two days that were remarkably similar in meteorology, and in PM_{10} and ozone impact. During the SCAQS, many pollutants were measured at surface monitoring sites and aloft using aircraft. A summary of where and when these measurements were made and the data available was presented in Section 2. This section begins with a summary description of the meteorology during the June 24-25 episode and continues with a description of pollutant concentrations at both surface monitoring sites and aloft; including spatial and temporal concentration patterns, vertical profiles of pollutants aloft, and comparisons of pollutant concentrations at the surface and aloft. A comparison of ozone concentrations measured during aircraft spirals with aloft ozone concentrations generated in model simulations is also included.

3.1 EPISODE METEOROLOGY

The meteorology during the SCAQS has been well-described elsewhere (e.g. Surface winds - Zeldin et al., 1989; Aloft winds - Douglas et al., 1991 and SCAQMD, 1990). The following paragraphs summarize the meteorology during the June 24-25, 1987 episode.

3.1.1 Synoptic Meteorology

The June 24-25 episode was characteristic of a classic late spring/early summer episode with a strong inversion, low-level stratus clouds, and a strong onshore flow with transport to the high and low deserts. A high pressure aloft centered over southern New Mexico began to spread north and west on June 23; it was over southern California on June 24. By June 25, the ridge had spread to southern Washington. The development of the ridge as it spread west was sufficient to intensify the strength of the inversion over southern California, but upper level flow remained southerly during the course of the episode keeping the inversion elevated. Gradients and station pressures were very similar on both days of this episode.

3.1.2 Summary of Daily Meteorology

Figures 3-1 and 3-2 show surface streamline analyses prepared by Zeldin et al. (1989) for June 24 and 25, 1987. Plots are shown for 0700, 1200, and 1700 PDT to illustrate the morning stagnation or drainage wind conditions, early stages of the sea breeze, and the well-developed sea breeze. The surface streamlines were nearly identical on the two days.

June 24. Coastal clouds and stratus were evident on each day, existing into the morning and then burning off to haze. Surface winds were light across the basin with numerous local swirls or eddies. Generally southerly flow occurred along the Orange County coastal region with westerly flow along the coast north of Palos Verdes. Southerly flow dominated the central Los Angeles area. Aloft winds were light.

By 1200 PDT on June 24, surface winds across much of the basin were south-westerly, reaching a depth of about 300 meters msl. South-easterly flow in the Coachella Valley and easterly flow through the Banning Pass were apparent both at the surface and 300 m agl. Southerly to south-easterly flow dominated at 1000 m agl. In the afternoon, south-westerly flow dominated the basin with westerly winds in the eastern basin and upslope flow developed along the foothills. The wind shifted to westerly at Banning Pass by 1600 PDT. Winds aloft were south-easterly over much of the basin; at 1000 meters, winds were south-westerly.

June 25. On the morning of June 25, surface winds were similar to June 24 with light winds across the basin with numerous local swirls or eddies. Generally southerly flow occurred along the Orange County coastal region with westerly flow along the coast north of Palos Verdes. Easterly flow was observed across the central Los Angeles area. Weak south-easterly flow was apparent at 300 m agl. At 1000 meters agl, winds were southerly. The sea breeze developed more quickly on this day than on the previous day.

The vertical temperature structure exhibited a well-mixed marine environment capped by an elevated inversion hovering at about 500 m agl. As on June 24, by 1200 PDT, surface winds across most of the basin were south-westerly. In the afternoon, the winds were nearly identical to June 24. Upslope flow developed along the foothills. The wind shifted to westerly at the Banning Pass by 1400 PDT (two hours earlier than June 24). South-westerly flow dominated the basin with westerly winds in the eastern basin. Airflow at 300 m agl was south-westerly over the basin, and south-easterly at Burbank and over the Coachella Valley. Winds at 1000 m agl were southerly to south-easterly. Upward propagation of westerly flow was slower than on the previous day.

3.1.3 Mixing Heights

Figures 3-3 and 3-4 show the mixing heights as determined from surface-based soundings and aircraft spirals for June 24-25 by T.B. Smith (T.B. Smith and Associates). The mixing height at coastal and some mid-basin stations generally ranged from 300 to 600 m msl and did not exhibit much diurnal variation. In the mid- and eastern-basin, the mixing height ranged from 800 to 1000 m msl in the afternoon and fell to about 400 m msl at night. The mixing heights determined from aircraft spirals matched the nearby surface-based meteorological soundings very well, except the PADDR spirals were flown over the ocean and thus were dominated by the marine environment. The Fullerton spiral was several kilometers from the Yorba Linda and Santa Fe Springs soundings; this comparison demonstrates that there is some spatial variation in mixing heights.

3.2 DIURNAL POLLUTANT PROFILES AT THE SURFACE

3.2.1 Ozone, NO, and NO_2

On June 24, SoCAB maximum ozone concentrations occurred at Glendora, Claremont, San Bernardino, and Redlands (23 to 25 pphm). On June 25, the

maximum surface ozone concentrations occurred at Glendora, Fontana, San Bernardino, and Redlands (22 to 24 pphm).

Figures 3-5 and 3-6 show the diurnal profiles of ozone at the eight summer SCAQS surface B-sites. Ozone concentrations at Hawthorne, Anaheim, and Long Beach were the lowest, while ozone concentrations at Claremont, Azusa, and Rubidoux were the highest. At night, ozone concentrations dropped to nearly zero at most sites except Hawthorne and Long Beach.

The diurnal profiles of NO and NO_2 are shown in Figures 3-7 and 3-8 for the same sites. NO concentrations typically peaked in the early morning when traffic emissions were high and mixing heights were low. The highest NO concentrations were observed at Rubidoux. NO_2 concentrations were typically highest after the NO peak (oxidation of fresh NO). NO_2 concentrations remained relatively high, 4 to 11 pphm, throughout the episode at Azusa, Burbank, and Los Angeles. NO_2 concentrations at the western-basin sites were typically less than half these levels. The relatively high NO_2 concentrations observed in the afternoon were probably due to both transported pollutants and the oxidation of fresh (local) emissions.

3.2.2 Particulate and Gaseous Species

Figures 3-9 to 3-21 show the diurnal profiles of the gaseous and particulate pollutants measured at the eight surface B-sites during the June episode. The plots show PM_{10} mass and $PM_{2.5}$ mass and species concentrations for the most abundant $PM_{2.5}$ species; and formic, acetic, and nitric acids. One-hour averages for PAN and NMOC are also provided. Observations from these figures include the following:

- On June 24-25, PAN data (Figure 3-9) were only available at Claremont. PAN peaked at about the same time as ozone. Peak concentrations were 23 and 16 ppb on June 24 and 25, respectively.

- Morning peaks in PM_{10} and $PM_{2.5}$ mass (Figures 3-10, 3-11) were observed at Anaheim and Hawthorne. Peak concentrations occurred midday or in the afternoon at Azusa, Burbank, Claremont, and Rubidoux, indicating photochemical activity and transport. PM_{10} and $PM_{2.5}$ mass concentrations were highest at Rubidoux on both days; PM_{10} mass concentrations also were high at Azusa. The lowest concentrations were observed at Long Beach and Anaheim, where the diurnal variations in particulate mass concentrations were small.

- Nitric acid concentrations (Figures 3-12, 3-13) were highest at Azusa, Burbank, Claremont, and Los Angeles. Sites east of Los Angeles had peak concentrations in the afternoon, while Los Angeles and sites to the west had peak concentrations midday. Peak concentrations at Long Beach, Anaheim, and Rubidoux were low, below 5 ppb.

- $PM_{2.5}$ nitrate ion concentrations (Figures 3-12, 3-13) were highest at Rubidoux and at Hawthorne on June 25, with relatively high concentrations also observed at Azusa, Claremont, and Burbank. At Hawthorne, nitrate ion peak concentrations occurred in the afternoon, while at Rubidoux, peak nitrate ion concentrations occurred during the

night. At the other sites, the timing of peak nitrate ion concentrations varied.

- Ammonia concentrations (Figures 3-14, 3-15) were generally below 3 ppb at all sites except Rubidoux, where peak concentrations were up to 90 ppb. Peak ammonia concentrations occurred during the day.

- Ammonium ion concentrations (Figures 3-14, 3-15) were highest at Rubidoux. The Long Beach and Anaheim ammonium ion concentrations were lowest, with little temporal change (similar to PM_{10}). Ammonium ion concentrations at Azusa, Claremont, Los Angeles, and Burbank were similar and peak concentrations occurred midday. Hawthorne had low concentrations of ammonium ion, with peak concentrations occurring in the morning. At Rubidoux, the nitrate ion concentration peaks and valleys were opposite timing of the ammonia and ammonium ion peaks and valleys; peak ammonia and ammonium ion concentrations occurred midday.

- The highest organic carbon (OC) concentrations (Figures 3-16, 3-17) were measured at Azusa, Burbank, Los Angeles, and Claremont. Rubidoux OC concentrations were also relatively high. OC concentrations at Long Beach, Hawthorne, and Anaheim were low and varied little during the episode. At the central- and eastern-basin sites, OC concentrations peaked midday, corresponding to the peak ozone, PAN, and nitric acid concentration peaks.

- Elemental carbon (EC) concentrations (Figures 3-16, 3-17) were about an order of magnitude lower than OC concentrations. Concentrations were about the same at the central- and eastern-basin sites. The timing of peak concentrations at these sites varied: EC concentrations peaked in the morning at Los Angeles and Burbank; while EC concentrations peaked in the afternoon at Claremont and Azusa. The coastal sites and Anaheim had the lowest concentrations and showed little change with time of day. Rubidoux EC concentrations also did not change substantially with time of day.

- SO_2 concentrations (Figures 3-18, 3-19) were highest at Hawthorne and Azusa during the daytime. SO_2 concentrations were below 3 ppb at the other sites. SO_2 and sulfate ion concentrations went up and down together at Azusa, Burbank, Claremont, Hawthorne, and Los Angeles.

- Sulfate ion concentrations (Figures 3-18, 3-19) were highest at Hawthorne, Burbank, Azusa, and Los Angeles with peak concentrations occurring in the morning at Hawthorne, midday at Los Angeles, and afternoon at Azusa and Burbank. The lowest concentrations were observed at Anaheim, Long Beach, and Rubidoux. Sulfate ions were present mostly in the fine aerosol, which is consistent with emissions and formation mechanisms.

- Formic and acetic acids (Figure 3-20) were significantly more abundant at Claremont than at Long Beach. Concentrations of both species peaked midday at Claremont.

- NMOC concentrations (Figure 3-21) were similar on both days. Concentrations were highest at Los Angeles and Burbank and lowest at coastal sites and Rubidoux. NMOC concentrations varied with time of day.

3.3 VERTICAL POLLUTANT PROFILES

The air quality aircraft typically flew three flights daily during the summer: early morning, midday, and afternoon. However, on June 24 the midday flight was about three hours later and the afternoon flight was about two hours later than the flights on June 25. Measurements were described in Section 2 and spiral and orbit locations were shown in Figure 2-10.

Vertical profiles of ozone, b_{scat}, NO, and NO_x by site, date, and time of day are shown in Figures 3-22 to 3-35. In these plots the continuous data, which were collected every second (about every 3 meters) during each spiral, were averaged into 30 meter vertical bins. Data are plotted versus altitude in meters above mean sea level (m msl). During each time period, the pollutant profiles showed similar shapes, as a function of altitude, across the basin. Observations from these figures include the following:

Morning:

- Relatively high b_{scat} levels and NO, NO_x concentrations were observed in the surface layer on both days (see Figures 3-30 to 3-33, for example). Ozone concentrations were low at these altitudes, probably because of titration by fresh NO emissions.

- On June 24, above the mixed layer, there were two layers with high pollutant levels. The topmost layer was observed at about 1100 to 1300 m msl over the eastern basin, above the top of the previous day's inversion. At Cable, elevated levels of both ozone and b_{scat} were present in the layer, although b_{scat} levels were relatively low. At El Monte and Rubidoux, this layer contained relatively high ozone concentrations (130 to 150 ppb) but low b_{scat} levels. This top layer appears to be aged and may have been injected above the inversion layer by upslope flow the day before. Ozone concentrations in a layer between 700 to 900 m msl were as high as 250 ppb; this layer was observed at all spiral locations. At the western and offshore spiral locations, low pollutant levels were observed above about 900 m msl (top of the inversion).

- On June 25, three layers of ozone and b_{scat} were apparent above the surface layer at Burbank, Rubidoux, El Monte, and Cable. The topmost layer was at about 1000-1200 m msl (typically above the top of the previous day's inversion) and contained moderately high ozone and b_{scat} levels. A separate layer just below the top layer contained similar or higher pollutant levels. The third layer was just above the surface layer. Ozone concentrations aloft on the morning of June 25 were higher than on June 24. On June 25, concentrations above 1000 m msl at offshore and western basin spiral locations, and above 1200 m msl at central and eastern basin locations, were similar to those on June 24.

Ozone and b_{scat} values were significantly higher between 1000 and 1200 m msl on June 25 than on June 24.

Midday and afternoon:

- On both days at midday, below about 750 m msl, ozone concentrations were higher than in the morning. The same trend was observed in the b_{scat} data except at Fullerton, Hawthorne, and Riverside, where morning b_{scat} levels were the same or somewhat greater than the midday levels. Above this layer, midday pollutant levels were similar to morning levels. Midday pollutant profiles were very similar to afternoon profiles.

- In the afternoon, below about 500 m msl, ozone concentrations and b_{scat} levels were reduced by the sea breeze influence at all onshore sites except Cable. Above 500 m msl, ozone and b_{scat} levels were similar to or higher than earlier in the day. The sea breeze appeared to undercut the original mixed layer of pollutants. This phenomenon was observed at the western and central basin sites and as far east as Riverside (b_{scat} reduction). The marine layer did not reach Cable since its depth was only about 450 m msl at this time.

- Above the surface layer, two pollutant layers (with elevated levels of both b_{scat} and ozone) were observed over El Monte, Cable, Burbank, and Riverside. The top layer may be due to slope flow. At El Monte, this top layer had very similar b_{scat} and ozone levels to the layer below it. At slightly different altitudes, two to three layers with high b_{scat} and ozone were also observed between 400 and 900 m msl over PADDR, Fullerton, and Hawthorne (approximately between the marine layer and the top of the inversion).

- On June 25 in the afternoon mixed layer, ozone concentrations and b_{scat} levels were significantly different from midday (except at PADDR and Fullerton). Rubidoux ozone concentrations and b_{scat} levels were lower than earlier in the day; and Cable, El Monte, Burbank, and Hawthorne ozone concentrations were higher, while b_{scat} levels were lower than earlier in the day. Above the surface layer, ozone and b_{scat} levels were similar or higher than levels earlier in the day except at Hawthorne. The sea breeze appeared to undercut the original mixed layer pollutants at the western and central basin sites. The sea breeze front, with a depth of about 500 to 600 meters, again did not appear to have reached Cable.

3.4 CHARACTERISTICS OF ALOFT INTEGRATED SAMPLES TAKEN DURING ORBITS

Integrated aerosol and gaseous samples were made during constant-altitude orbits using a modified version of the SCAQS sampler. These samples were later analyzed for nitric acid, SO_2, PAN, carbonyls, and particulate sulfur and nitrogen species similar to the surface samples. Orbit locations are shown in Figure 2-10. Samples were collected by both the UW and STI aircraft during the SCAQS as described in section 2.2.2. The spatial distribution of these species aloft has not been investigated in much detail in past studies.

We computed the mean values of air quality parameters measured during the orbits and combined these parameters with the results of the integrated samples. Figures 3-36 to 3-41 show the orbit-averages of nitric acid, PAN, ozone, ammonia, SO_2, NO_x, and $PM_{2.5}$ mass, organic and elemental carbon, nitrate ion, sulfate ion, and NMOC by date, time of day (morning and afternoon), and orbit location. All but one of the samples were collected above the mixing height. Note that samples were collected offshore at DOYLE and PADDR only in the morning and inland at Pomona and Riverside only in the afternoon. No afternoon samples were collected on June 24. All $PM_{2.5}$ mass samples were invalid.

Observations from these figures include the following:

- Ozone, nitric acid, PAN, and NO_x concentrations were significantly higher in the afternoon than in the morning.
- Ozone, nitric acid, and PAN concentrations went up and down together.
- All of the orbit-average ozone concentrations were well above background, varying from 120 to over 220 ppb.
- Elemental carbon, nitrate ion, ammonia, ammonium ion, and SO_2 concentrations were low. Nitrate ion concentrations were highest in the afternoon except at Riverside, where nitrate ion concentrations were below detection.
- $PM_{2.5}$ sulfate ion concentrations were generally higher in the afternoon.
- NMOC and organic carbon concentrations were highest at AMTRA. The afternoon NMOC and OC concentrations were higher than the morning.
- Ozone, carbonyl compound, NMHC, and organic carbon concentrations were highest at AMTRA (near Los Angeles) and lower at coastal and inland sites on the afternoon of June 25. This is the pattern observed for surface hydrocarbon concentrations.
- Carbonyl compounds comprised a significant fraction of the NMOC aloft (typically more than 30 % of the carbon).

3.5 COMPARISON OF SURFACE AND ALOFT POLLUTANTS

Air quality data at the surface are abundant both spatially and temporally in the SoCAB. In contrast, aloft measurements of air quality are rarely available. In this section, we compare the aloft measurements of ozone, NMOC, and $PM_{2.5}$ mass and species made during June 24 and 25 with surface measurements.

3.5.1 Comparison of Aloft and Surface Ozone

We investigated how well the aloft ozone concentrations at the spiral locations compared to the measurements made at nearby surface sites. Figures 3-42 to 3-44 show the surface and aloft measurements made during the

June 24-25, 1987 episode. Two ozone values are shown in the figures for the aircraft, the mixed-layer-average (MLA) and the 45-m average. The MLA was computed by averaging the ozone concentrations over the mixing height (determined by T.B. Smith and Associates) in the midday and afternoon. The 45-m average is the average ozone concentration in the lowest 45 m of the aircraft spiral. Most of the spirals during the summer SCAQS reached altitudes below 30 m agl.

At all sampling locations, the aircraft ozone measurements were slightly higher than the surface in midday and afternoon. The Burbank and Cable aircraft data differed the most from the corresponding surface data, with the largest differences occurring in the afternoon. Over all SCAQS intensive days, MLA and 45-m average ozone concentrations were about 25 ppb higher than nearby surface concentrations (Roberts and Main, 1992).

3.5.2 Comparison of Aloft and Surface Gaseous and Particulate Species

Three of the aloft hydrocarbon and carbonyl samples were collected within about one hour of surface samples at nearby sites. The composition of the 25 most abundant species in the matched samples correlated reasonably well, r^2 = 0.5 to 0.7. NMHC concentrations at the surface were greater than aloft in all three matched pairs. Carbonyl compound concentrations aloft, on the other hand, were equal to or greater than concentrations at the surface. Details are provided by Lurmann and Main (1992).

We matched aloft samples, collected during 30-minute orbits, with the nearest surface site data, collected during four-to six-hour periods. Ammonia, and $PM_{2.5}$ ammonium, nitrate, and sulfate ion concentrations aloft were almost always less than the matched surface concentrations. However, $PM_{2.5}$ organic carbon concentrations aloft were generally higher than at the surface. Nitric acid concentrations were sometimes higher and sometimes lower than matched concentrations at the surface.

3.6 THE PRESENCE AND STRUCTURE OF POLLUTED LAYERS ALOFT

3.6.1 Ozone and b_{scat} From West to East

In order to illustrate the structure of ozone concentrations aloft, we have constructed a 2-dimensional (2-D) plane from the surface to about 1500 m msl along a line from the coast to the eastern-basin (see map in Figure 3-45). This line passes near the Hawthorne, El Monte, Cable, and Riverside aircraft spiral locations. The PADDR, Burbank, and Fullerton spiral locations do not lie along this line, so we did not use these data in this analysis. We next interpolated and contoured data from spirals along the line to a 2-D plane which illustrates the pollutant structure aloft over the SoCAB: Figures 3-46 and 3-47 show ozone and b_{scat} on June 24, 1987.

In the figures, the darkened area along the bottom of the figure shows the approximate ground level in the SoCAB. Note that the ground level at Cable Airport is significantly higher than at either El Monte or Riverside; this is because Cable is part-way up the San Gabriel Mountains, as opposed to lower down along a straight line from El Monte to Riverside.

Figure 3-46 shows the 2-D ozone concentration plots for the morning, midday, and afternoon of June 24. On this morning, there was an aloft layer with ozone concentrations from 100 to over 200 ppb, similar to the next morning (see Figure 3-48). By midday, there was a layer at about this same altitude with ozone concentrations over 200 ppb. Note that data at Cable were missing from the surface to 1300 m msl; thus, the 150 and 200 ppb contours at Riverside do not intersect the contours to the west of Cable. By afternoon, there was a 300 m-thick layer at about this same altitude with ozone concentrations over 250 ppb covering most of the SoCAB. Peak surface ozone concentrations on this day reached 250 ppb at Claremont. The b_{scat} levels were lowest to the west and showed a steep gradient inland (see Figure 3-47). The b_{scat} levels were highest toward the ground and in the central and eastern basin. The sea breeze intrusion on the basin can be seen in Figure 3-47c.

On the morning of June 25, ozone concentrations near the ground were close to 0 ppb; probably titrated by fresh NO emissions (Figure 3-48a). Aloft, there was a layer about 300 m thick with ozone concentrations over 150 ppb (from about 750 to 1050 m msl), with peak concentrations over 200 ppb. The b_{scat} levels were also high in this layer (Figure 3-49a). This layer containing relatively high levels of ozone and b_{scat} was still present midday. By afternoon, ozone concentrations in this layer over the central and eastern basin exceeded 200 ppb. High ozone concentrations and b_{scat} levels were observed at Riverside above 900 m msl, providing evidence of a convergence zone carrying pollutants aloft.

Figure 3-50 shows aerosol lidar results for the morning of June 25, 1987 along a 2-D plane from South Pasadena to San Bernardino; ground level is indicated along the bottom of the plot by the thick dark band. The darker areas in the plot above the ground indicate higher particle backscatter and thus higher particle concentrations. Note that there is a layer of high particle backscatter between about 800-1000 m msl across the whole distance of the lidar image; this layer corresponds to the same ozone layer shown in Figure 3-48. This layer was evident on numerous other lidar images covering a much wider area.

Note that in Figures 3-46 through 4-50, the general structure of the polluted layers aloft is horizontal and not terrain-following; all of these figures were prepared based on altitude above mean sea level (msl), not based on altitude above ground level (agl).

3.6.2 Ozone and b_{scat} From North to South

To investigate the layer structure from the north to the south, we prepared 2-D contours of ozone and b_{scat} along a plane from Burbank through El Monte to Fullerton (see map in Figure 3-45). Ozone and b_{scat} data were interpolated and contoured as described in Section 3.6.1. Figures 3-51 and 3-52 show these ozone and b_{scat} 2-D contours.

On June 24, particularly in the afternoon, a layer with high ozone concentrations (>250 ppb) was observed from Burbank to Fullerton from about 500 to 800 m msl. This layer was also observed to stretch from Hawthorne to Riverside (Figure 3-46), indicating this layer was spread across most of the basin. Data collected at PADDR also showed the layer extended offshore

(Figure 3-22). The b_{scat} levels aloft were higher at Burbank than at Fullerton.

On the morning of June 25, a layer containing ozone concentrations greater than 150 ppb was still observed above 500 m msl from Burbank to Fullerton. Again, b_{scat} levels were higher at Burbank than at Fullerton. In the afternoon, the ozone layer observed in the central and eastern basin (Figure 3-48) at about 500 to 800 m msl (>200 ppb) also extended north to Burbank.

3.7 ALOFT LAYER FORMATION

Aloft layers of pollutants can be formed by a number of mechanisms (Edinger, 1963; Blumenthal et al., 1974; Smith et al., 1976), including the following: undercutting of the afternoon mixed layer by the sea breeze, isolation of polluted material aloft by the nocturnal boundary layer, upslope flow in the afternoon, injection of pollutants aloft by stationary source emissions, injection aloft at a convergence zone formed in the eastern SoCAB when the sea breeze meets a weak easterly flow, and transport of buoyant air parcels from the mixed layer into the inversion layer (convective debris).

Undercutting of the afternoon mixed layer by the sea breeze occurred regularly during the summer SCAQS. On most summer days, a shallow sea breeze penetrates the SoCAB and undercuts the afternoon mixed layer, pushing a shallow polluted layer in front of it and leaving the top portion of the mixed layer aloft. The sea breeze is composed of relatively clean, cool air which does not mix significantly with the more-polluted mixed layer. Figure 3-53 shows pollutant profiles at Fullerton on the afternoon of June 24, 1987. The elevated polluted layer (about 400 to 600 m msl) is formed at a relatively low altitude and thus, may be incorporated into the mixed layer the following day depending upon transport of this layer during the night. This type of undercutting of the mixed layer by the sea breeze was common during the SCAQS at locations from the coast inland to El Monte; the sea breeze seldom reached Cable or Riverside. The lidar gray-scale plot in Figure 3-54 shows that clean air due to the sea breeze (surface to about 500 m msl) has penetrated to about El Monte and isolated a polluted layer aloft on the afternoon of June 25, 1987.

Another way in which pollutants may be transported aloft is upslope flow. Past research efforts have shown that the heating of the slopes and inland valleys provide a major mechanism for ventilation of the SoCAB. Flow up the mountain slopes due to heating may carry pollutants aloft to form layers above the surface mixing layer. Dispersion of this aloft layer would be dependent on the aloft winds. Figure 3-55 shows a lidar gray-scale plot for a flight from Mt. Gleason to South Pasadena on the afternoon of June 25, 1987. In the figure, higher particle backscatter is denoted by a darker signal. The mixed layer is shown rising up the mountainside and being injected aloft; some material is even being injected above the top of the mountain. Similar evidence of upslope flow was found in past studies (Wakimoto and McElroy, 1986).

3.8 COMPARISON OF OZONE CONCENTRATIONS FROM MODEL SIMULATIONS AND AIRCRAFT MEASUREMENTS

The SCAQS meteorological and air quality data have been extensively used in the development and testing of models, such as the Urban Airshed Model (UAM). SCAQS data have been used by various investigators to test different methods for preparing wind fields (Wheeler, 1991b; Cassmassi et al., 1990) and mixing height fields (Wheeler, 1990; Cassmassi and Durkee, 1990). Others have investigated the model sensitivity to variations in wind fields (Wheeler, 1991a) and ozone deposition (Harley et al., 1992), changes in emissions, and initial and boundary conditions (Harley et al., 1992; SCAQMD, 1990, 1991). UAM simulation results have also been compared to tracer measurements (Chico et al., 1990).

One objective of this project was to determine how well model simulations of ozone concentrations aloft compared with aircraft measurements at various times and locations throughout the SoCAB. To accomplish this, we compared ozone concentrations measured during aircraft spirals with aloft ozone concentration results from model simulations. Model simulation results were available from the final Air Quality Management Plan (AQMP) UAM runs (SCAQMD, 1990, 1991). Days with both model simulation results and aircraft measurements included June 24-25, 1987 and August 27-28, 1987; in both cases, the model simulation started on the previous day.

Most past comparisons of model results and measurements have been performed only at the surface. Such comparisons have been made using time-series plots of hourly ozone measurements and hourly model predictions at a particular surface monitoring site and using spatial plots of differences between measurements and model results. Comparisons of aloft measurements and model predictions had to be done differently. In general, we prepared plots of ozone concentrations as a function of altitude for a given time and location, using measured aircraft data and model simulation results.

During each of three flights each day, the aircraft measured ozone concentrations from about 1500 m msl to the surface during vertical spirals. The model predicted average ozone concentrations in six vertical cells centered over a 5 km by 5 km surface grid cell. The size of the six vertical cells varied as a function of mixing height; three cells of equal height below the mixing height and three above. The model simulated the first 1000 m above the surface. For the model predictions, we computed a distance-weighted average over the four horizontal cells nearest the aircraft spiral location; this minimized the effects of any unusual peaks or valleys in the ozone concentration. For the model predictions, we used the hour-averaged ozone concentrations which included the time of the aircraft spiral.

Figure 3-56 shows an example comparison of measured and predicted ozone concentrations for June 25, 1987 at Cable Airport. Cable Airport is located about 5 km east-north-east of the Claremont monitoring site at an elevation of 442 m msl. The solid line shows 30-meter bin averages of the ozone concentrations measured during an aircraft spiral at 0513-0520 PDT. The dashed line shows the hour-averaged model prediction for 0500-0600 PDT. We have also included an average of the aircraft data on the same altitude intervals as the model results (the dotted line).

The morning aircraft data (Figure 3-56a) showed very low ozone concentrations (less than 10 ppb) within about 200 m of the ground and high ozone concentrations (over 150 ppb) in a layer from about 750 to 1200 m msl. The ozone concentrations were low near the ground because fresh emissions of NO had titrated any available ozone within the nocturnal boundary layer and that layer was not mixed with material at higher altitudes. The model simulation results indicated low ozone concentrations in the nocturnal boundary layer, less than 50 ppb, but higher concentrations than the aircraft measurements. Above about 650 m msl, the model predicted about 70 to 90 ppb ozone, while the averaged aircraft data showed ozone concentrations about 50 to 80 ppb higher. This comparison is typical of most early-morning comparisons: the model does not predict enough ozone aloft and predicts too much ozone in the surface layer. For midday and afternoon comparisons, the model simulation results were still significantly lower than the measured ozone concentrations (see Figures 3-56b and 3-56c), although the shapes of the simulated and measured ozone profiles were similar in the afternoon.

In order to evaluate the potential variations in comparisons between model predictions and aircraft measurements, we reviewed the variations in model predictions for surrounding grid cells and times. We then compared these predictions to the measured ozone concentrations. We performed this evaluation for the June 24-25, 1987 episode, since this episode displayed the largest differences between predicted and measured ozone concentrations. In addition, there may be variations in the measured ozone concentrations; however, much of the spatial variation has already been averaged out since the aircraft data were averaged over 30 m bins and since the aircraft spiral covered a circle about 1 to 2 km in diameter.

To evaluate the spatial variation, we compared the model predictions for the four nearest cells to the distance-weighted average of the four cells and to the measured ozone concentrations. In general, these spatial variations did not exceed about 10 percent of the predicted concentrations, while the difference between the predicted and measured ozone concentrations may have been as great as 150 percent.

To evaluate the temporal variation, we compared model predictions for the previous and following hours to predictions for the selected hour and to the measured ozone concentrations. In general, these temporal variations did not exceed 30 percent of the predicted concentrations, except when the ozone concentrations were low; however, these variations are still significantly smaller than the typical difference between predicted and measured ozone concentrations. For example, Figure 3-57 shows the measured and predicted ozone concentration profile for the afternoon of June 24, 1987 at Burbank. At all altitudes, the model predictions for all three hours were different from each other by 30 to 50 ppb; above about 550 m msl, this difference amounts to about 30 percent. However, all three sets of model predictions were still significantly different from the measured ozone concentrations: 10 to 70 ppb different above 550 m msl and 130 to 200 ppb lower than measured below 550 m msl.

We prepared comparisons for all days with both model simulation results and aircraft measurements: June 24-25, 1987 and August 27-28, 1987. Typically, data were taken in seven spirals during early morning, midday, and

afternoon flights. In most early-morning cases, the model does not predict enough ozone aloft and predicts too much ozone in the surface layer. During most midday and afternoon cases, the model predicted too little ozone throughout the whole range of altitudes. Figures 3-56 and 3-58 to 3-63 show ozone profiles for early morning, midday, and afternoon on June 25, 1987 for Cable, Hawthorne, PADDR, Fullerton, Burbank, El Monte, and Riverside, respectively.

The morning ozone profile measured at Hawthorne on June 25, 1987 showed low ozone concentrations (about 20 ppb) below about 500 m msl and high ozone concentrations (over 200 ppb) above 700 m msl, see Figure 3-58a. We would expect low ozone concentrations near the ground, due to titration of ozone in the nocturnal boundary layer by fresh NO emissions. The higher ozone concentrations above 500 m msl were probably due to carryover from the previous day; this material will be available to be mixed to the surface later in the day. The measured ozone profiles for midday and afternoon continued to show a layer of high ozone concentrations above 600 m msl and increasing ozone concentrations in the mixed layer below about 600 m msl, see Figure 3-58b and 3-58c.

As seen on Figure 3-58a, the morning model predictions for Hawthorne were similar to the measured ozone concentrations below 500 m msl and significantly lower than measured above 700 m msl. During the midday, the model predictions were again similar to the measured ozone concentrations below 500 m msl and lower than measured above 700 m msl, see Figure 3-58b. However, during the afternoon, the model predictions were significantly lower than measured ozone concentrations at all altitudes, see Figure 3-58c. This pattern, of model predictions being significantly lower than measured ozone concentrations above about 500 m msl in the morning and at all altitudes in the midday and afternoon, was typical for most of our comparisons. A few of the important features of Figures 3-56 through 3-63 are discussed below. Additional ozone profiles for June 24 are shown in Appendix B.

The ozone profiles measured at PADDR showed a significant layer of high ozone concentrations at about 500 to 1000 m msl throughout the day, with lower concentrations below 500 m msl (see Figure 3-59). In contrast, the model predictions showed a fairly-flat profile of 60 to 80 ppb ozone all day; the model simulation had not generated the layer of ozone carried-over from the previous day. Instead, the model appeared to be predicting boundary conditions at this offshore site.

The comparisons at Burbank, El Monte, Cable, and Riverside fit a similar pattern: during the morning, high model predictions below 500 m msl and low predictions above 500 m msl; and low predictions at most altitudes during the midday and afternoon. The model predictions were especially poor at Cable in the morning and at Riverside at midday. Of all the ozone profile comparisons, only two model-generated profiles showed shapes very similar to the measured shapes: afternoon model-generated profiles at Burbank and Cable. However, the model-generated profiles in these cases were still 30 to 100 ppb low.

The general bias between the model predictions of ozone and the measured ozone concentrations is illustrated in Figure 3-64, which shows the average ozone concentrations above and below the model-predicted mixing height for the

predicted and measured data. For each data point in this figure, the model-generated data and the measured data were each averaged over the same altitude range. The data are further identified by time of day. Above the model-predicted mixing height, the model under-predicted ozone concentrations in all but six cases; three were similar to the measured and three were higher than the measured ozone. The three cases for which the model over-predicted ozone concentration occurred on June 24 in the central SoCAB (at Burbank, El Monte, and Cable). The same comparison is made for average ozone concentrations below the model-predicted mixing height in Figure 3-64b. The model over-predicted ozone below the mixing height in most of the morning samples. The model under-predicted nearly all of the midday and afternoon ozone concentrations.

Since model predictions were worst above the mixing height, we prepared times-series plots of the average ozone concentration above the model-predicted mixing height for each spiral location. Figures 3-65, 3-66, 3-67, and 3-68 show these plots for El Monte, Hawthorne, Fullerton, PADDR, Cable, Burbank, and Riverside. At El Monte, while the model began with the correct amount of ozone above the mixing height on June 24, the average measured ozone exceeded the model predictions as the episode continued. At Hawthorne, Fullerton, and PADDR, the model values began more than 50 ppb lower than the measured values and maintained this difference throughout the episode. At Cable, model predictions were about 50 ppb low throughout the second day (June 25). At Burbank, the model predictions were much closer to the measured values. The model predicted relatively constant ozone concentrations over Riverside, while the measured values increased significantly from the morning of June 24 to the afternoon of June 25.

The primary emphasis in the model runs performed by the SCAQMD was in achieving performance goals for ozone. The performance of the model for NO_2 and hydrocarbon species were of secondary importance. In this report, we have only compared model output to ozone concentrations, since the model was expected to produce the best results for this species. Since the model-generated ozone concentrations were significantly different from the measured ozone concentrations, we did not pursue comparisons for any other species.

In summary, these model simulations regularly predicted ozone concentrations of about 100 ppb at altitudes above 500 m msl when measured concentrations were often 150 to over 200 ppb. These model simulations seem to transport these aloft pollutants out of the SoCAB instead of recirculating them within the SoCAB. In addition, the model predictions in the lower 200 m during the morning are often significantly higher than measured concentrations. This indicates that these model simulations do not produce enough ozone titration by fresh NO.

3.9 POLLUTANT CONCENTRATIONS AT SAN NICOLAS ISLAND

During the summer SCAQS, particulate and gaseous pollutants were measured at San Nicolas Island which is located about 120 km offshore. These data were collected to characterize the background levels of pollutants flowing into the SoCAB. PAN data were not available for the June 25-25 episode.

Figure 3-69 shows ozone, NO, NO_2, and PM_{10} and $PM_{2.5}$ mass concentrations for June 24-25, 1987 at San Nicolas Island. Unfortunately, most of the ozone data are missing from this episode. NO concentrations were below 1 pphm for all but one hour during the episode. NO_2 concentrations were also low, reaching a maximum of 2 pphm during only two hours midday on June 25.

Particulate mass concentrations at San Nicolas Island were a factor of two to ten lower than onshore SoCAB PM_{10} and $PM_{2.5}$ mass concentrations. All pollutant concentrations were low; in fact, nitric acid, ammonia, $PM_{2.5}$ elemental carbon, and SO_2 were near or below the detection limits (Figures 3-69 and 3-70). Sulfate ion and organic carbon comprised the largest portion of the PM_{10} mass. Chloride and sodium ions also were significant contributors to the PM_{10} mass. In addition to sulfate ion and organic carbon, nitrate and ammonium ions were a significant portion of the $PM_{2.5}$ mass. The composition of the particulate mass is consistent with its location and land cover. The composition reflected contributions from crustal, marine, and traces of urban sources.

NMOC concentrations (Figure 3-71) were significantly lower than NMOC concentrations measured onshore. The carbonyl fraction of the NMOC was higher than onshore surface samples and similar to aircraft samples. The unidentified fraction of the NMOC was also significantly higher than onshore samples. Detailed summaries of the average hydrocarbon and carbonyl compounds at San Nicolas Island are provided Main et al., 1990.

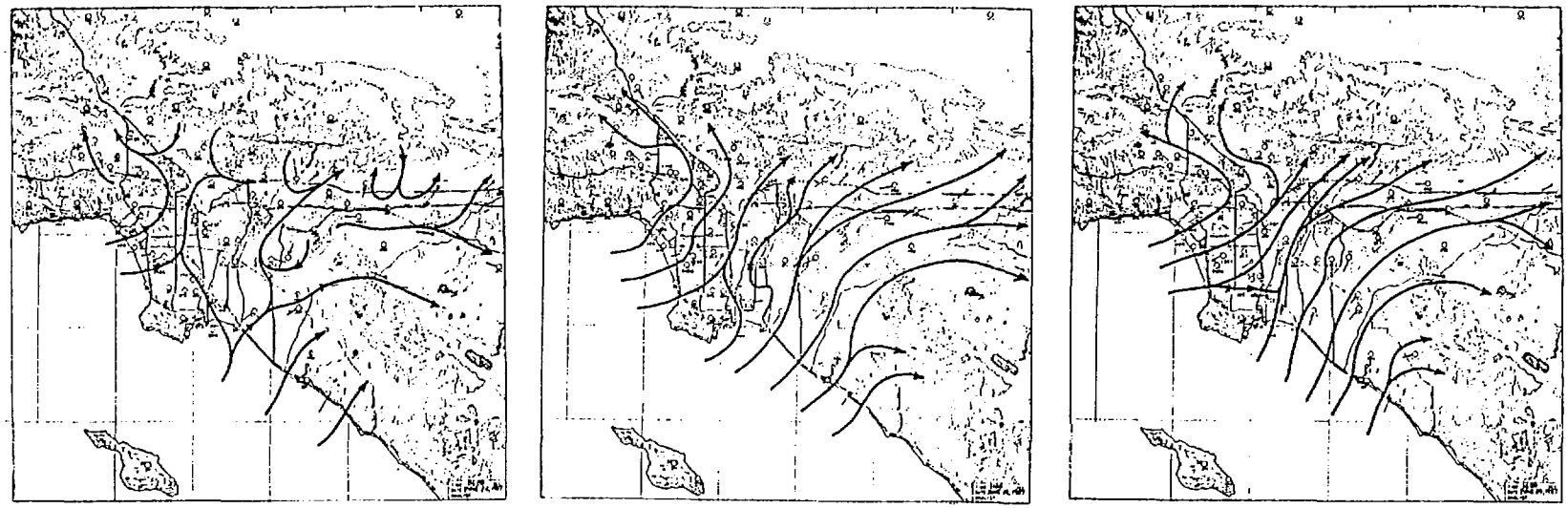

(a) (b) (c)

Figure 3-1. Surface Wind Streamline Analyses for June 24, 1987 at (a) 0700 PDT, (b) 1200 PDT, and (c) 1700 PDT (From Zeldin et al., 1989).

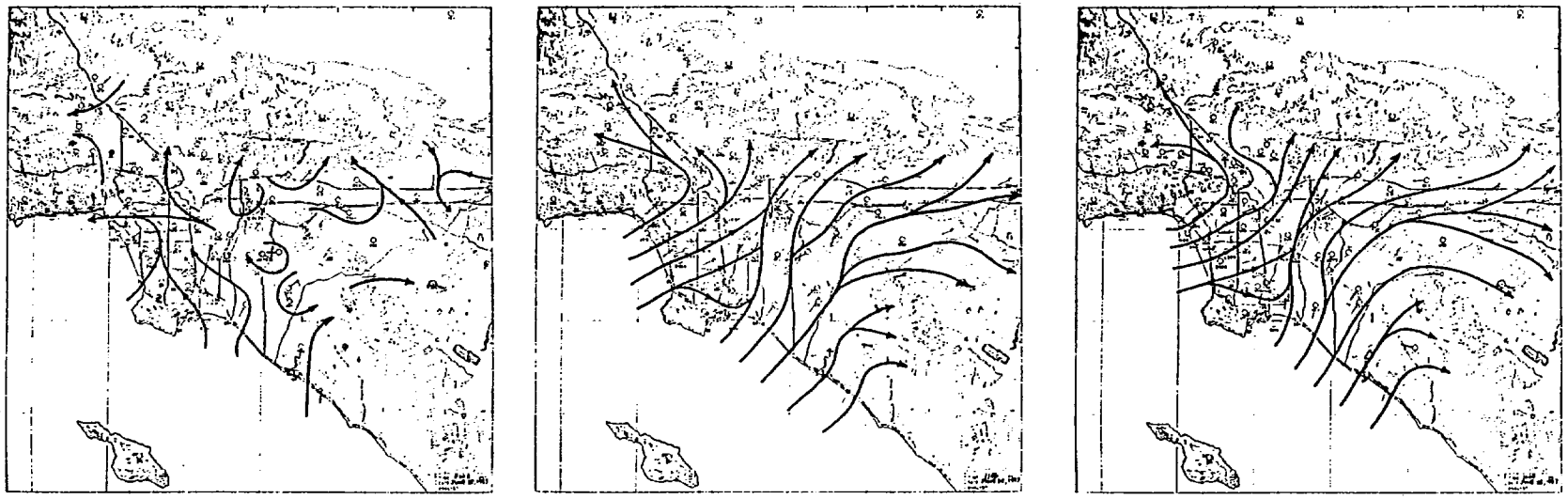

(a) (b) (c)

Figure 3-2. Surface Wind Streamline Analyses for June 25, 1987 at (a) 0700 PDT, (b) 1200 PDT, and (c) 1700 PDT (From Zeldin et al., 1989).

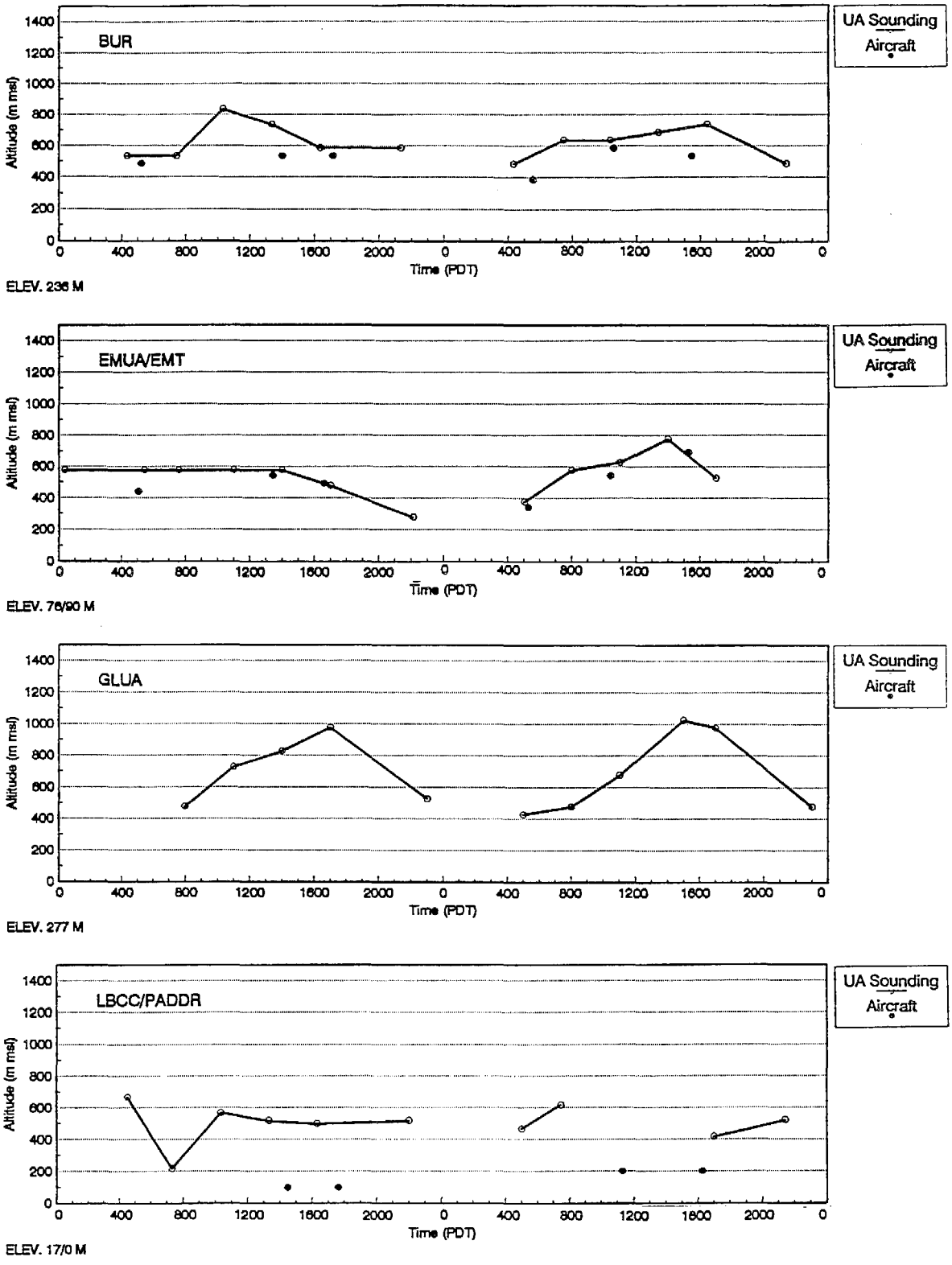

Figure 3-3. Estimated Mixing Heights on June 24-25, 1987 at Burbank, El Monte, Glendora, and Long Beach Using Rawinsonde Temperature Data and Nearby Aircraft Temperature and Air Quality Data. Elevations are given for the upper air and aircraft measurement locations.

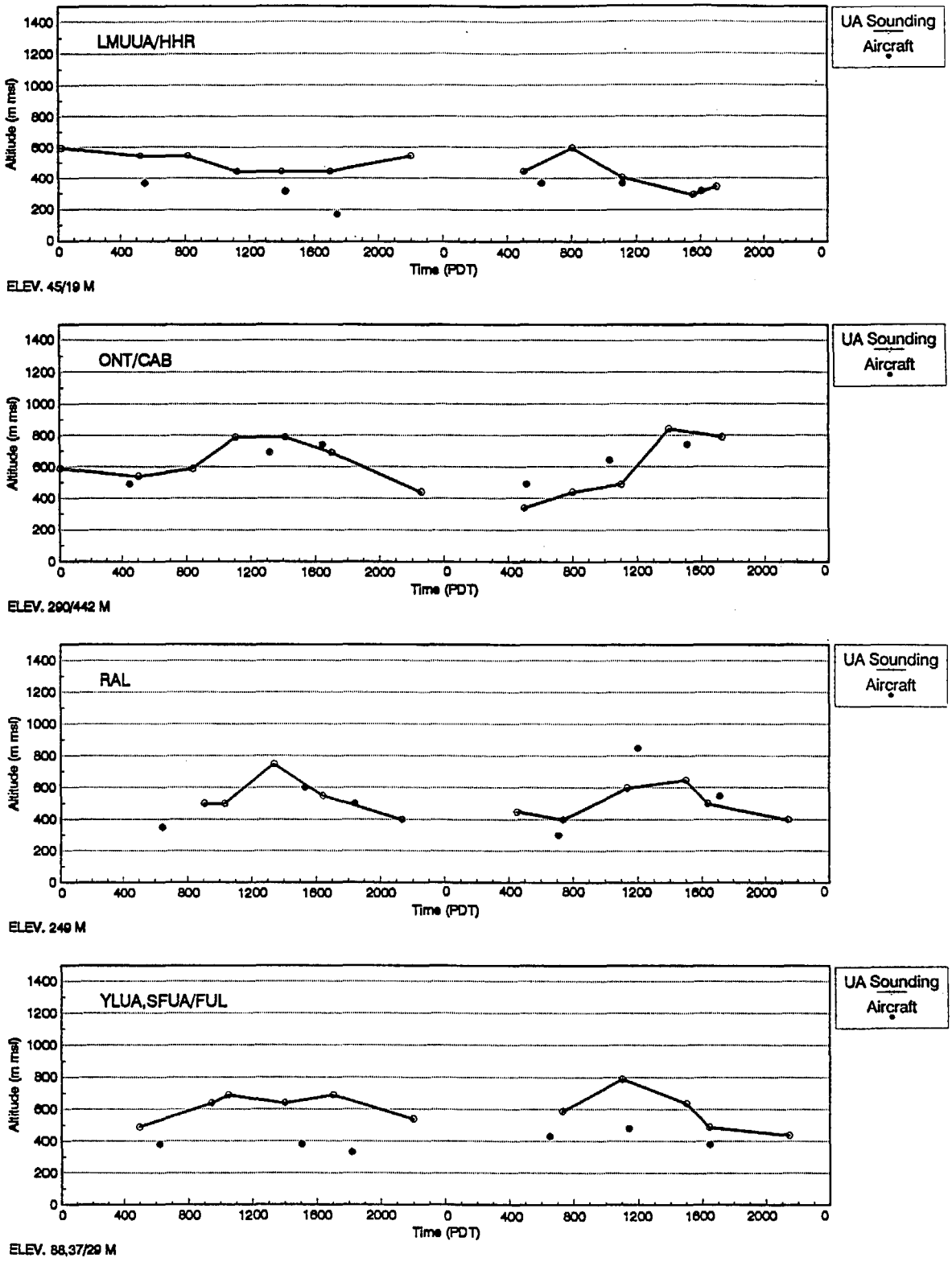

Figure 3-4. Estimated Mixing Heights on June 24-25, 1987 at Loyola-Marymount University, Ontario, Riverside, and Yorba Linda Using Rawinsonde Temperature Data and Nearby Aircraft Temperature and Air Quality Data. Elevations are given for the upper air and aircraft measurement locations.

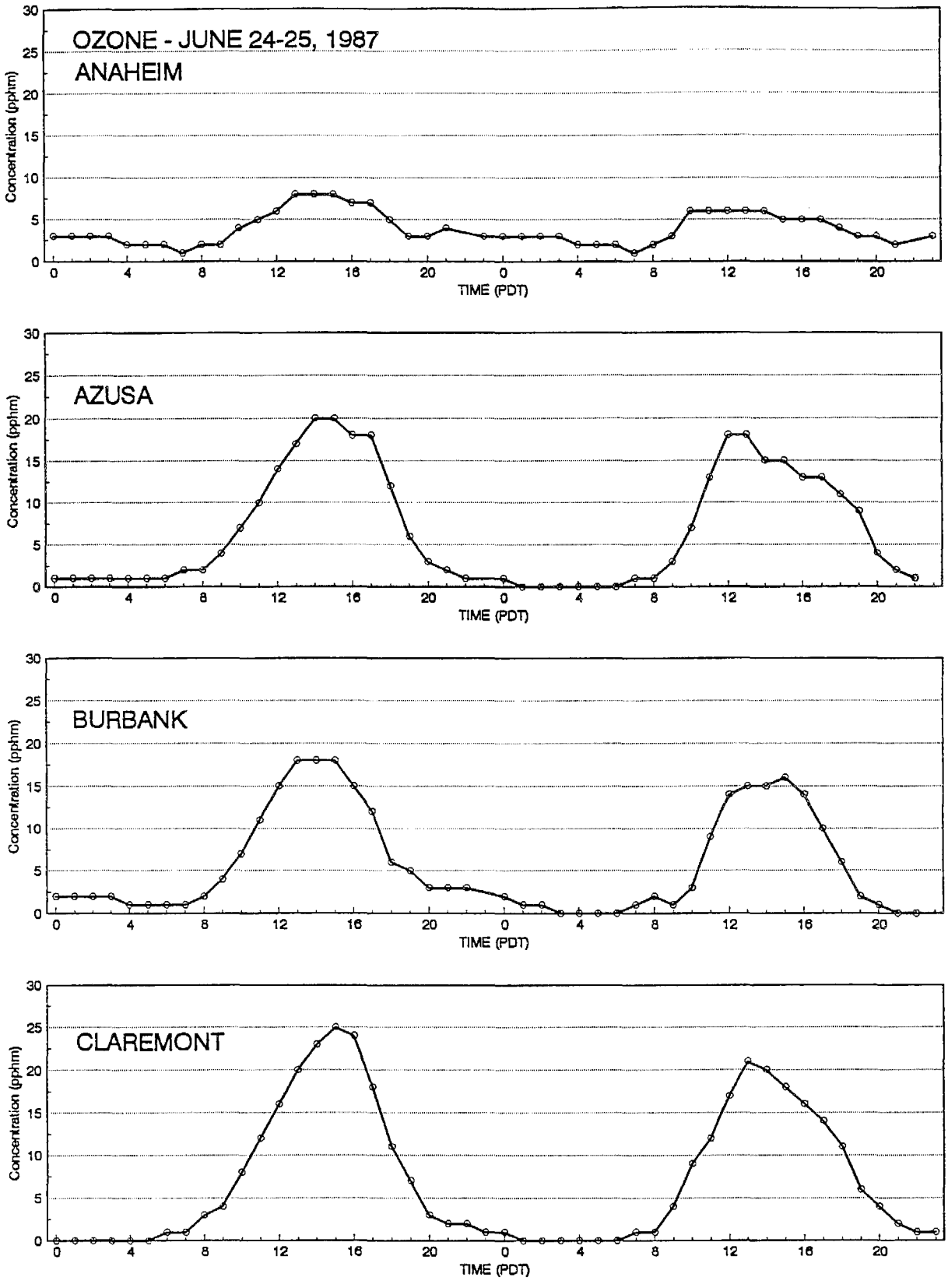

Figure 3-5. Diurnal Ozone Concentrations on June 24-25, 1987 at Anaheim, Azusa, Burbank, and Claremont.

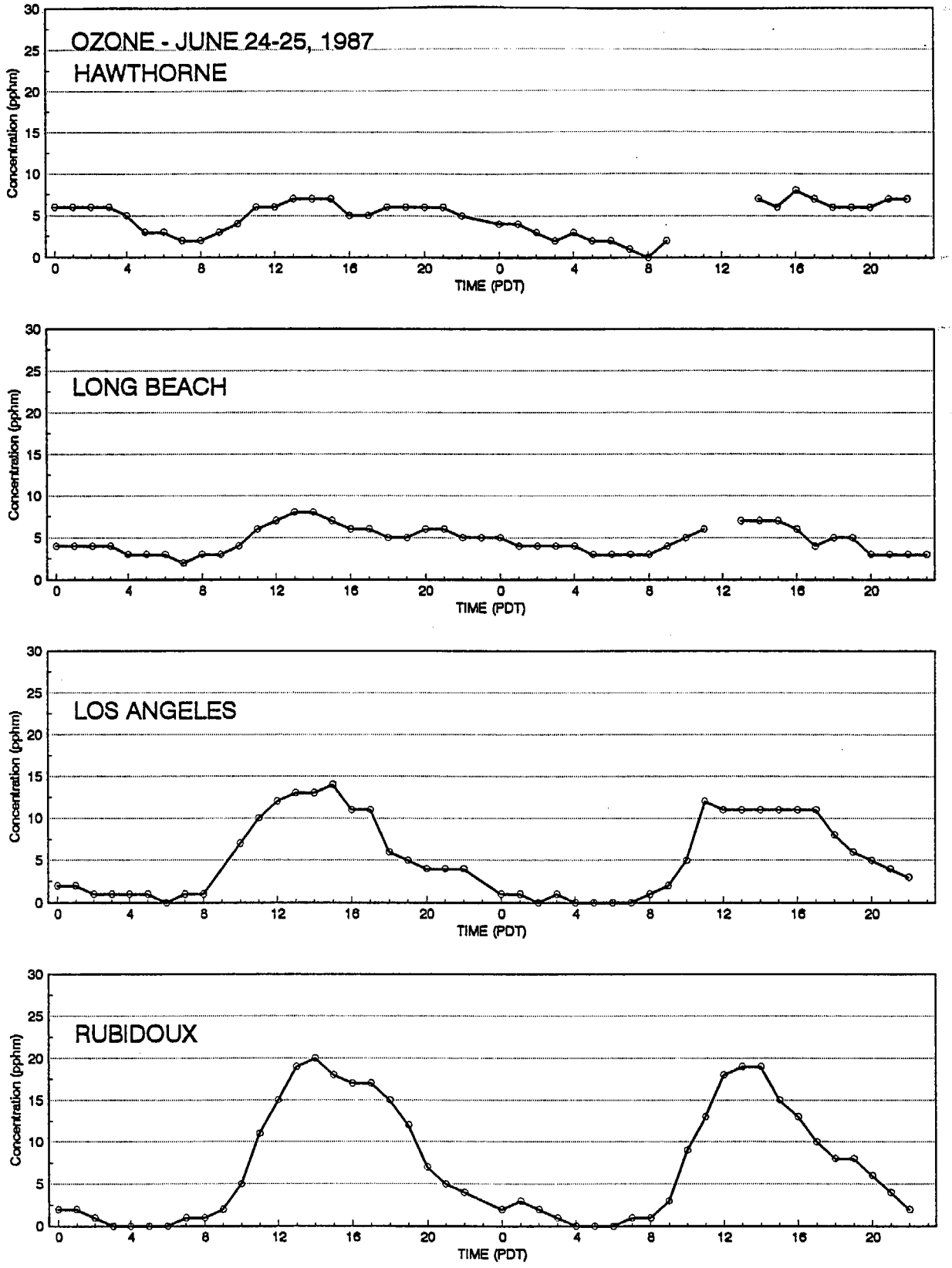

Figure 3-6. Diurnal Ozone Concentrations on June 24-25, 1987 at Hawthorne, Long Beach, Los Angeles, and Rubidoux.

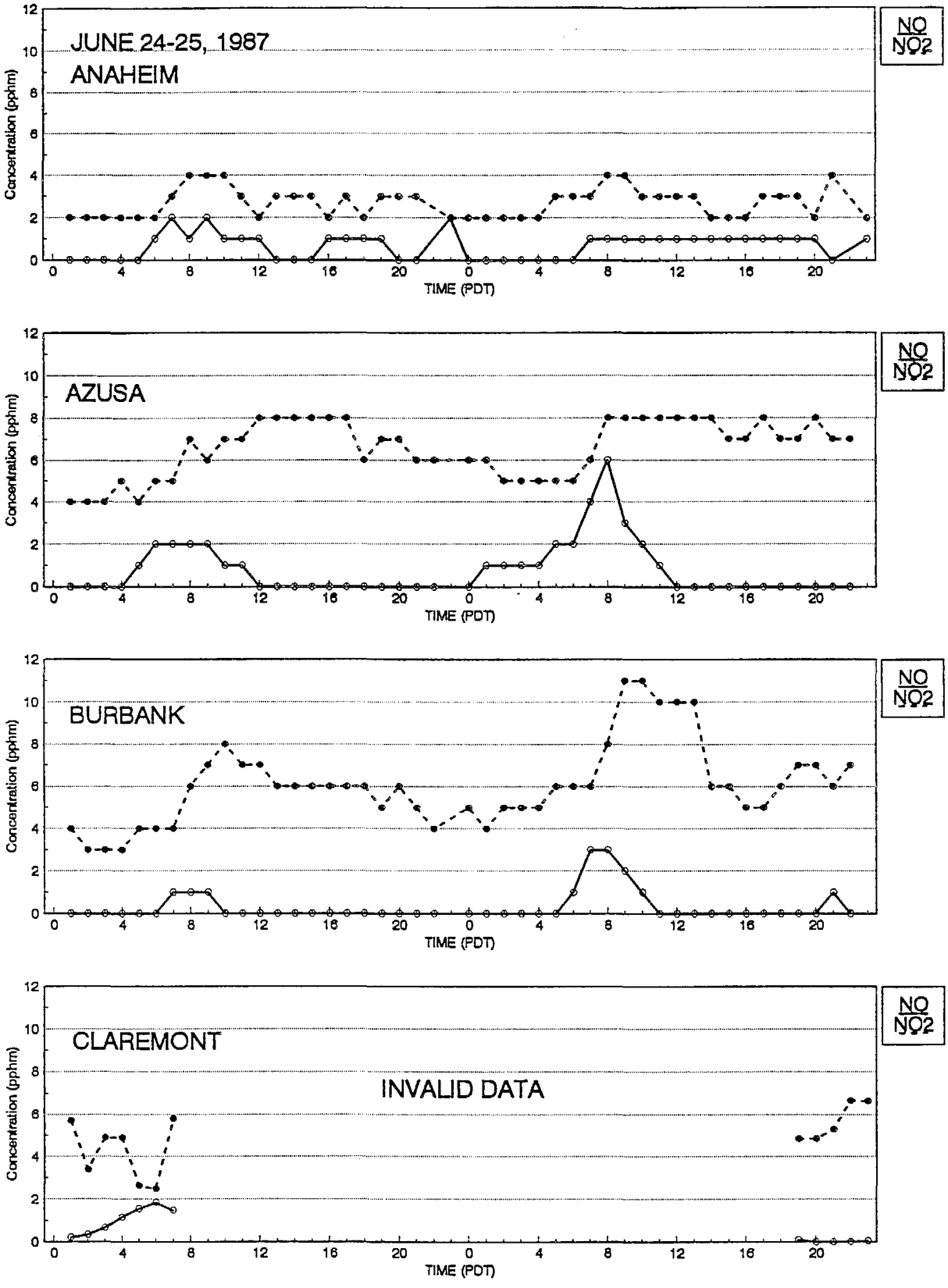

Figure 3-7. Diurnal NO and NO_2 Concentrations on June 24-25, 1987 at Anaheim, Azusa, Burbank, and Claremont.

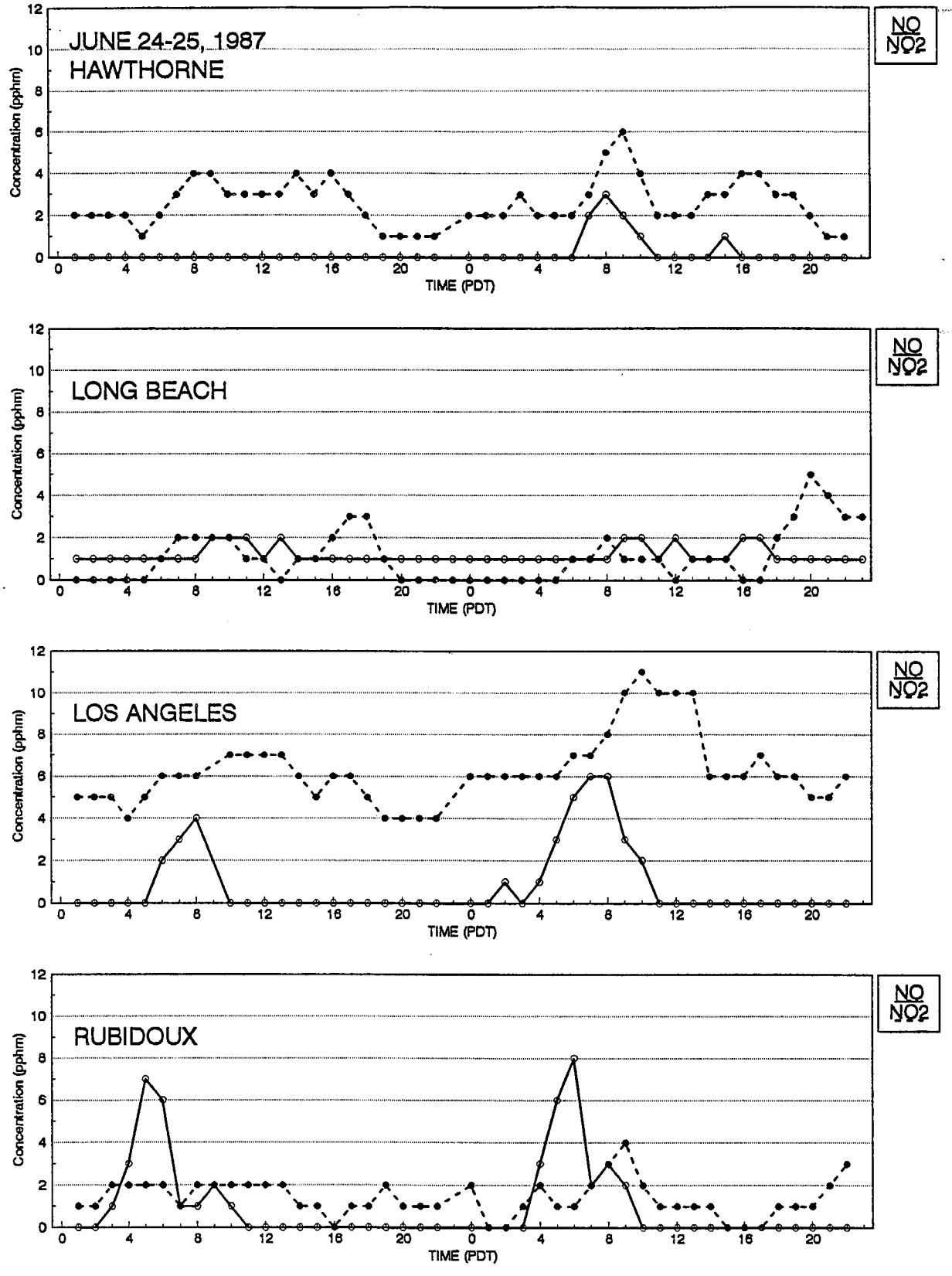

Figure 3-8. Diurnal NO and NO_2 Concentrations on June 24-25, 1987 at Hawthorne, Long Beach, Los Angeles, and Rubidoux.

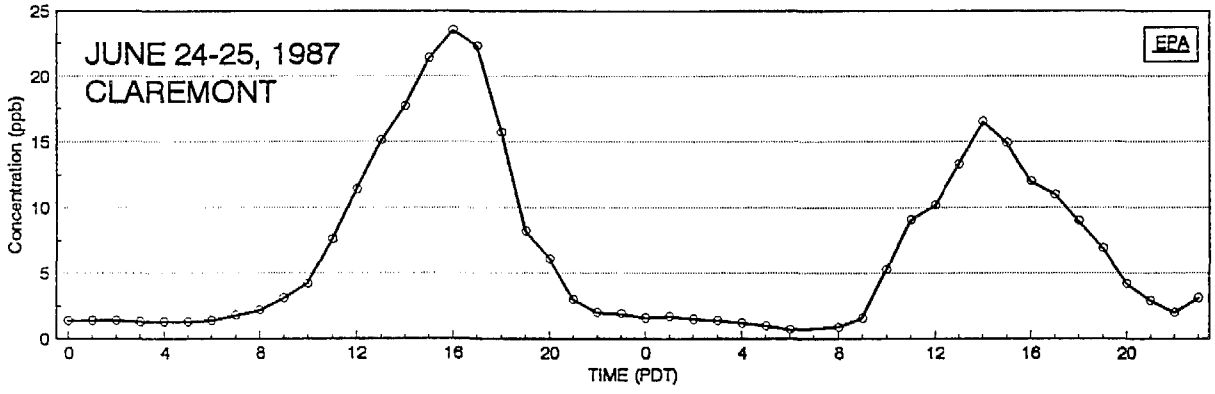

Figure 3-9. Diurnal PAN Concentrations by EPA on June 24-25, 1987 at Claremont. PAN data reported by DGA were suspect at all sites because of calibration problems; EPA only sampled PAN at Claremont.

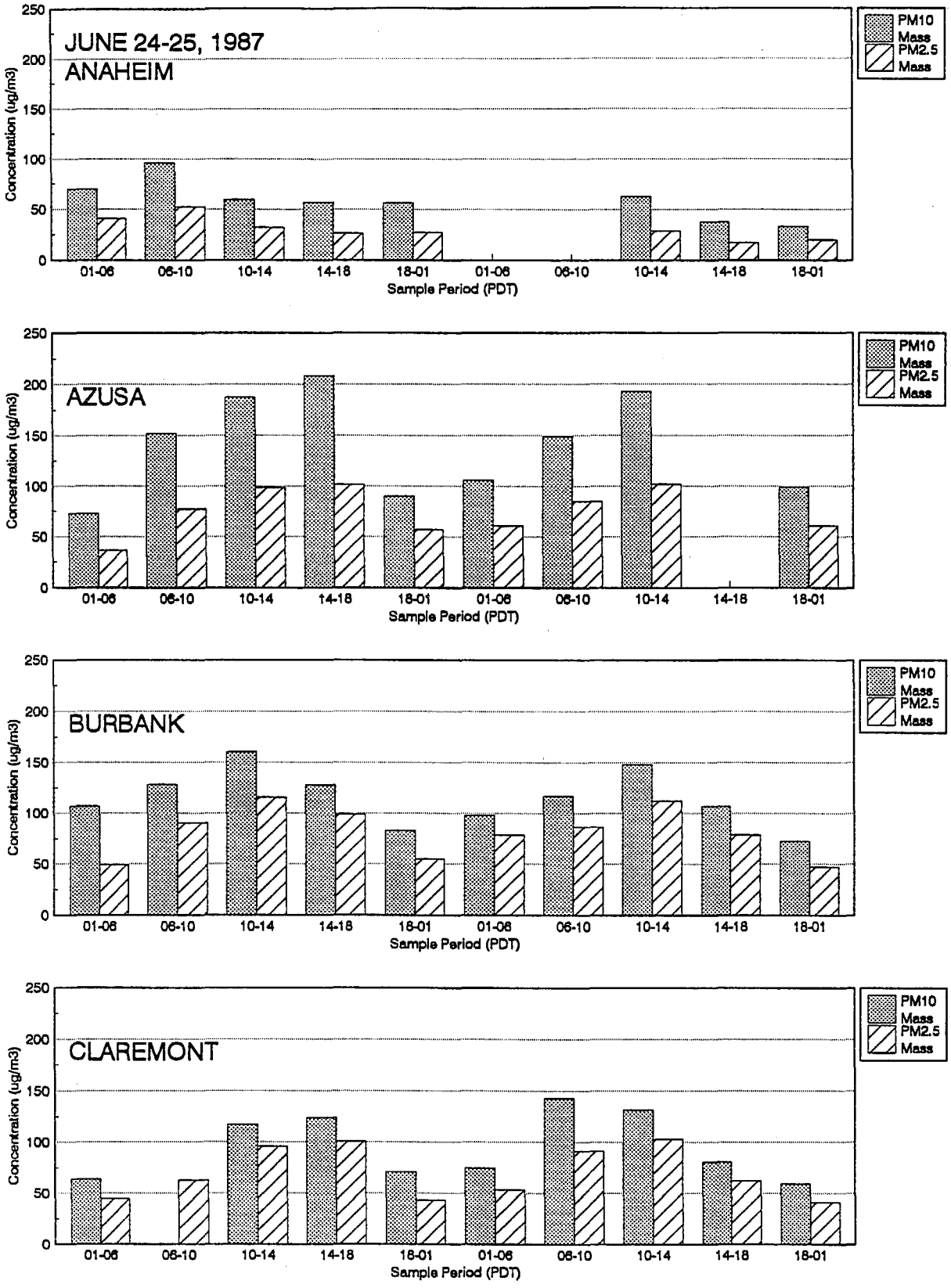

Figure 3-10. PM_{10} and $PM_{2.5}$ Mass Concentrations on June 24-25, 1987 at Anaheim, Azusa, Burbank, and Claremont.

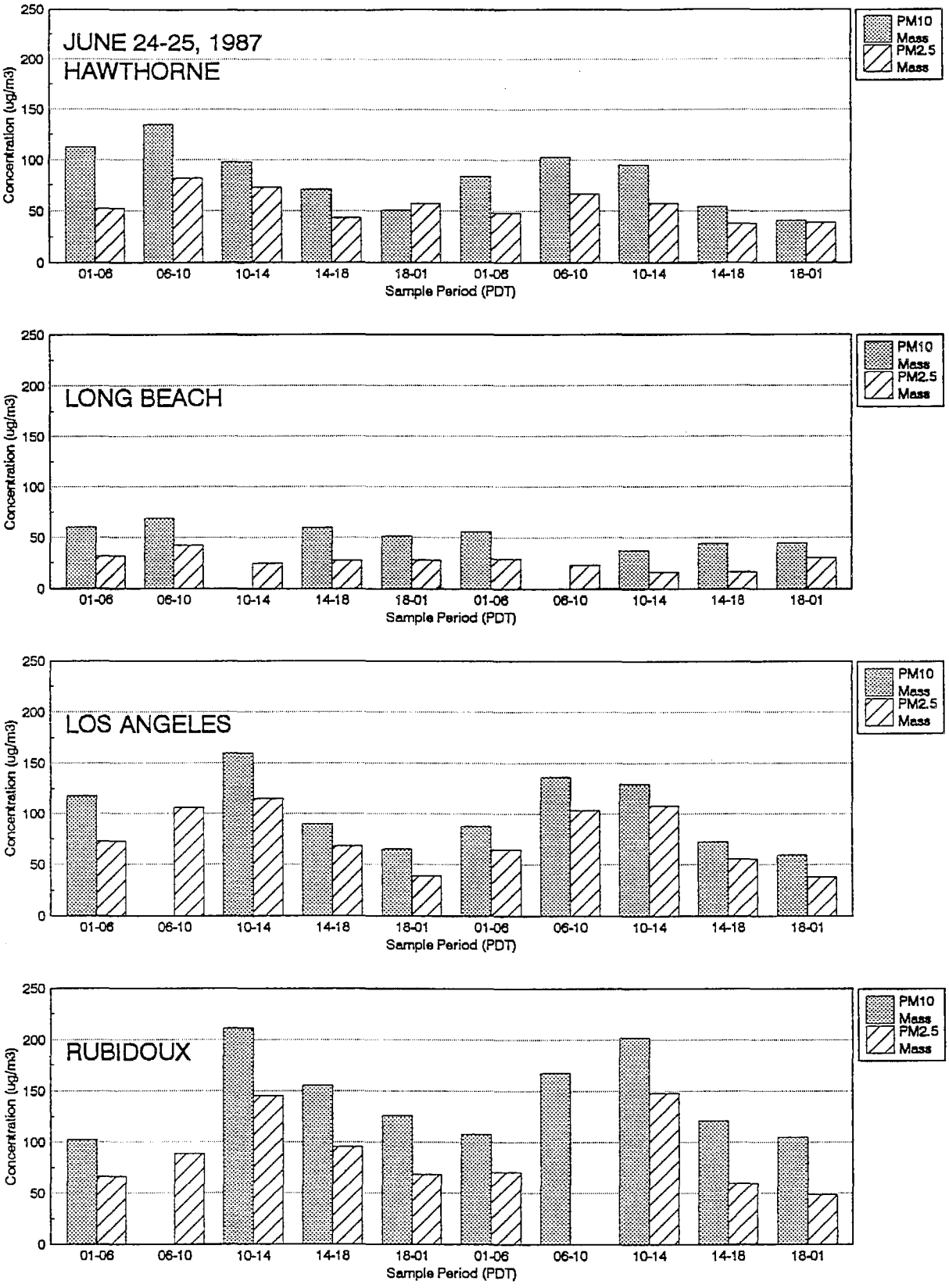

Figure 3-11. PM_{10} and $PM_{2.5}$ Mass Concentrations on June 24-25, 1987 at Hawthorne, Long Beach, Los Angeles, and Rubidoux.

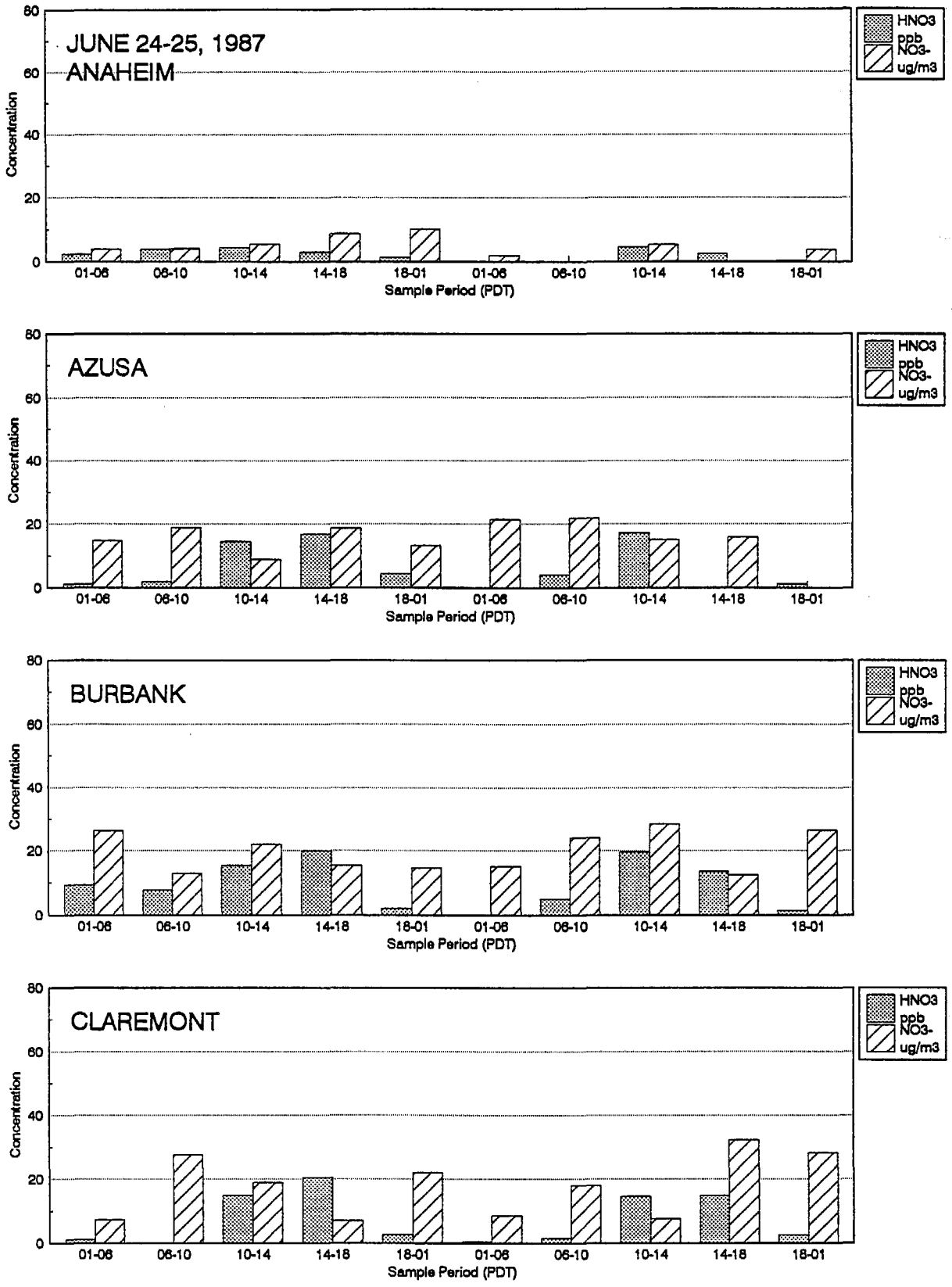

Figure 3-12. Nitric Acid and $PM_{2.5}$ Nitrate Ion Concentrations on June 24-25, 1987 at Anaheim, Azusa, Burbank, and Claremont.

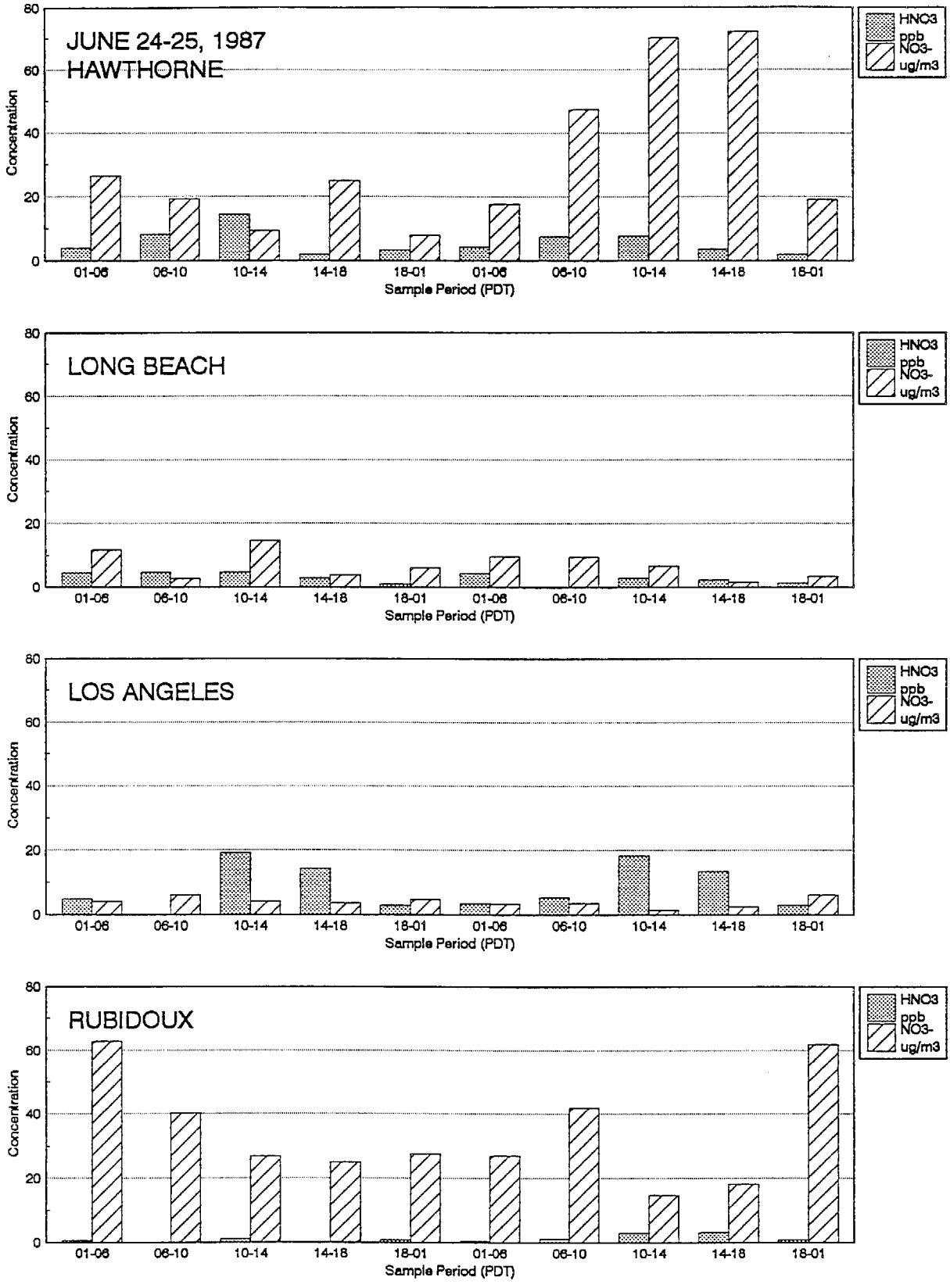

Figure 3-13. Nitric Acid and $PM_{2.5}$ Nitrate Ion Concentrations on June 24-25, 1987 at Hawthorne, Long Beach, Los Angeles, and Rubidoux.

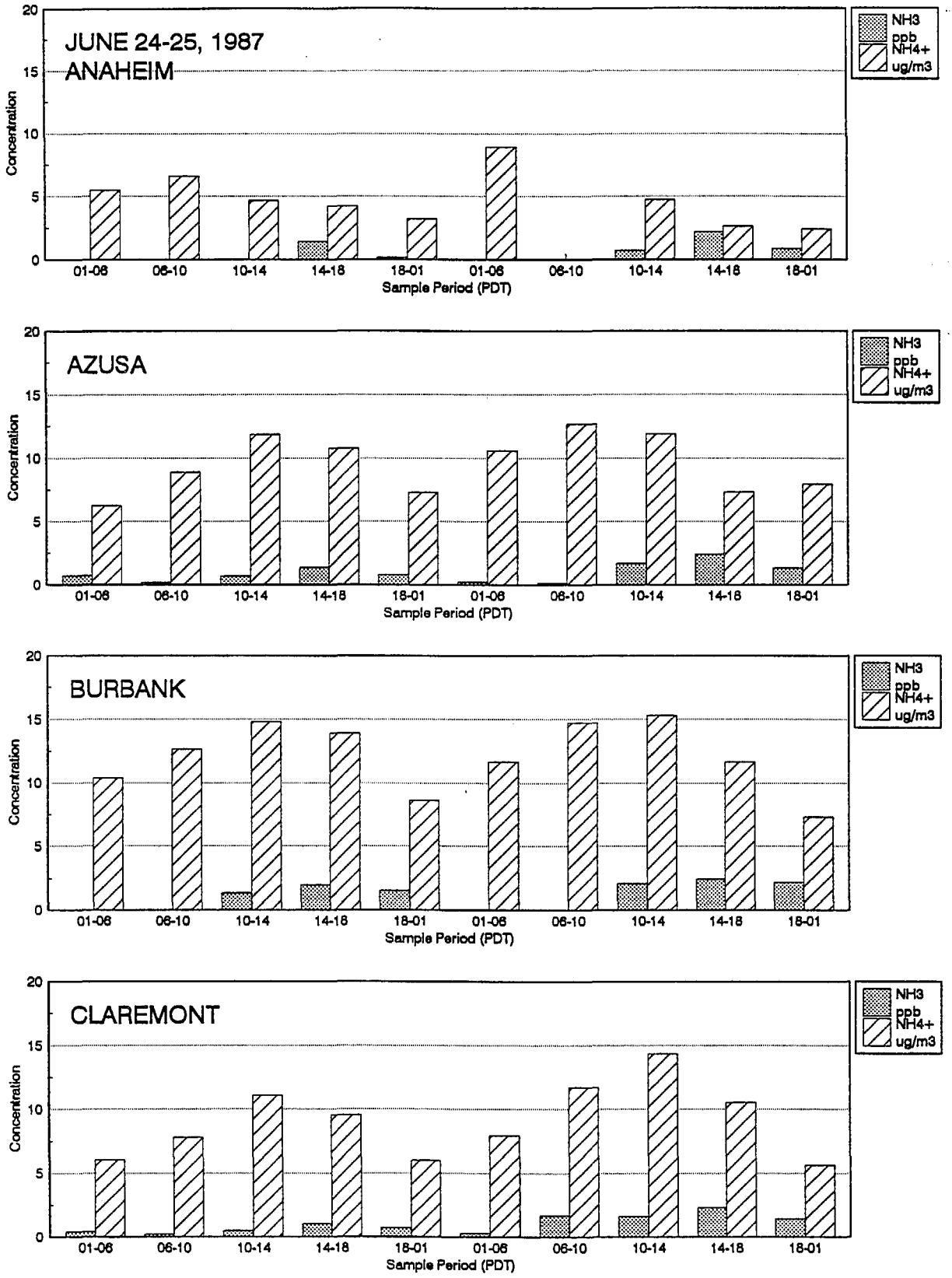

Figure 3-14. Ammonia and $PM_{2.5}$ Ammonium Ion Concentrations on June 24-25, 1987 at Anaheim, Azusa, Burbank, and Claremont.

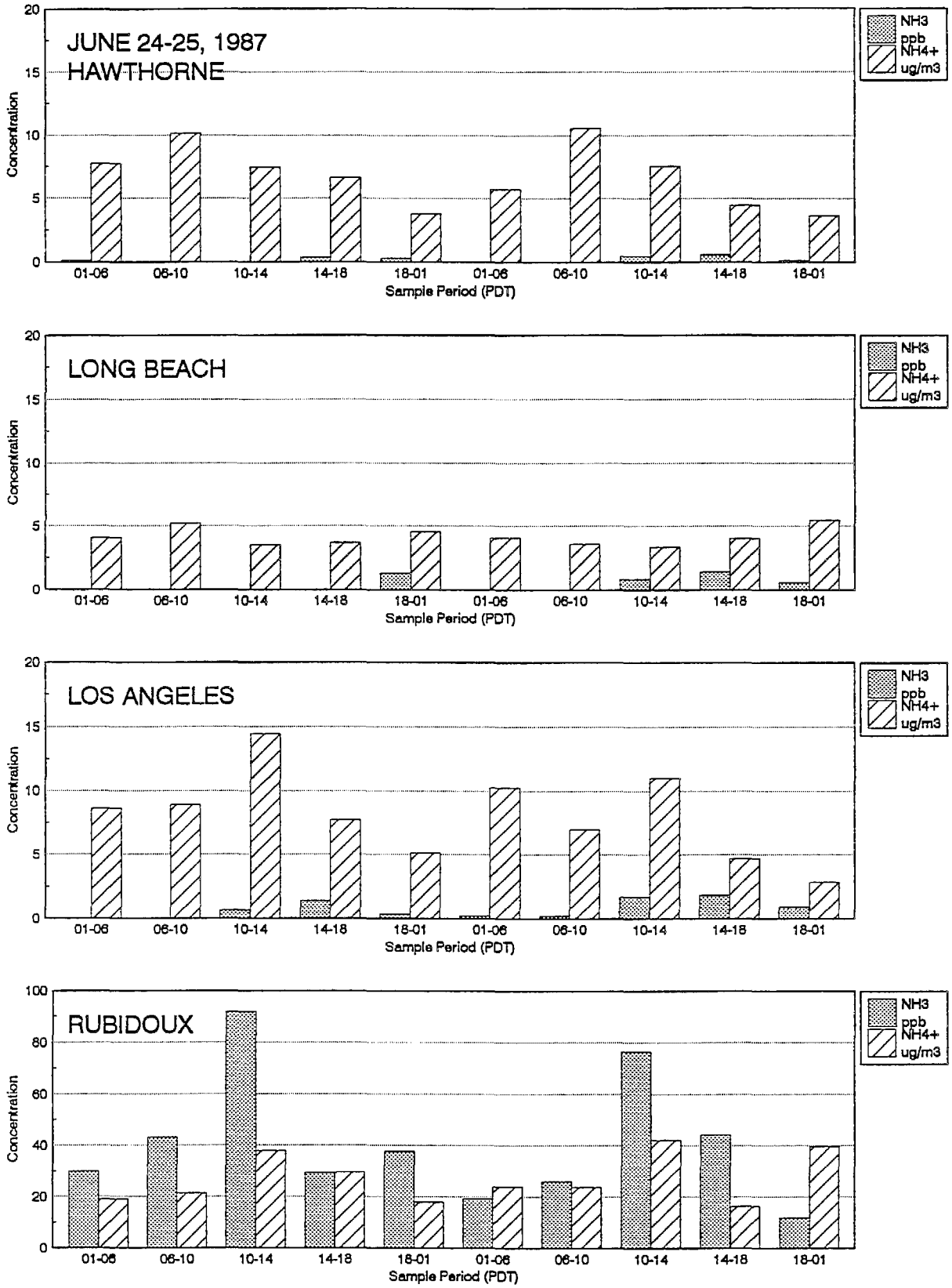

Figure 3-15. Ammonia and $PM_{2.5}$ Ammonium Ion Concentrations on June 24-25, 1987 at Hawthorne, Long Beach, Los Angeles, and Rubidoux. Note that the scale for ammonia and NH_4^+ at Rubidoux is five times higher than the scale the for other sites in Figures 3-14 and 3-15.

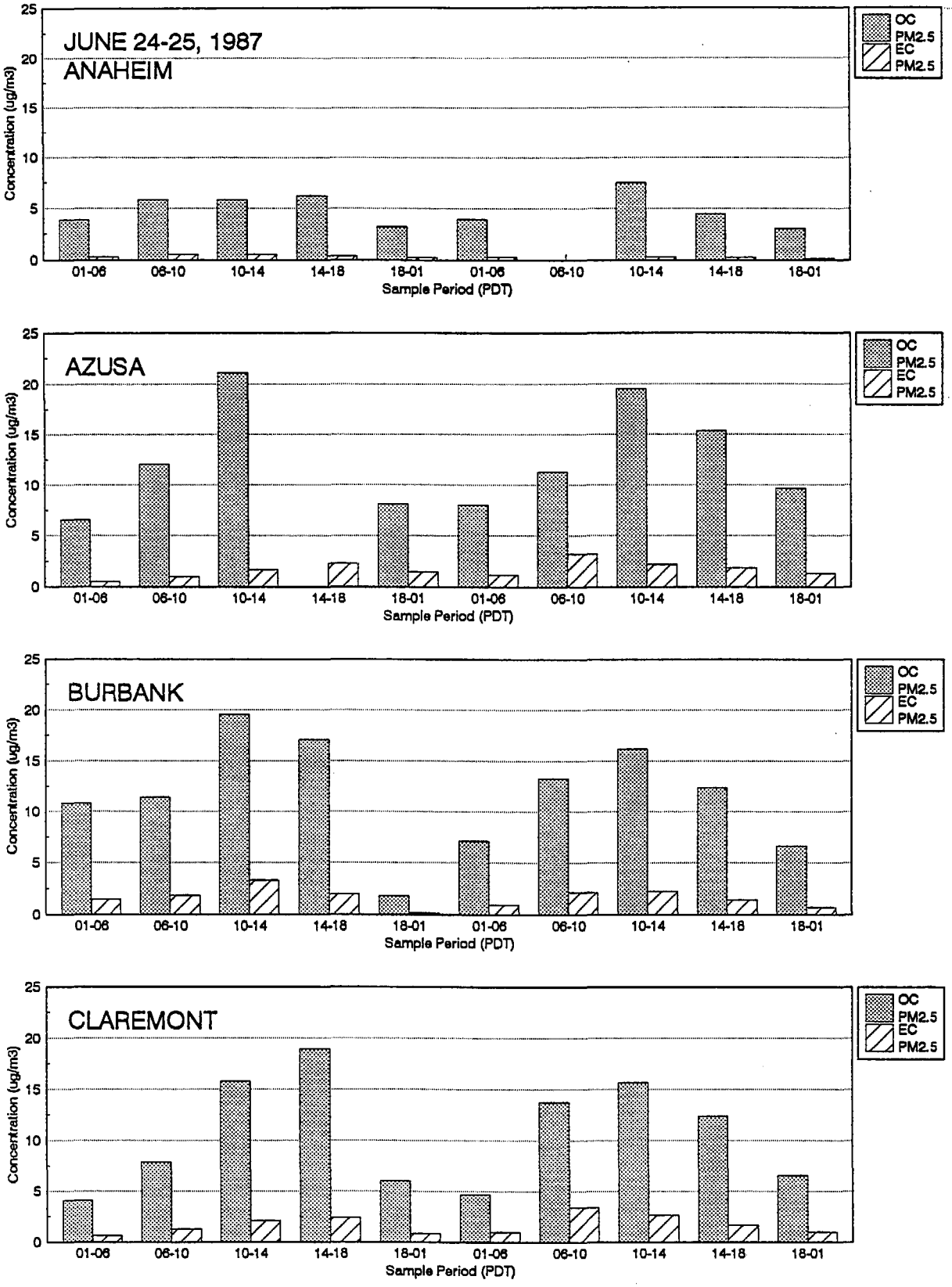

Figure 3-16. $PM_{2.5}$ Organic and Elemental Carbon Concentrations on June 24-25, 1987 at Anaheim, Azusa, Burbank, and Claremont.

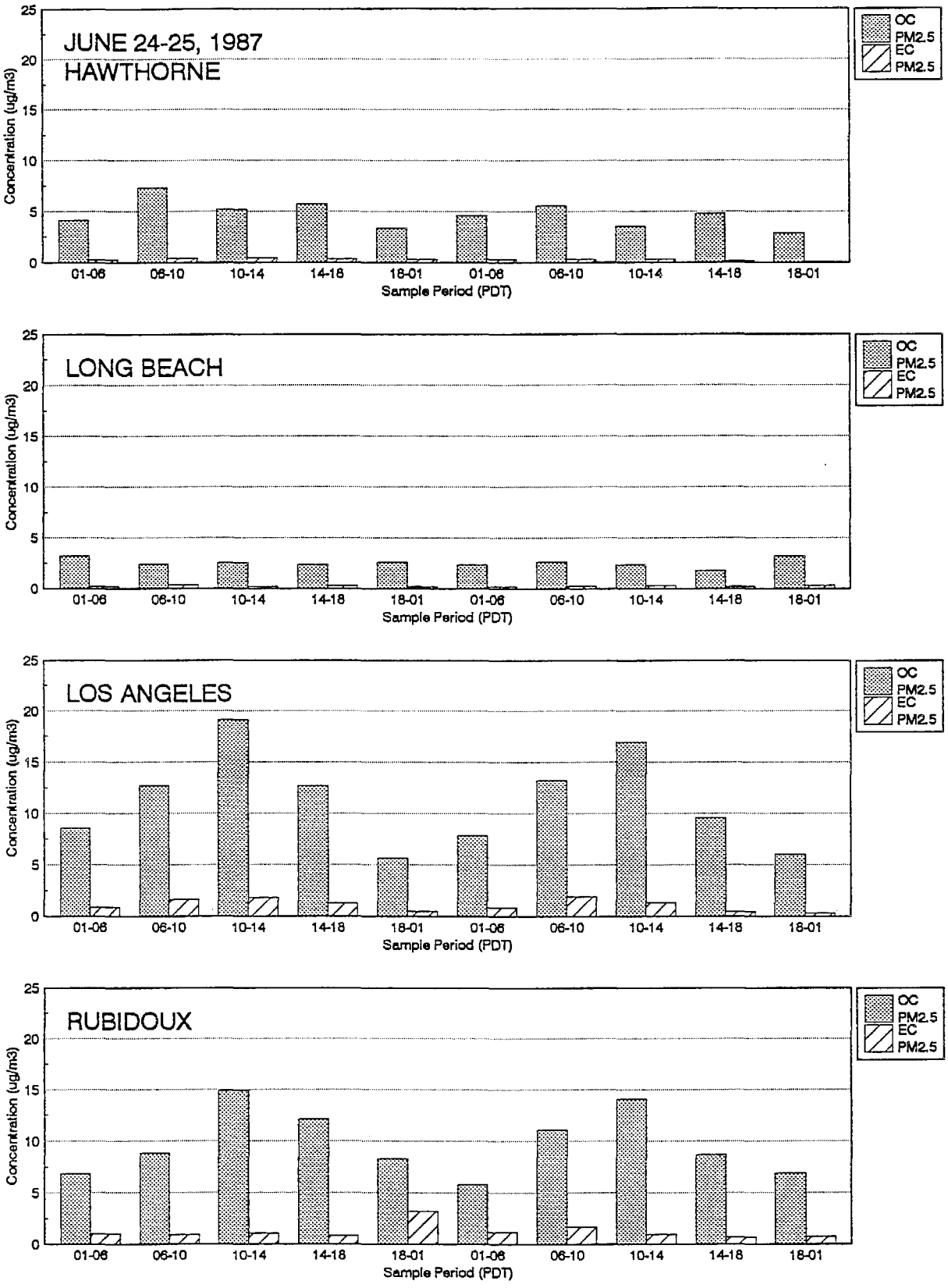

Figure 3-17. $PM_{2.5}$ Organic and Elemental Carbon Concentrations on June 24-25, 1987 at Hawthorne, Long Beach, Los Angeles, and Rubidoux.

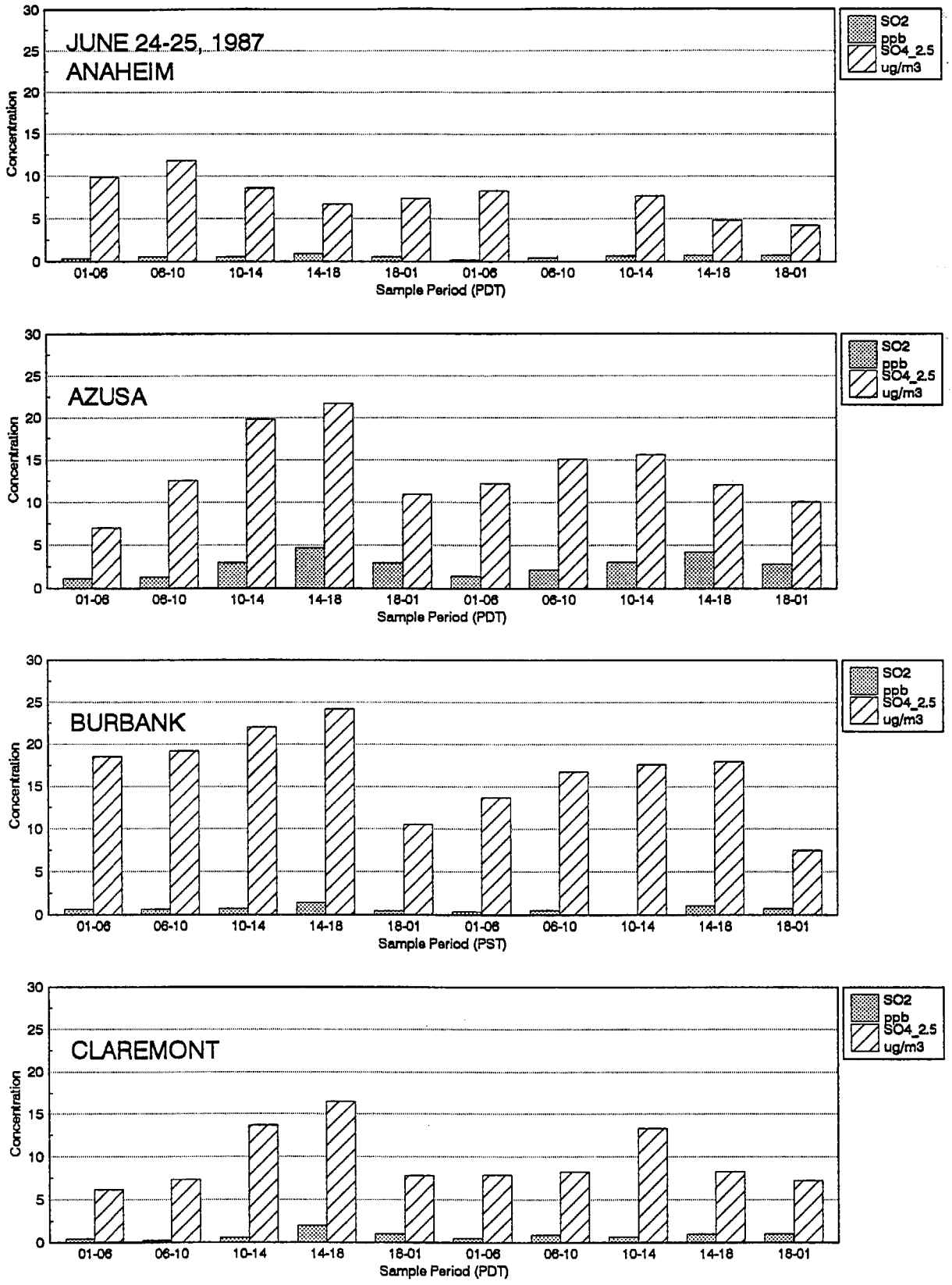

Figure 3-18. SO_2 and $PM_{2.5}$ Sulfate Ion Concentrations on June 24-25, 1987 at Anaheim, Azusa, Burbank, and Claremont.

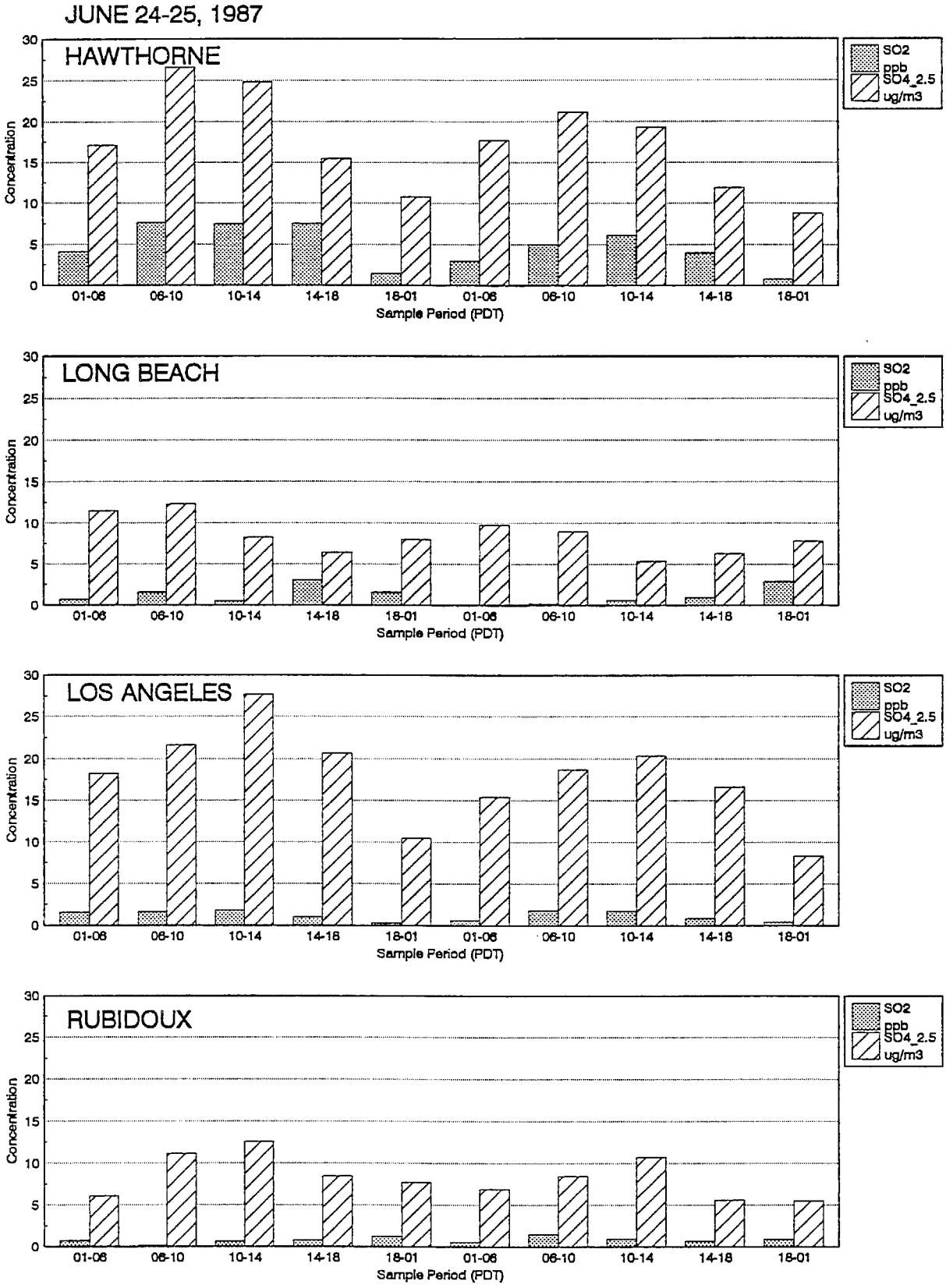

Figure 3-19. SO_2 and $PM_{2.5}$ Sulfate Ion Concentrations on June 24-25, 1987 at Hawthorne, Long Beach, Los Angeles, and Rubidoux.

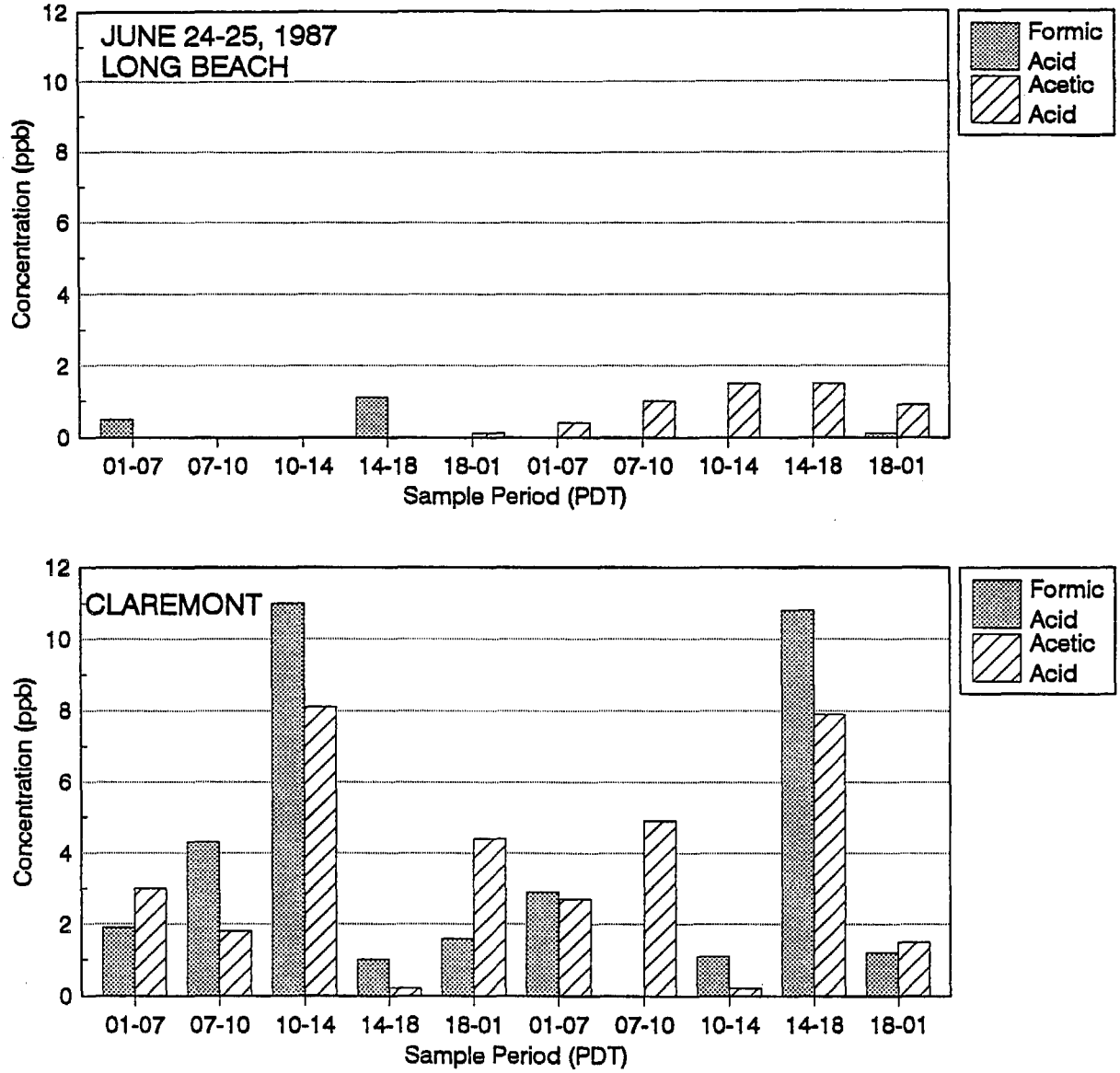

Figure 3-20. Formic and Acetic Acid Concentrations on June 24-25, 1987 at Long Beach and Claremont.

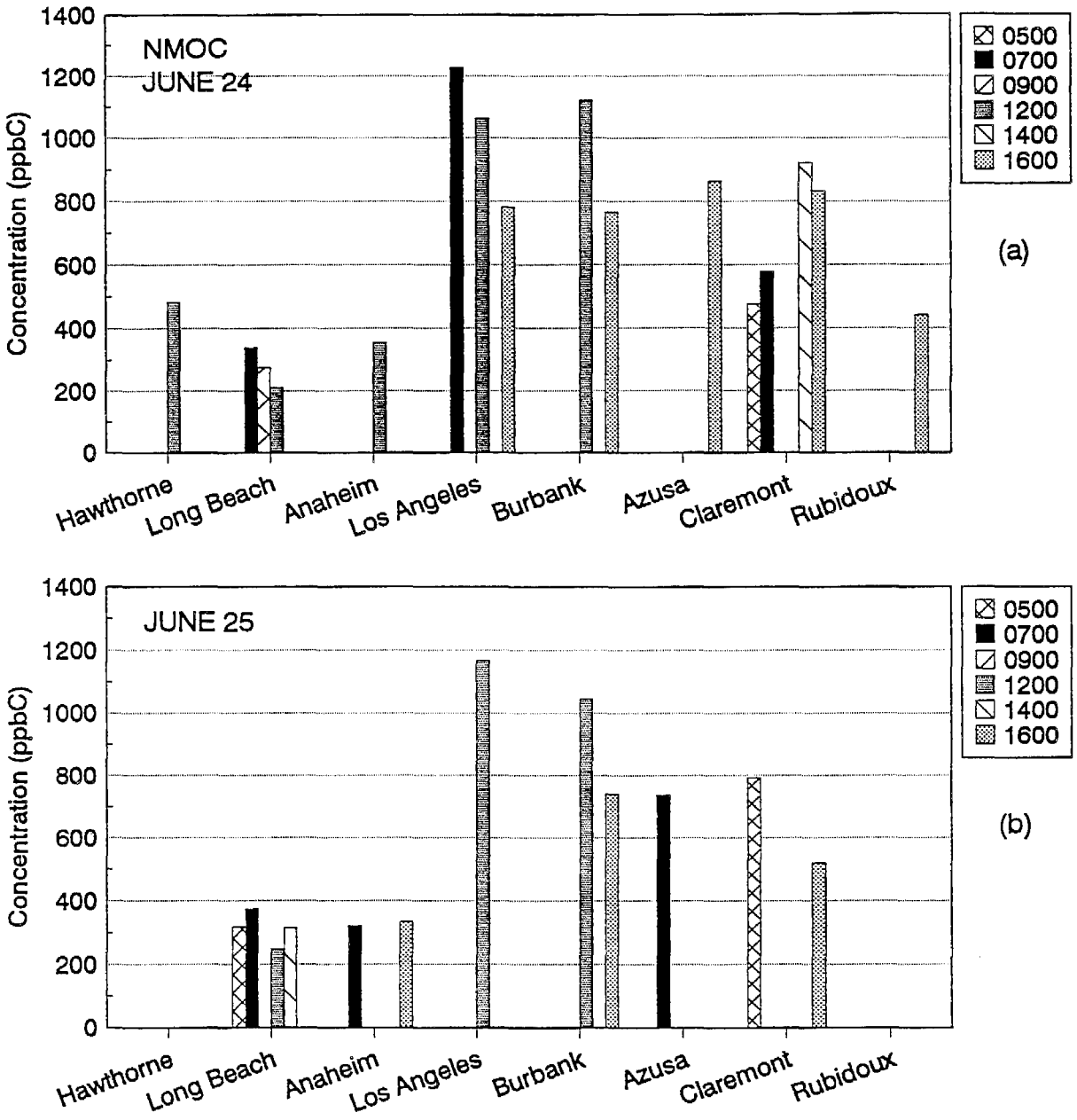

Figure 3-21. NMOC Concentrations at Each Sampling Location on a) June 24, and b) June 25. Samples were not taken at all times at all sites and numerous samples were invalid (see Section 2.1.3).

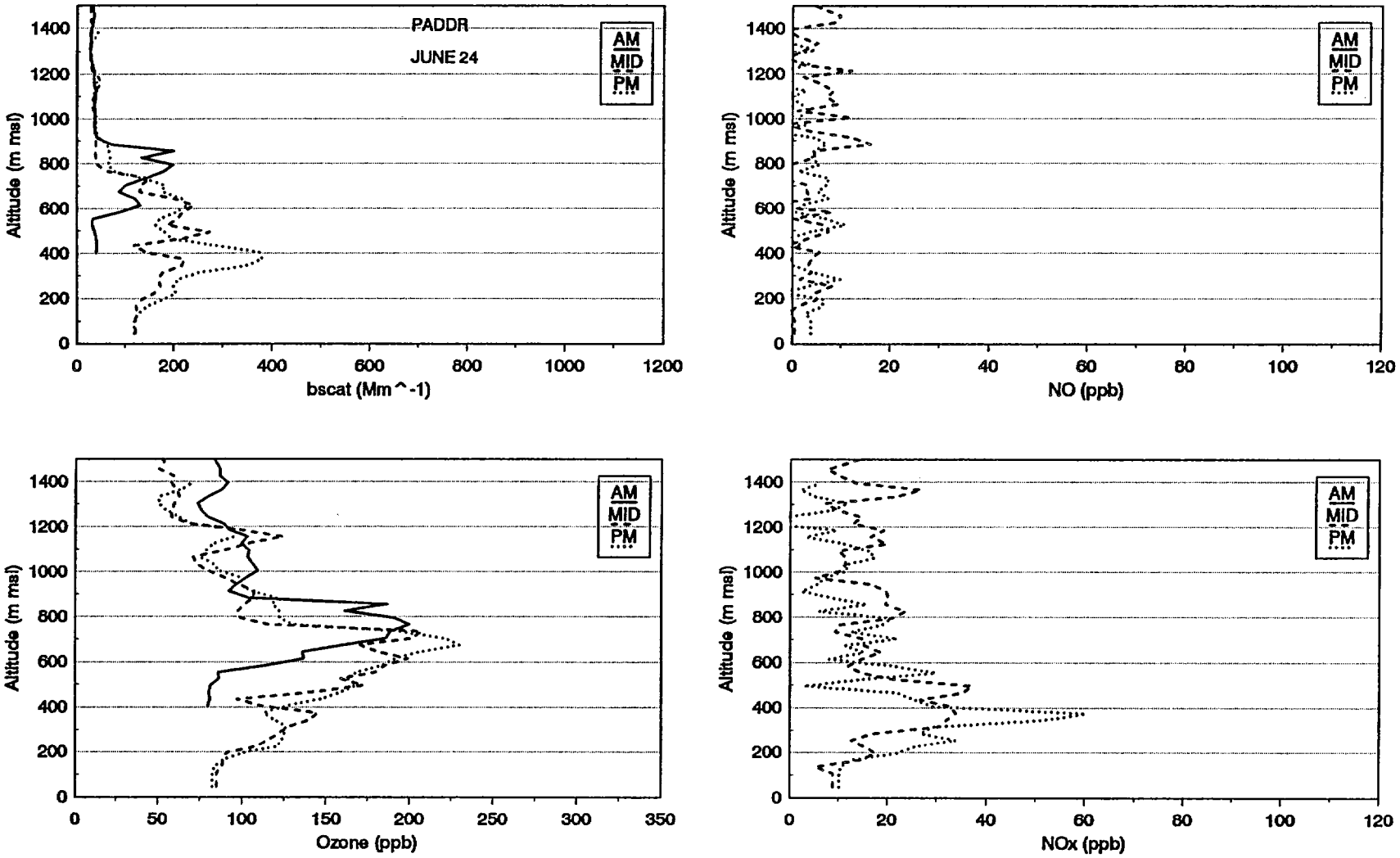

Figure 3-22. Light Scattering (b_{scat}), and Ozone, NO, and NO_x Concentrations for Morning, Midday, and Afternoon Aircraft Spirals on June 24, 1987 at PADDR. The NO_x monitor was inoperable during the morning flight. Morning data were not collected below about 400 m msl because of reduced visibility due to clouds.

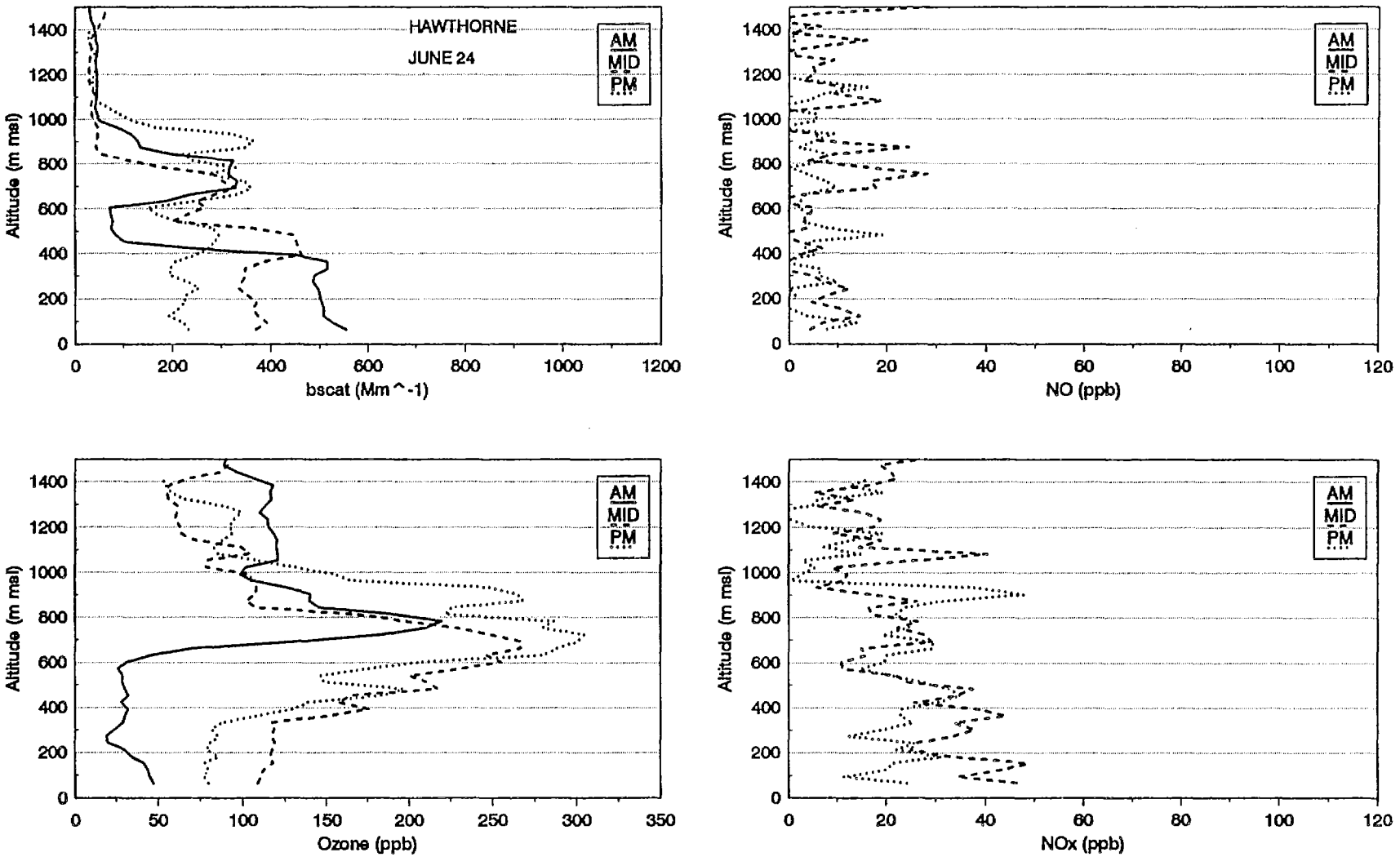

Figure 3-23. Light Scattering (b_{scat}), and Ozone, NO, and NO_x Concentrations for Morning, Midday, and Afternoon Aircraft Spirals on June 24, 1987 at Hawthorne. The NO_x monitor was inoperable during the morning flight.

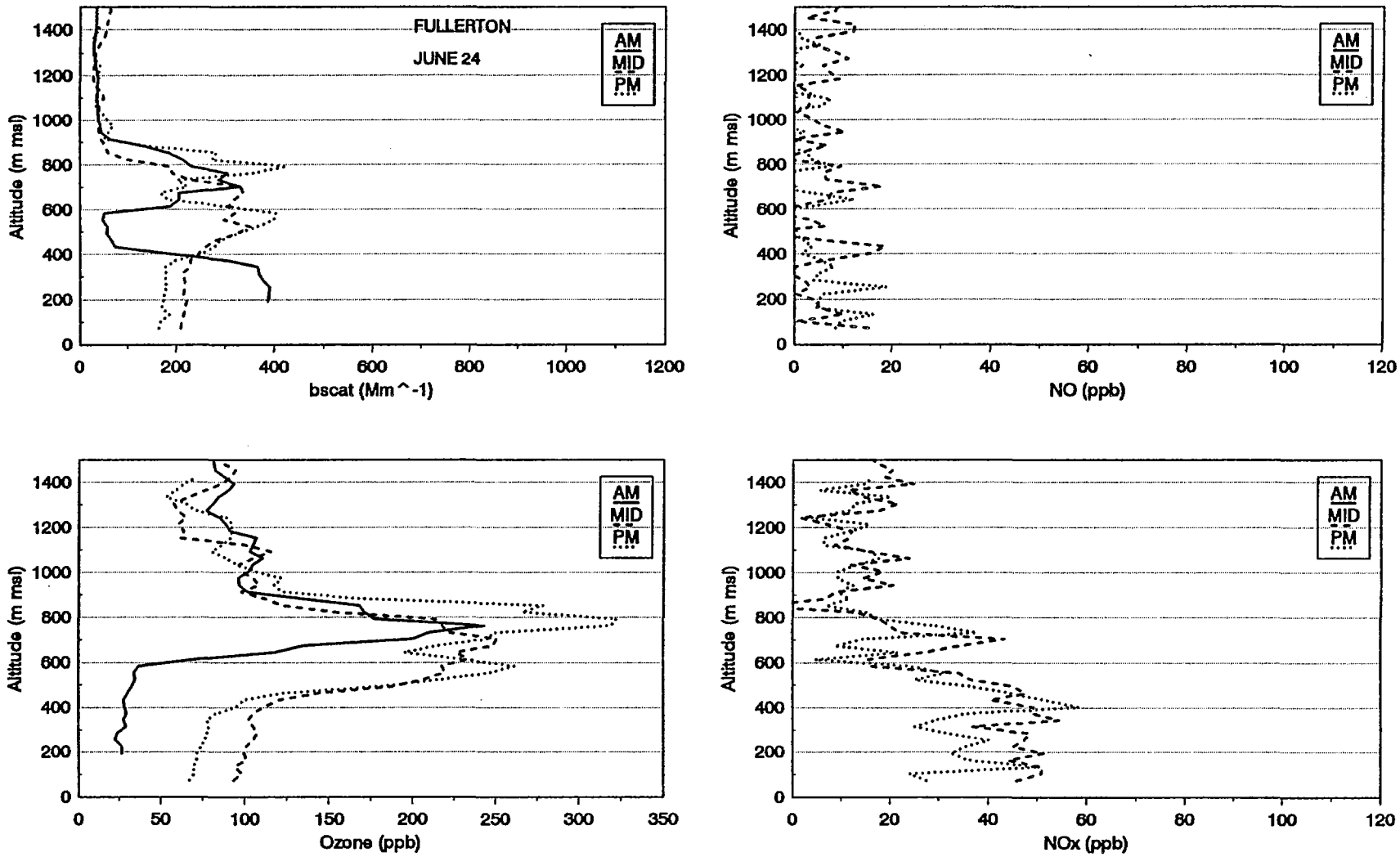

Figure 3-24. Light Scattering (b_{scat}), and Ozone, NO, and NO_x Concentrations for Morning, Midday, and Afternoon Aircraft Spirals on June 24, 1987 at Fullerton. The NO_x monitor was inoperable during the morning flight. Morning data were not collected below about 200 m msl because of reduced visibility due to clouds.

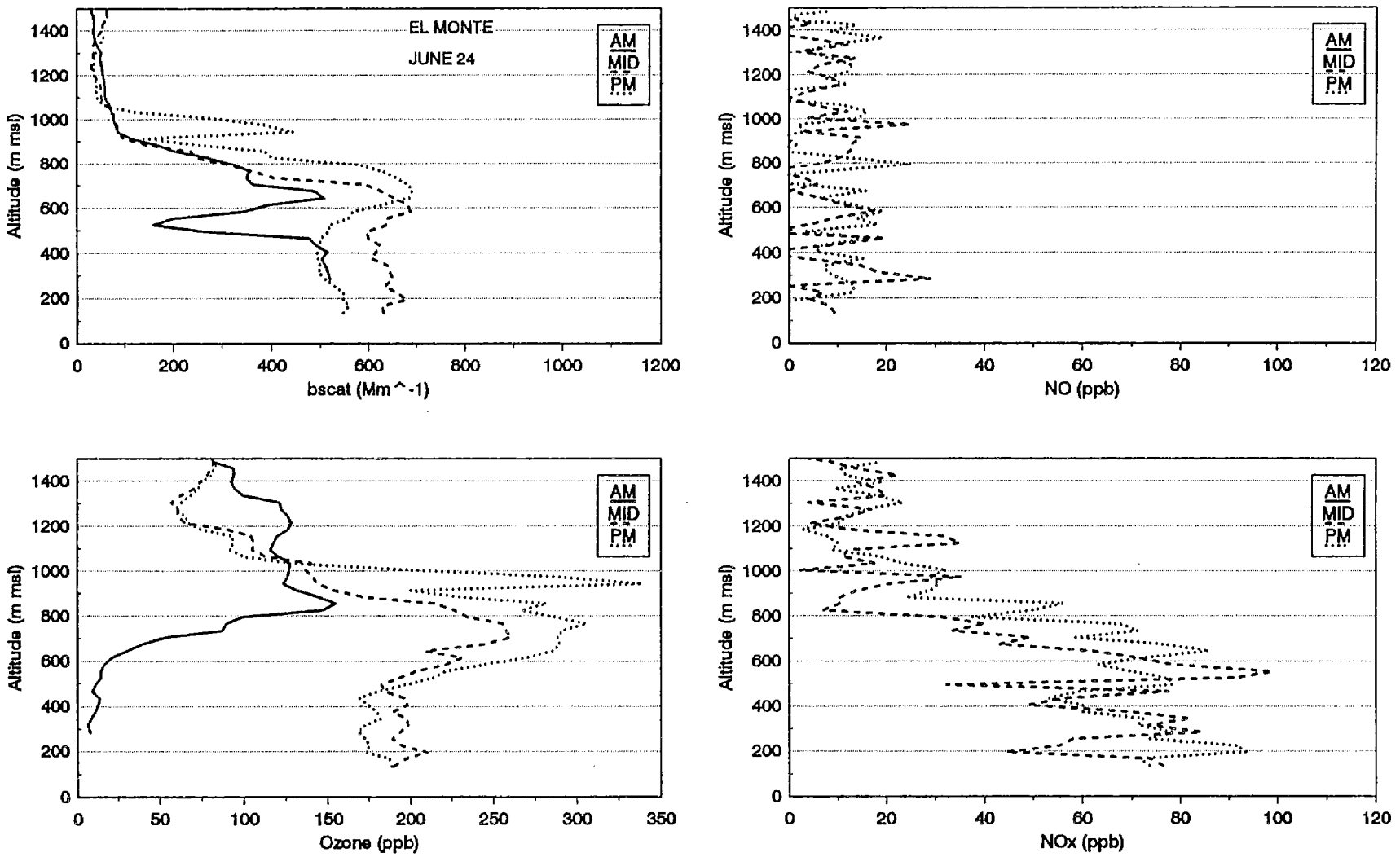

Figure 3-25. Light Scattering (b_{scat}), and Ozone, NO, and NO_x Concentrations for Morning, Midday, and Afternoon Aircraft Spirals on June 24, 1987 at El Monte. The NO_x monitor was inoperable during the morning flight. Morning data were not collected below about 300 m msl because of reduced visibility due to clouds.

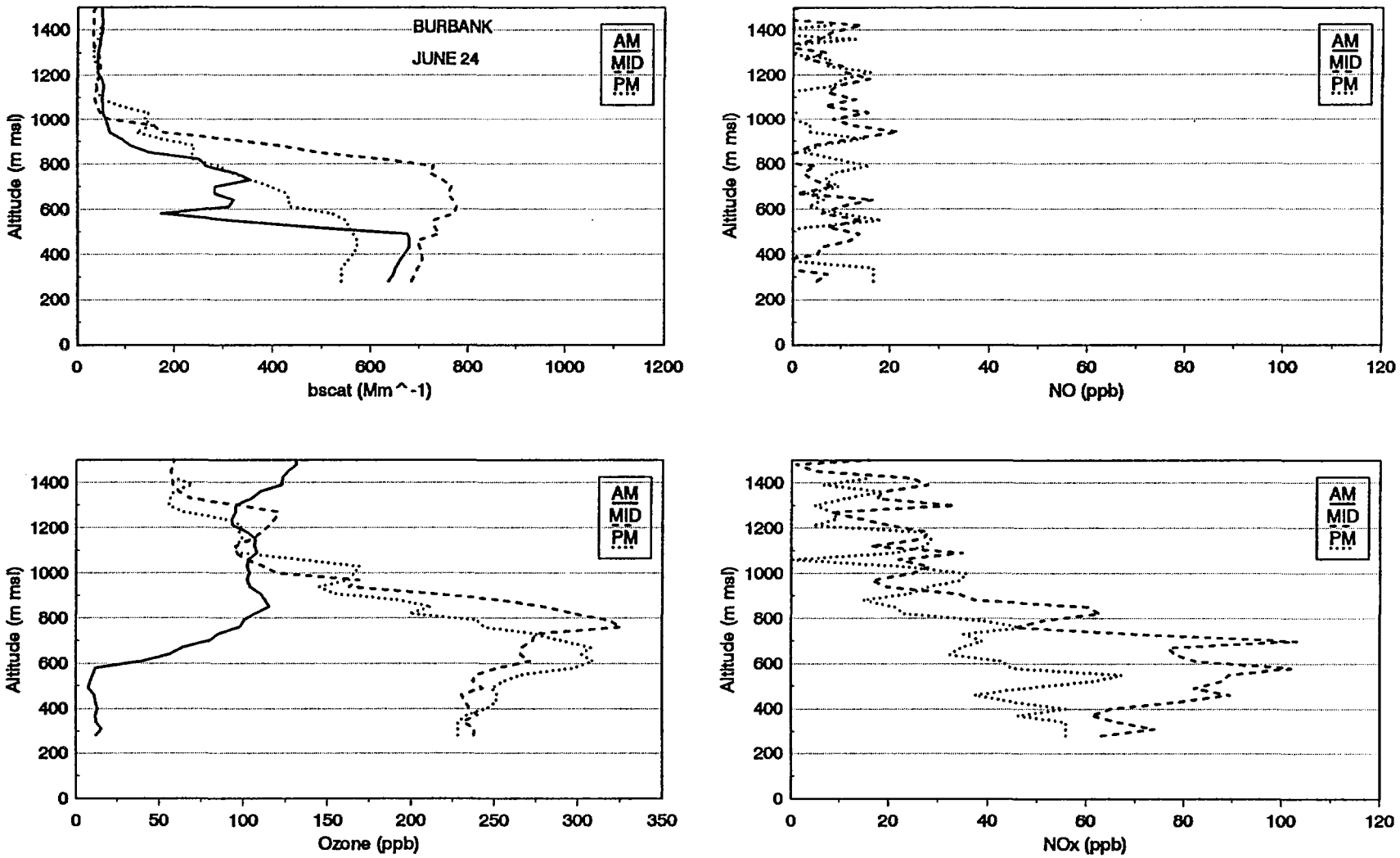

Figure 3-26. Light Scattering (b_{scat}), and Ozone, NO, and NO_x Concentrations for Morning, Midday, and Afternoon Aircraft Spirals on June 24, 1987 at Burbank. The NO_x monitor was inoperable during the morning flight.

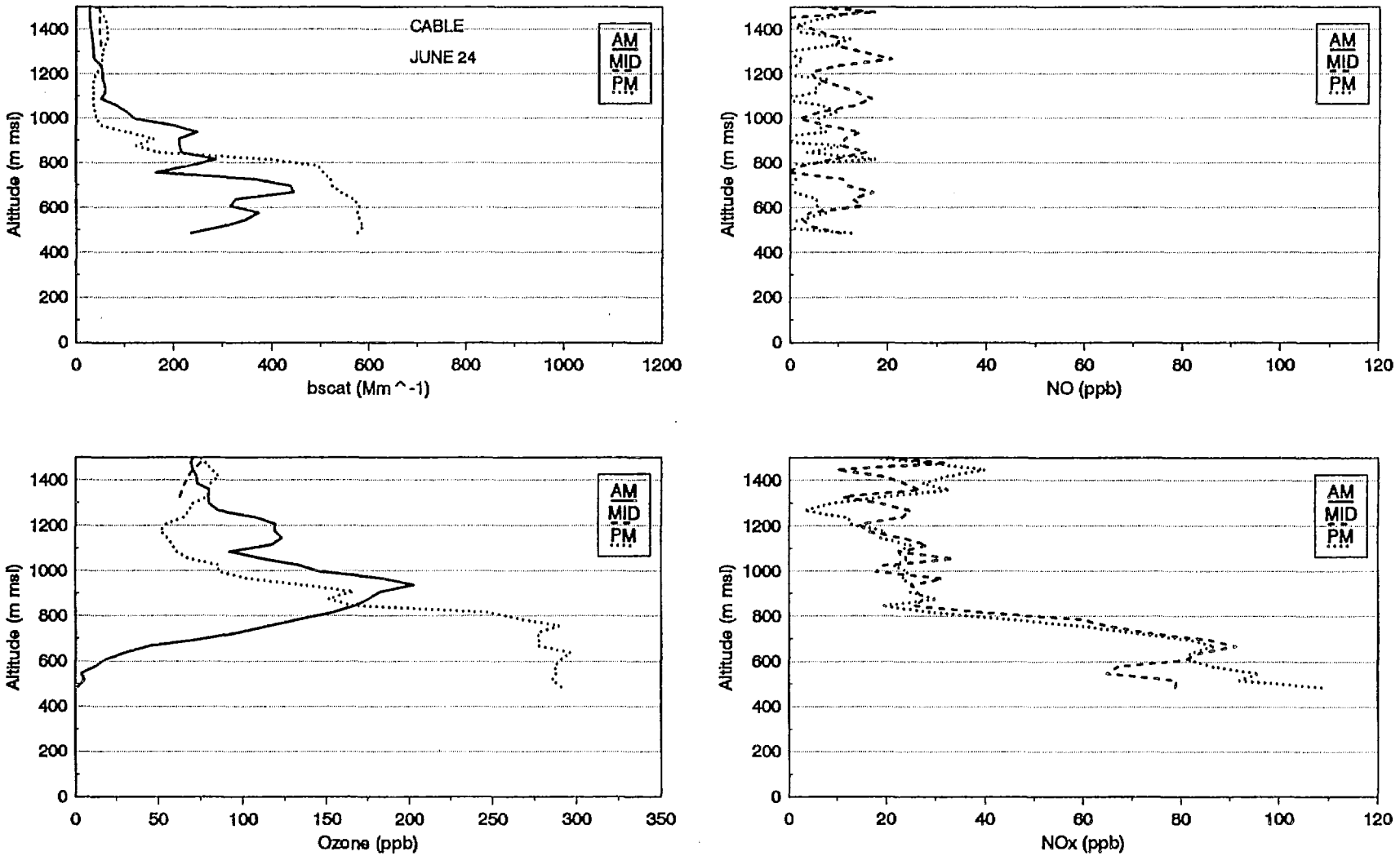

Figure 3-27. Light Scattering (b_{scat}), and Ozone, NO, and NO_x Concentrations for Morning, Midday, and Afternoon Aircraft Spirals on June 24, 1987 at Cable. The NO_x monitor was inoperable during the morning flight.

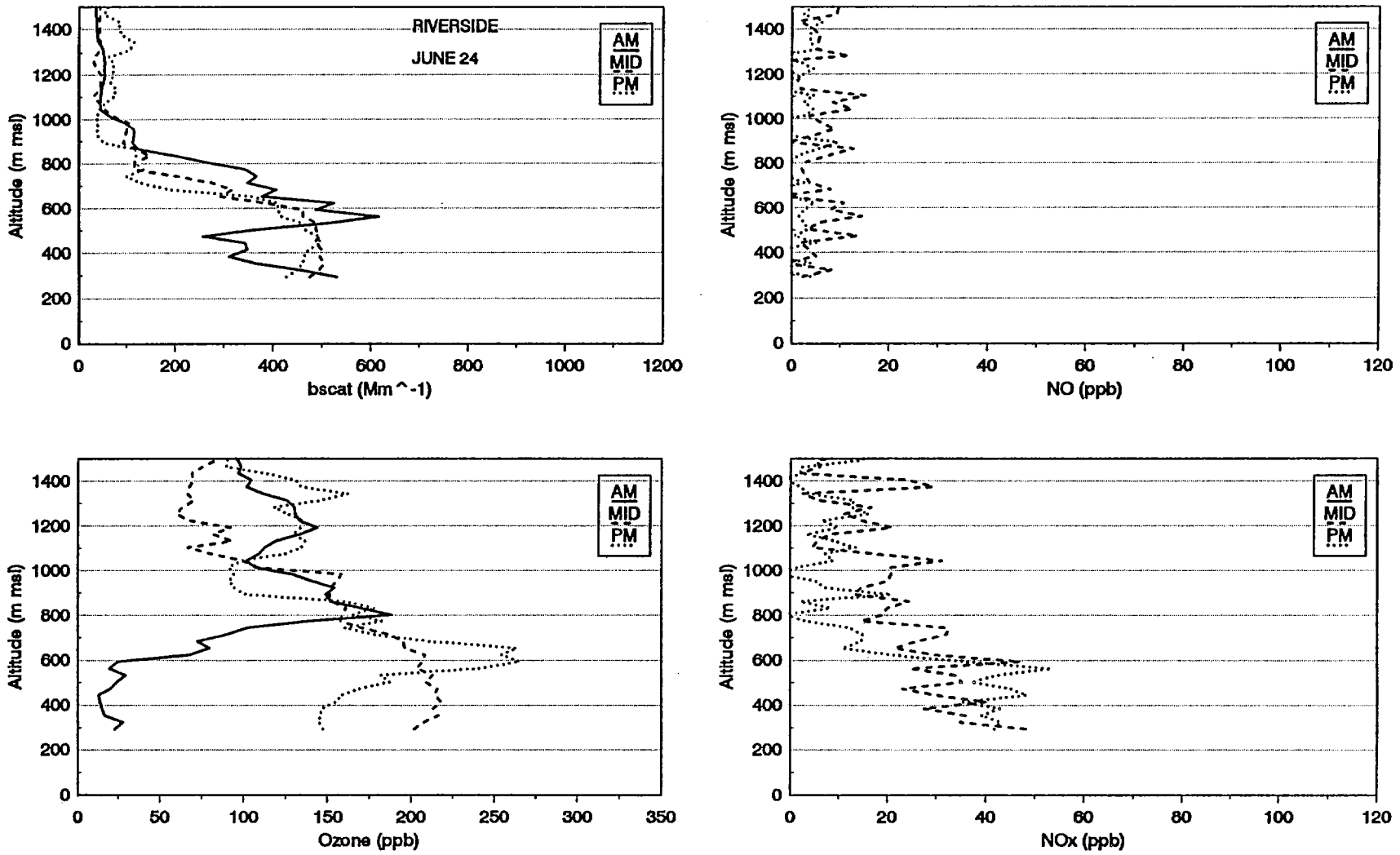

Figure 3-28. Light Scattering (b_{scat}), and Ozone, NO, and NO_x Concentrations for Morning, Midday, and Afternoon Aircraft Spirals on June 24, 1987 at Riverside. The NO_x monitor was inoperable during the morning flight.

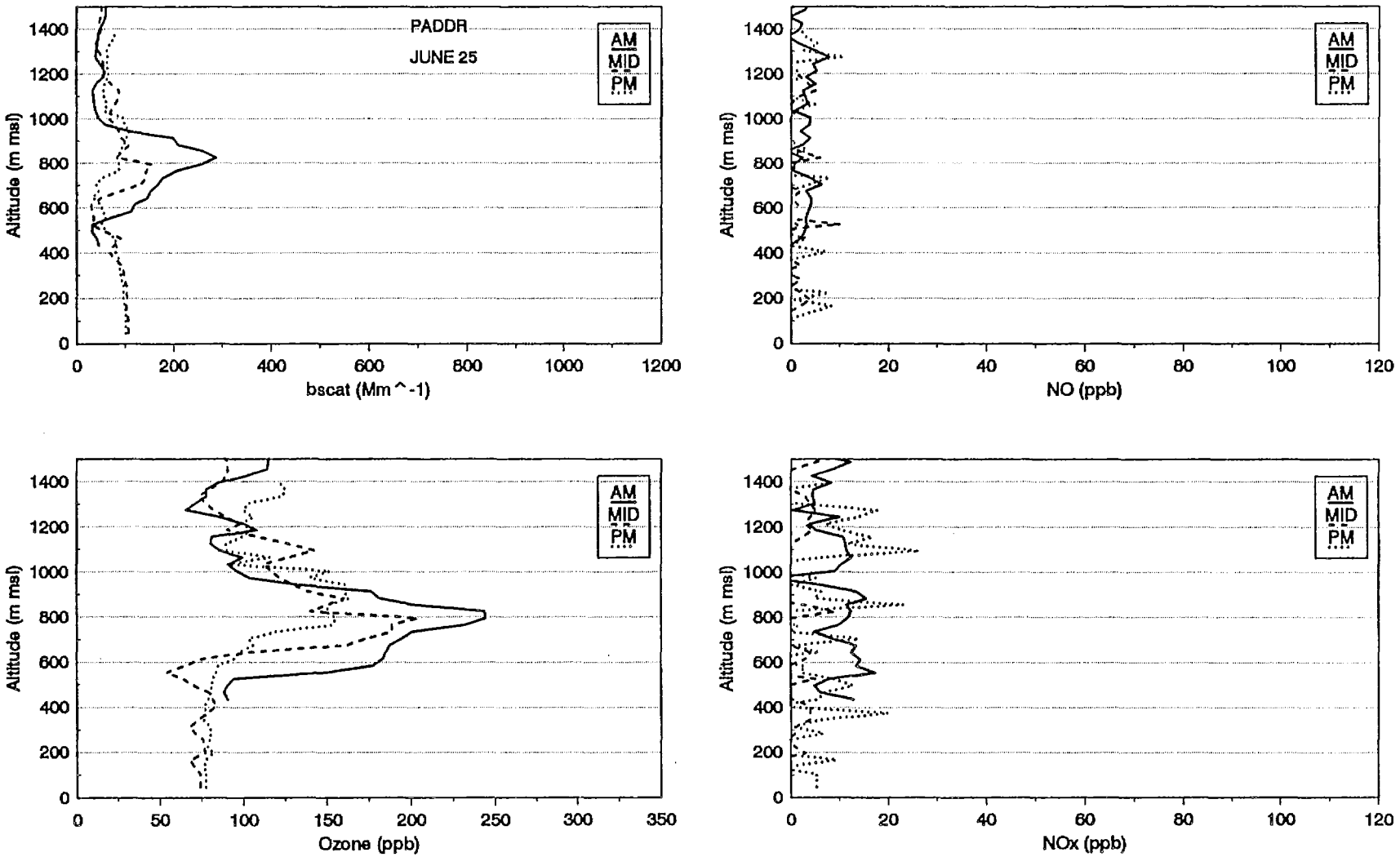

Figure 3-29. Light Scattering (b_{scat}), and Ozone, NO, and NO_x Concentrations for Morning, Midday, and Afternoon Aircraft Spirals on June 25, 1987 at PADDR. Morning data were not collected below about 400 m msl because of reduced visibility due to clouds.

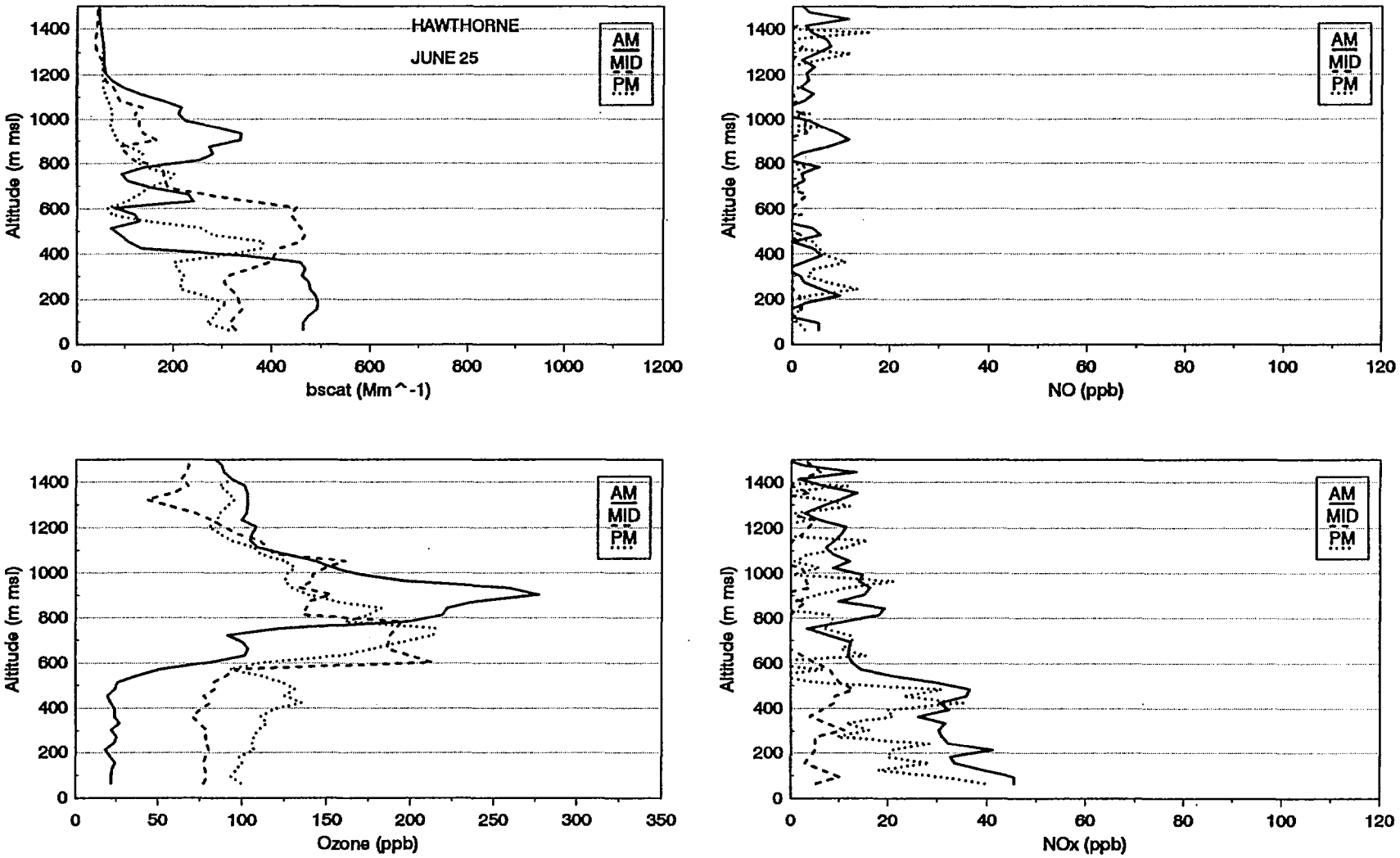

Figure 3-30. Light Scattering (b_{scat}), and Ozone, NO, and NO_x Concentrations for Morning, Midday, and Afternoon Aircraft Spirals on June 25, 1987 at Hawthorne.

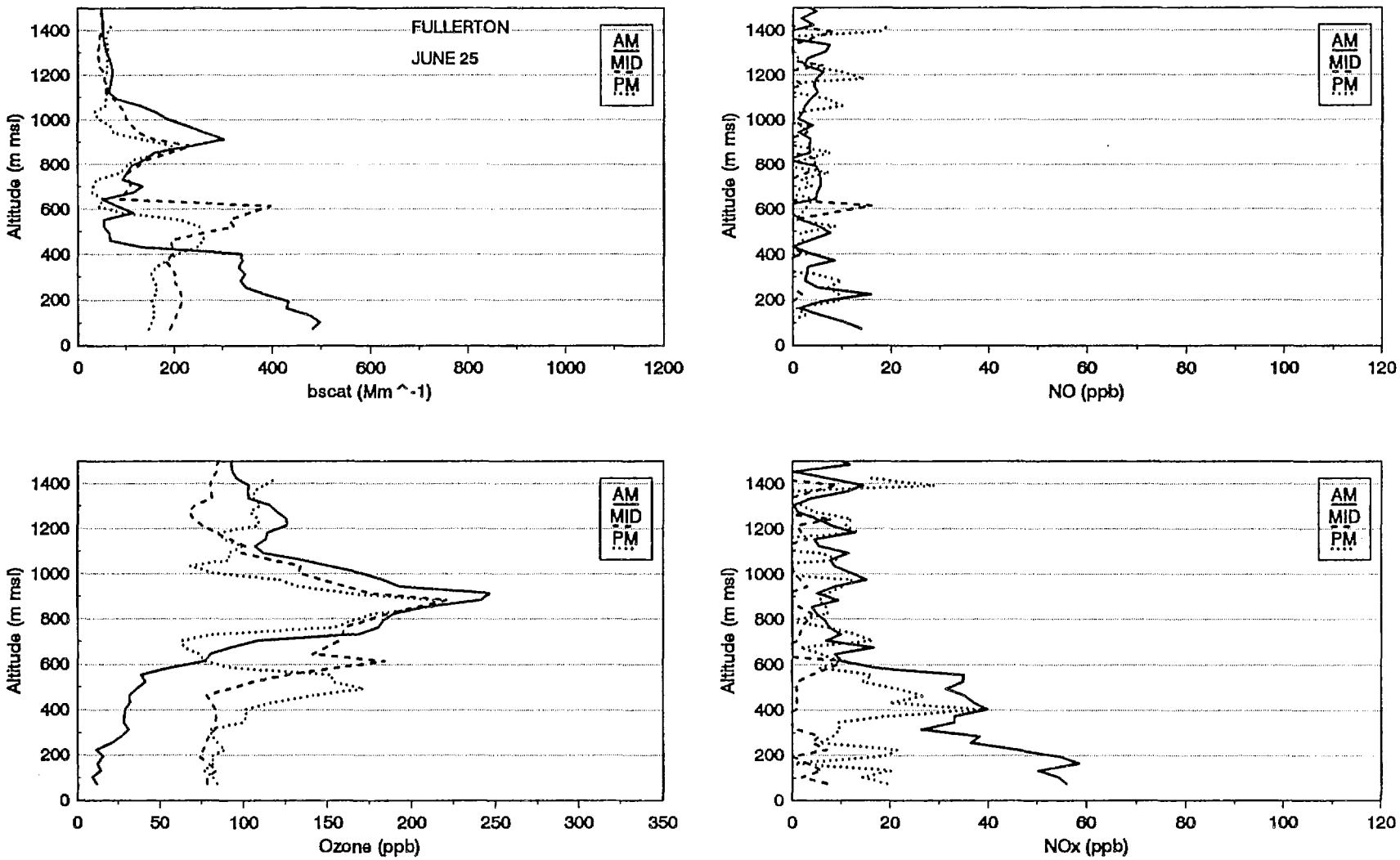

Figure 3-31. Light Scattering (b_{scat}), and Ozone, NO, and NO_x Concentrations for Morning, Midday, and Afternoon Aircraft Spirals on June 25, 1987 at Fullerton.

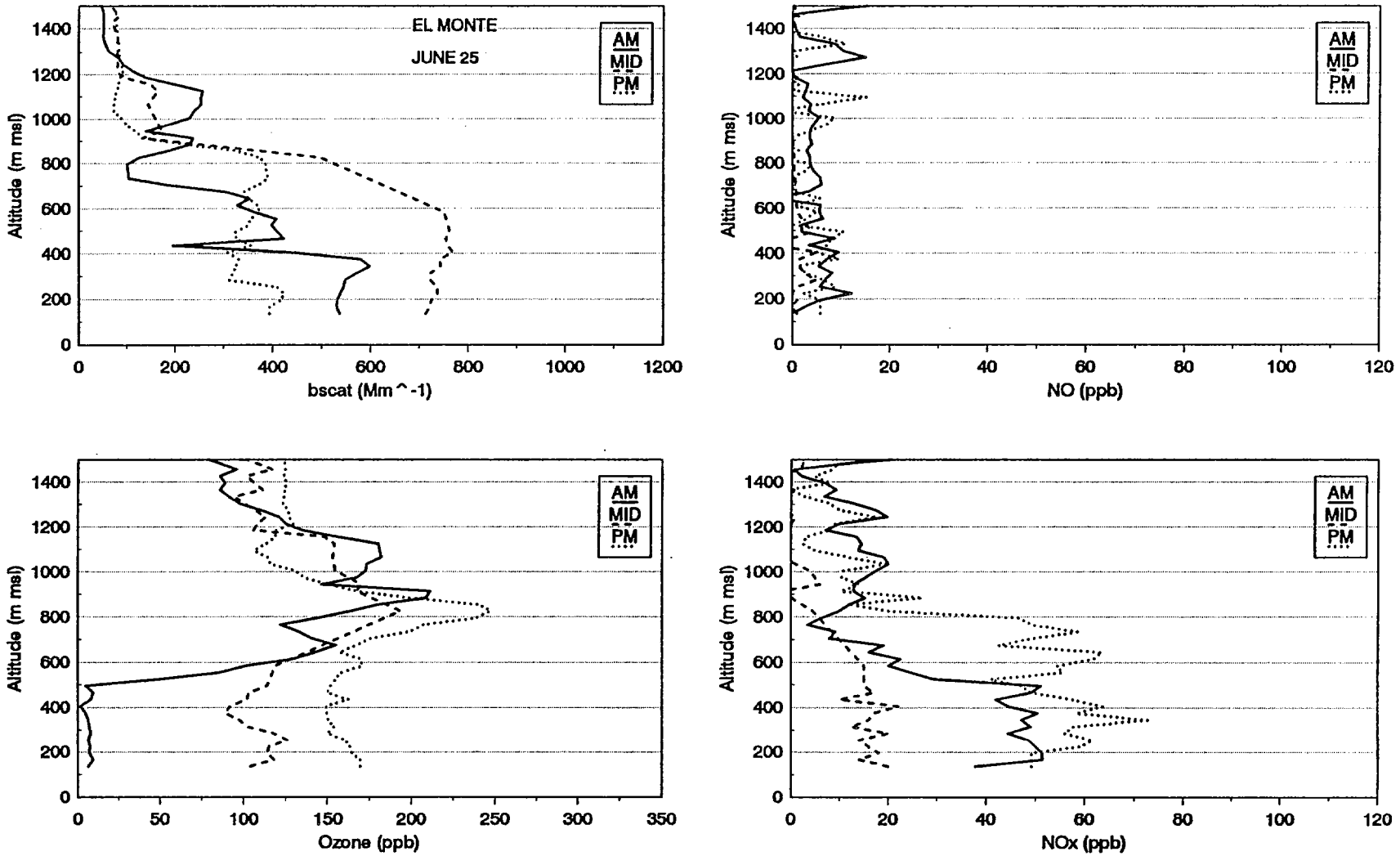

Figure 3-32. Light Scattering (b_{scat}), and Ozone, NO, and NO_x Concentrations for Morning, Midday, and Afternoon Aircraft Spirals on June 25, 1987 at El Monte.

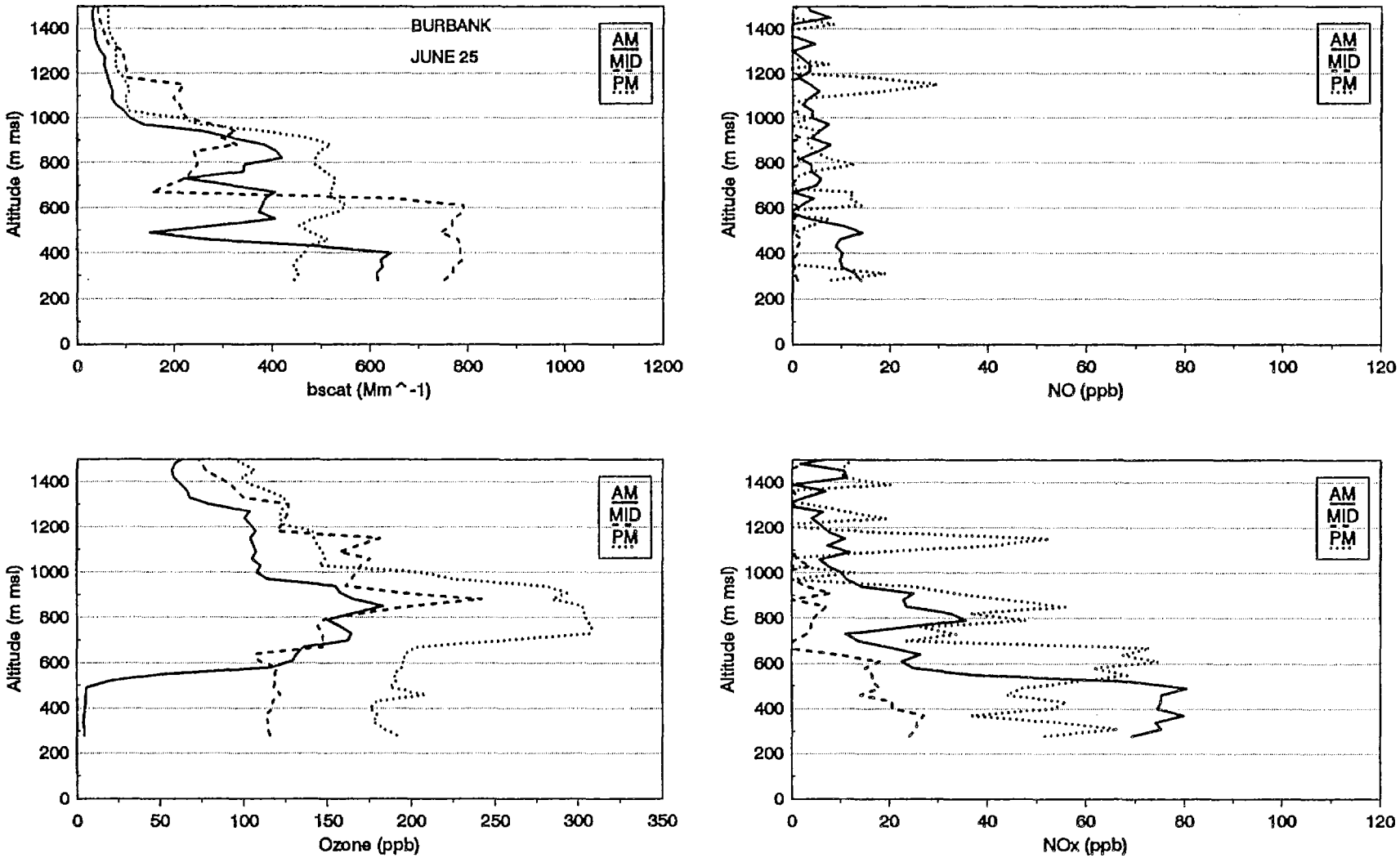

Figure 3-33. Light Scattering (b_{scat}), and Ozone, NO, and NO_x Concentrations for Morning, Midday, and Afternoon Aircraft Spirals on June 25, 1987 at Burbank.

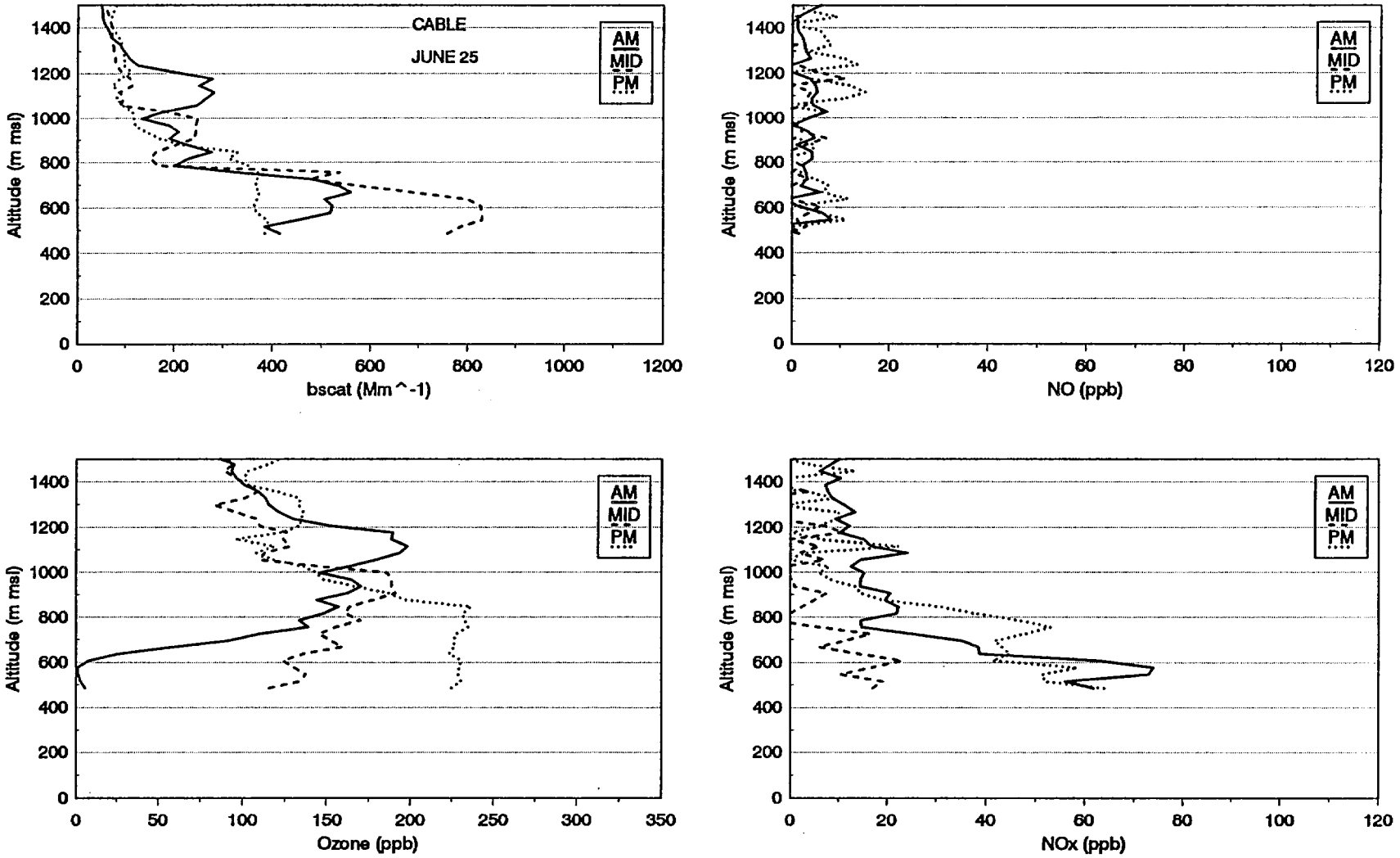

Figure 3-34. Light Scattering (b_{scat}), and Ozone, NO, and NO_x Concentrations for Morning, Midday, and Afternoon Aircraft Spirals on June 25, 1987 at Cable.

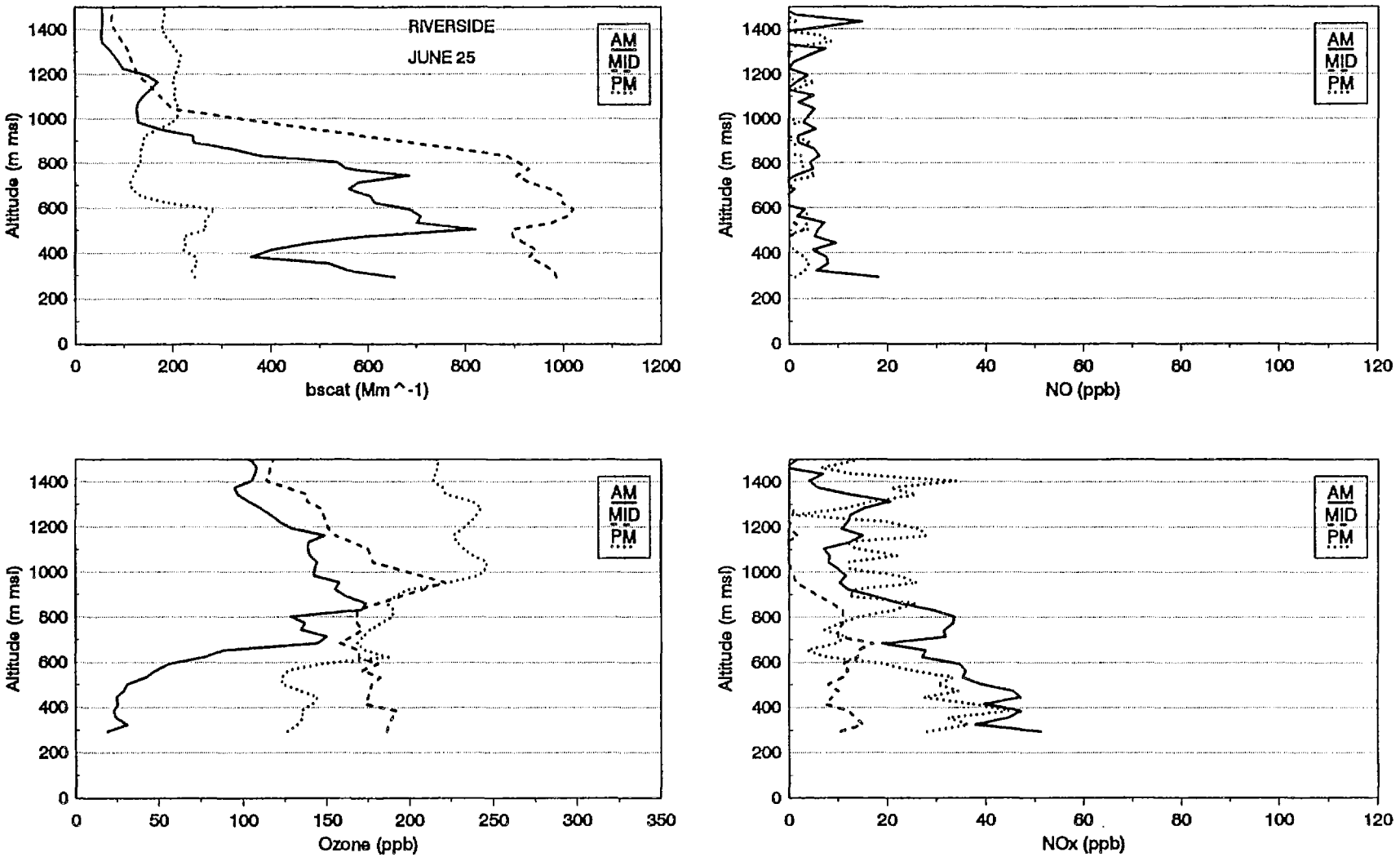

Figure 3-35. Light Scattering (b_{scat}), and Ozone, NO, and NO_x Concentrations for Morning, Midday, and Afternoon Aircraft Spirals on June 25, 1987 at Riverside.

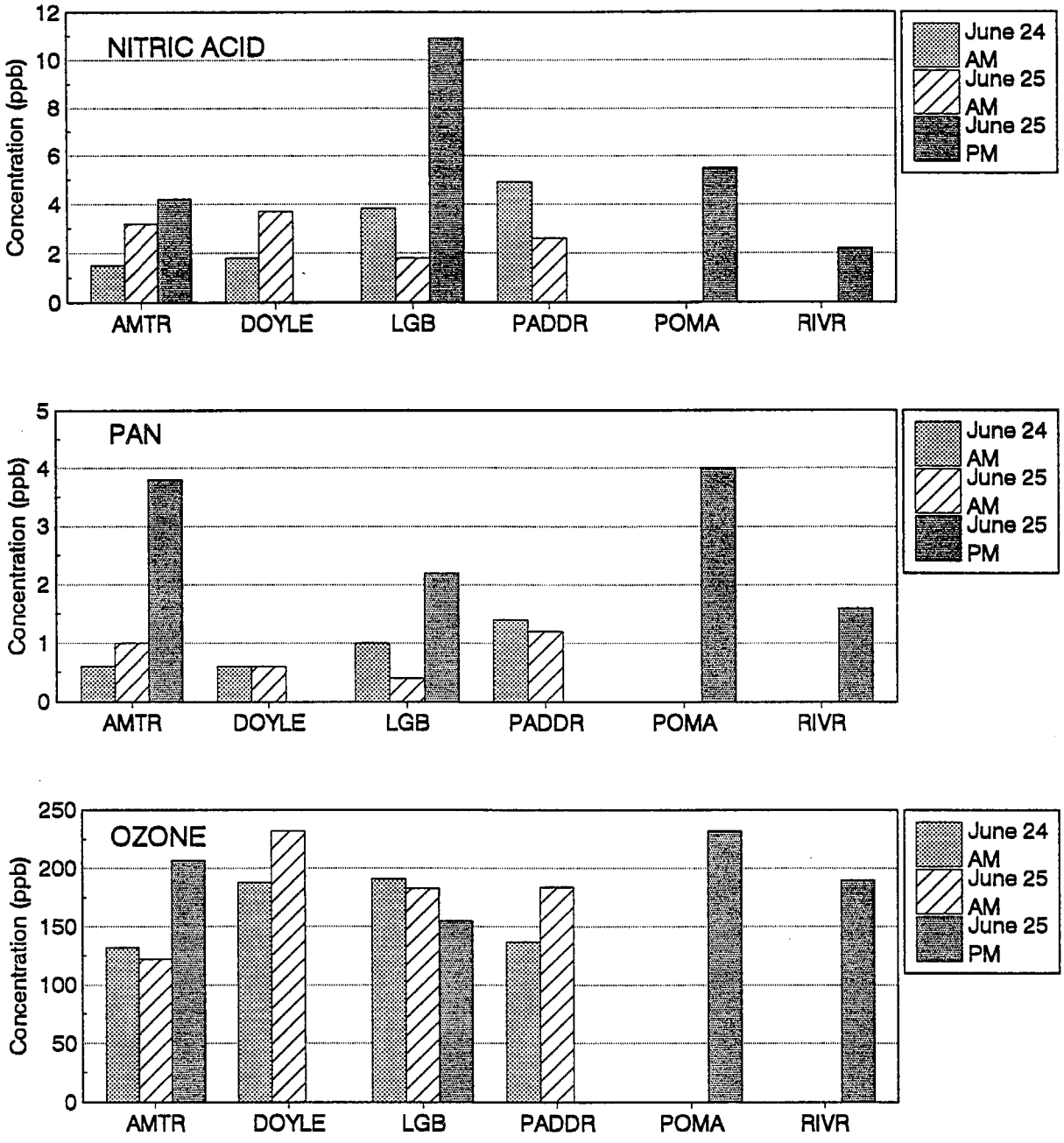

ALL SAMPLES COLLECTED ABOVE THE MIXED LAYER
EXCEPT POMONA, WHICH WAS COLLECTED WITHIN THE MIXED LAYER

Figure 3-36. Orbit-Averages of Nitric Acid, PAN, and Ozone Measured Aloft on June 24-25 for Each Orbit Location. All samples were collected above the mixed layer except the sample collected at Pomona on the afternoon of June 25.

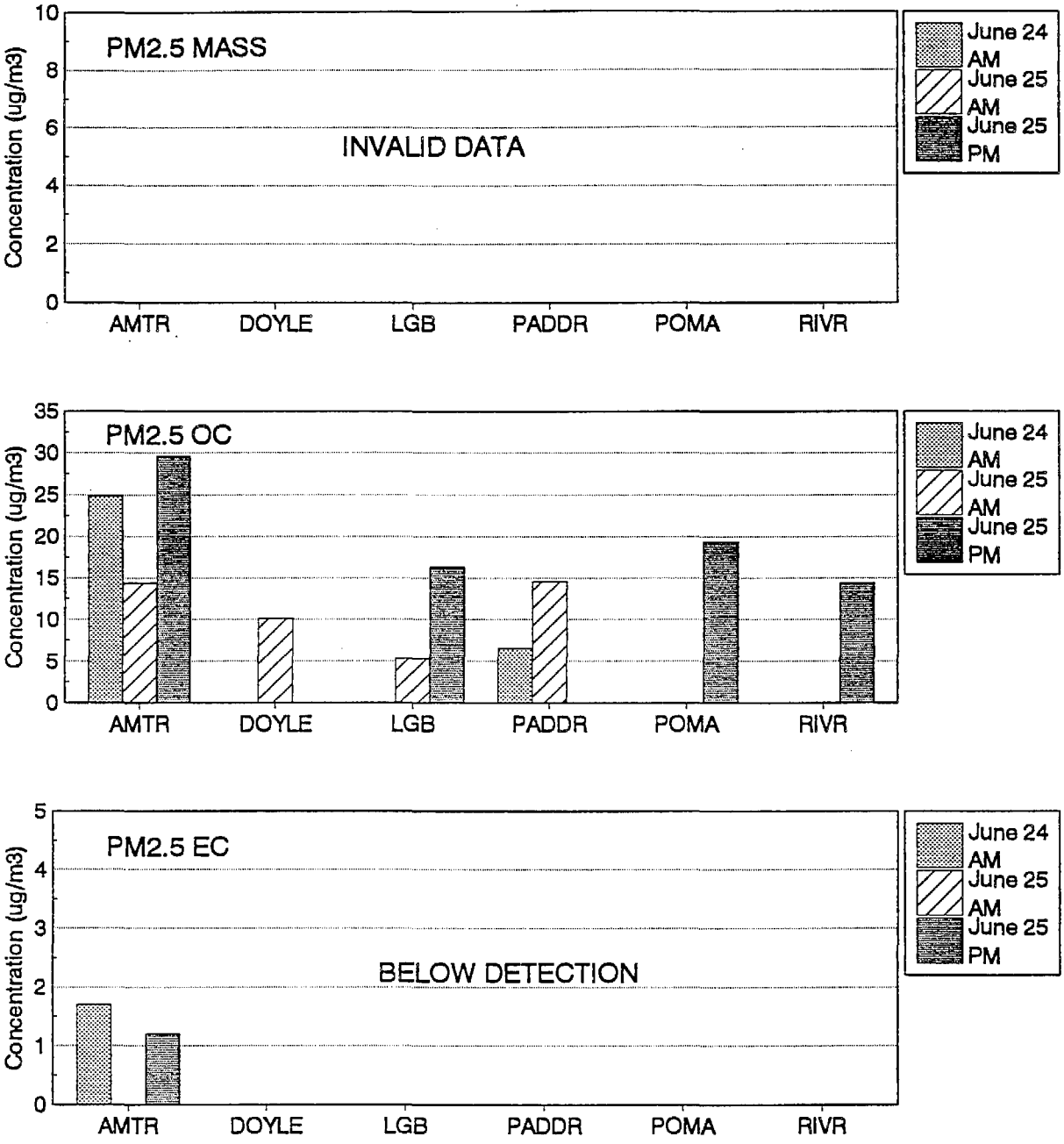

ALL SAMPLES COLLECTED ABOVE THE MIXED LAYER
EXCEPT POMONA, WHICH WAS COLLECTED WITHIN THE MIXED LAYER

Figure 3-37. Orbit-Averages of $PM_{2.5}$ Mass, Organic Carbon, and Elemental Carbon Measured Aloft on June 24-25 for Each Orbit Location. All samples were collected above the mixed layer except the sample collected at Pomona on the afternoon of June 25.

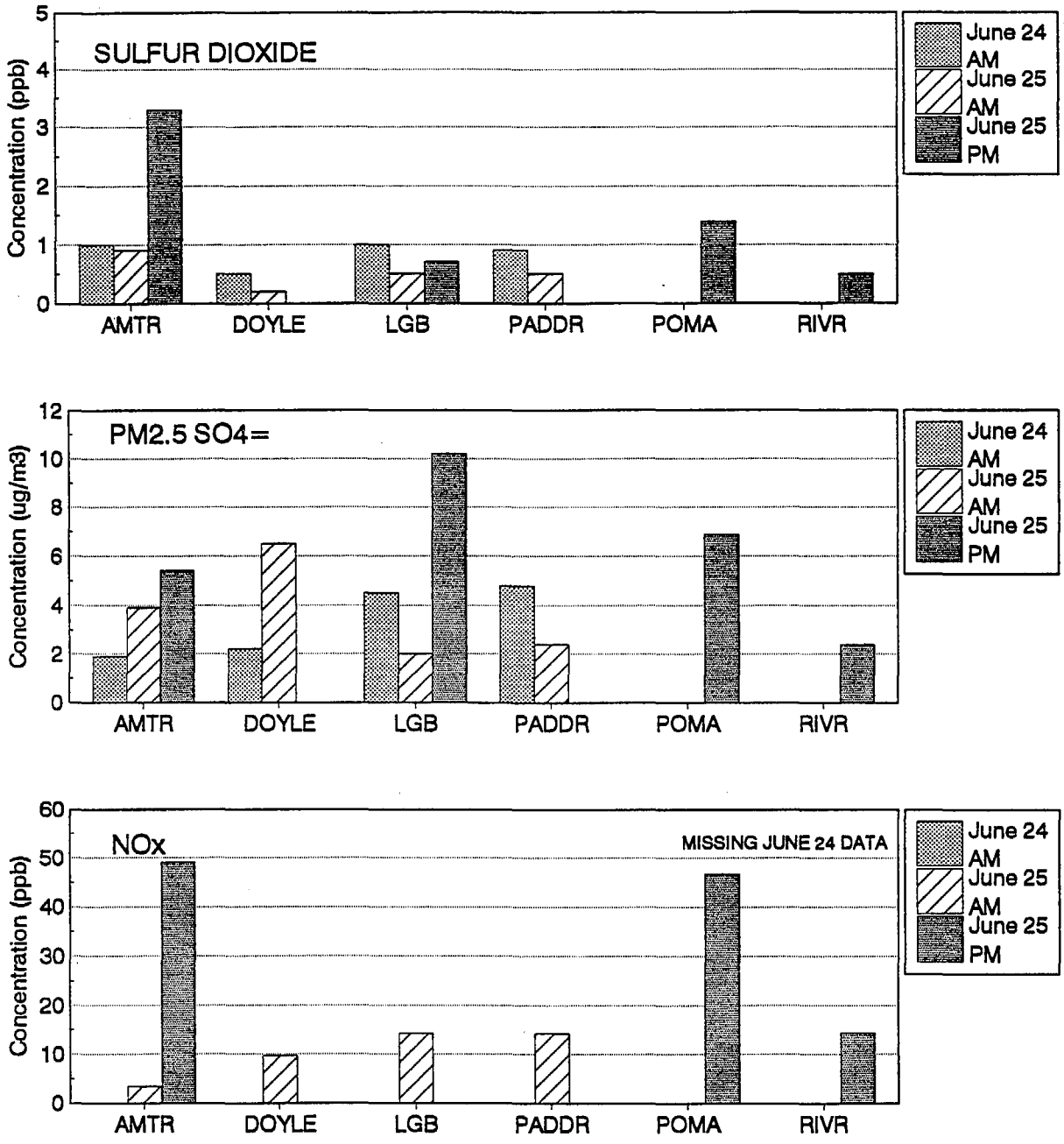

ALL SAMPLES COLLECTED ABOVE THE MIXED LAYER
EXCEPT POMONA, WHICH WAS COLLECTED WITHIN THE MIXED LAYER

Figure 3-38. Orbit-Averages of SO_2, $PM_{2.5}$ Sulfate Ion, and NO_x Measured Aloft on June 24-25 for Each Orbit Location. All samples were collected above the mixed layer except the sample collected at Pomona on the afternoon of June 25.

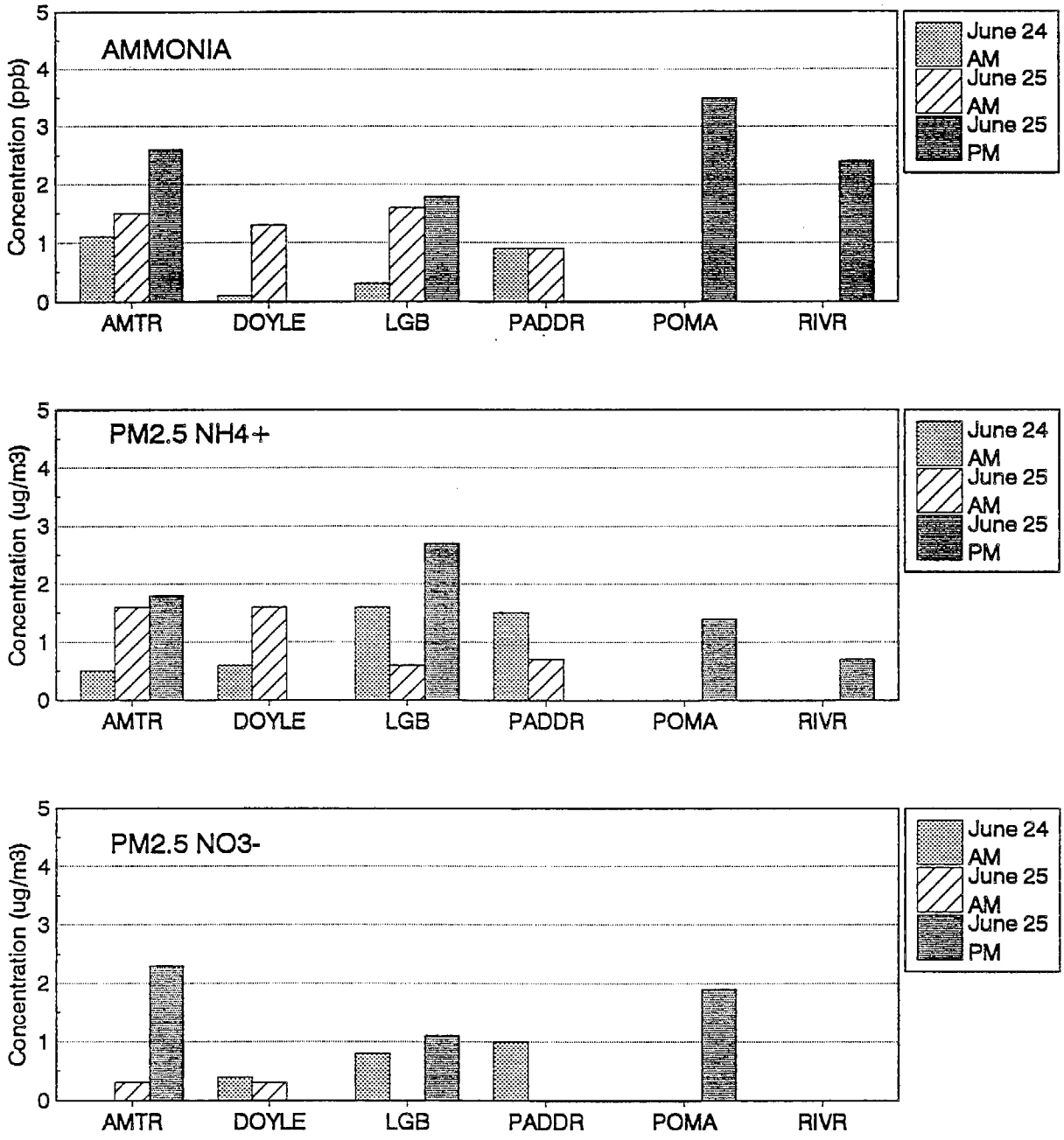

ALL SAMPLES COLLECTED ABOVE THE MIXED LAYER
EXCEPT POMONA, WHICH WAS COLLECTED WITHIN THE MIXED LAYER

Figure 3-39. Orbit-Averages of Ammonia and $PM_{2.5}$ Ammonium and Nitrate Ions Measured Aloft on June 24-25 for Each Orbit Location. All samples were collected above the mixed layer except the sample collected at Pomona on the afternoon of June 25.

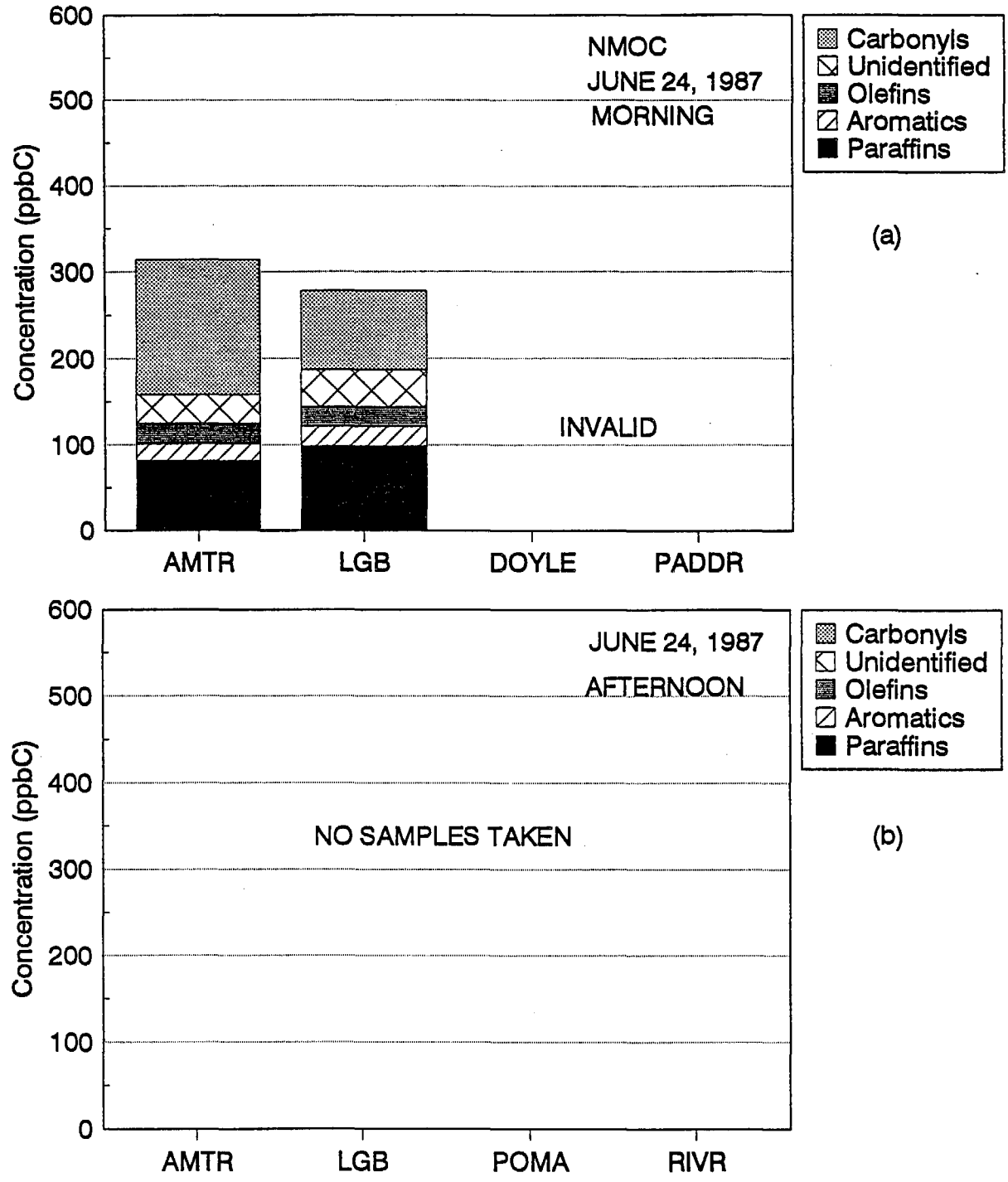

Figure 3-40. Orbit-Averages of NMOC Measured Aloft on the (a) Morning and (b) Afternoon of June 24 for Each Orbit Location. All samples were collected above the mixed layer.

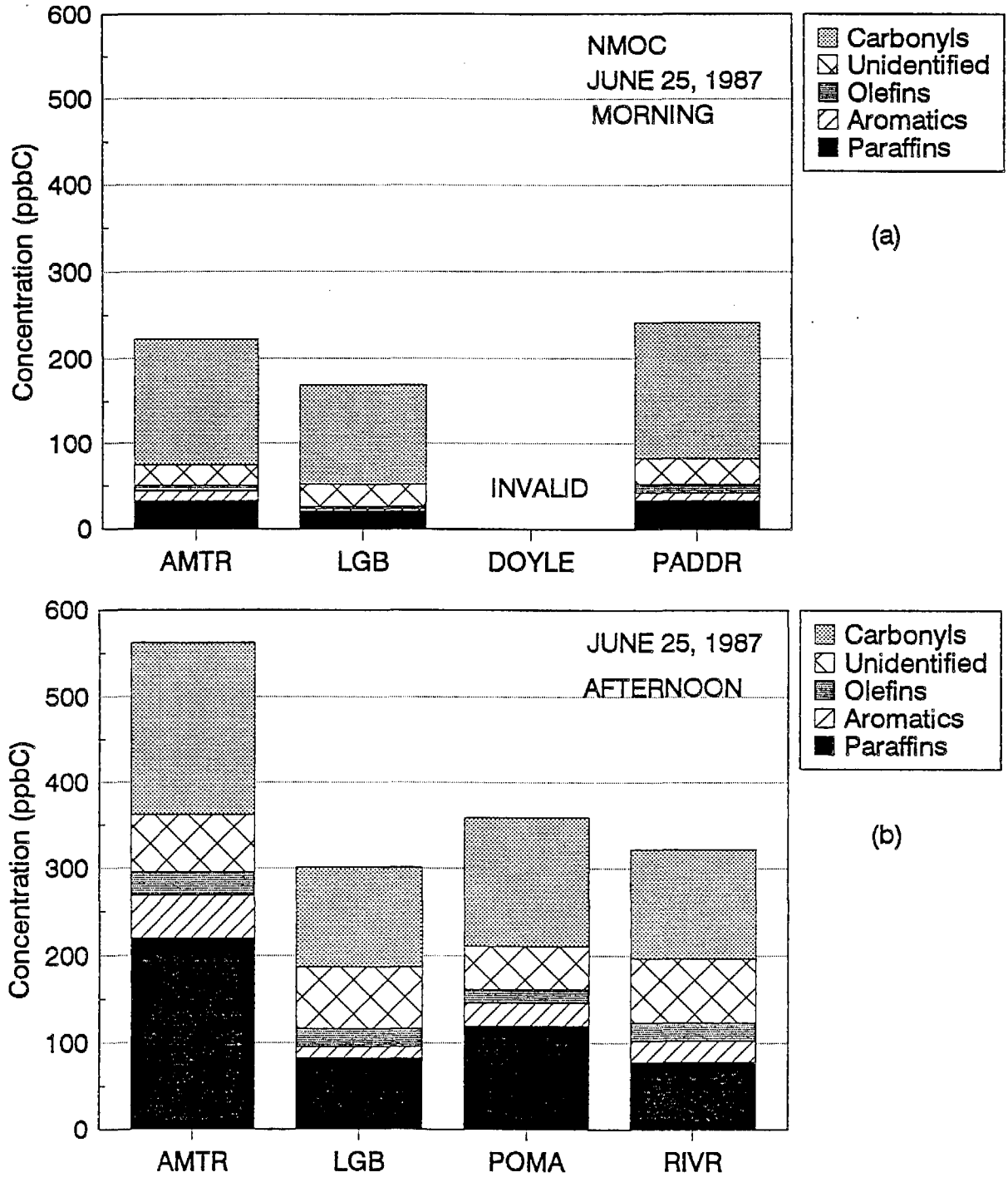

ALL SAMPLES COLLECTED ABOVE THE MIXED LAYER
EXCEPT POMONA, WHICH WAS COLLECTED WITHIN THE MIXED LAYER

Figure 3-41. Orbit-Averages of NMOC Measured Aloft on the (a) Morning and (b) Afternoon of June 25 for Each Orbit Location. All Samples were collected above the mixed layer except the sample collected at Pomona. The hydrocarbon concentrations appear low (suspect) in the morning samples.

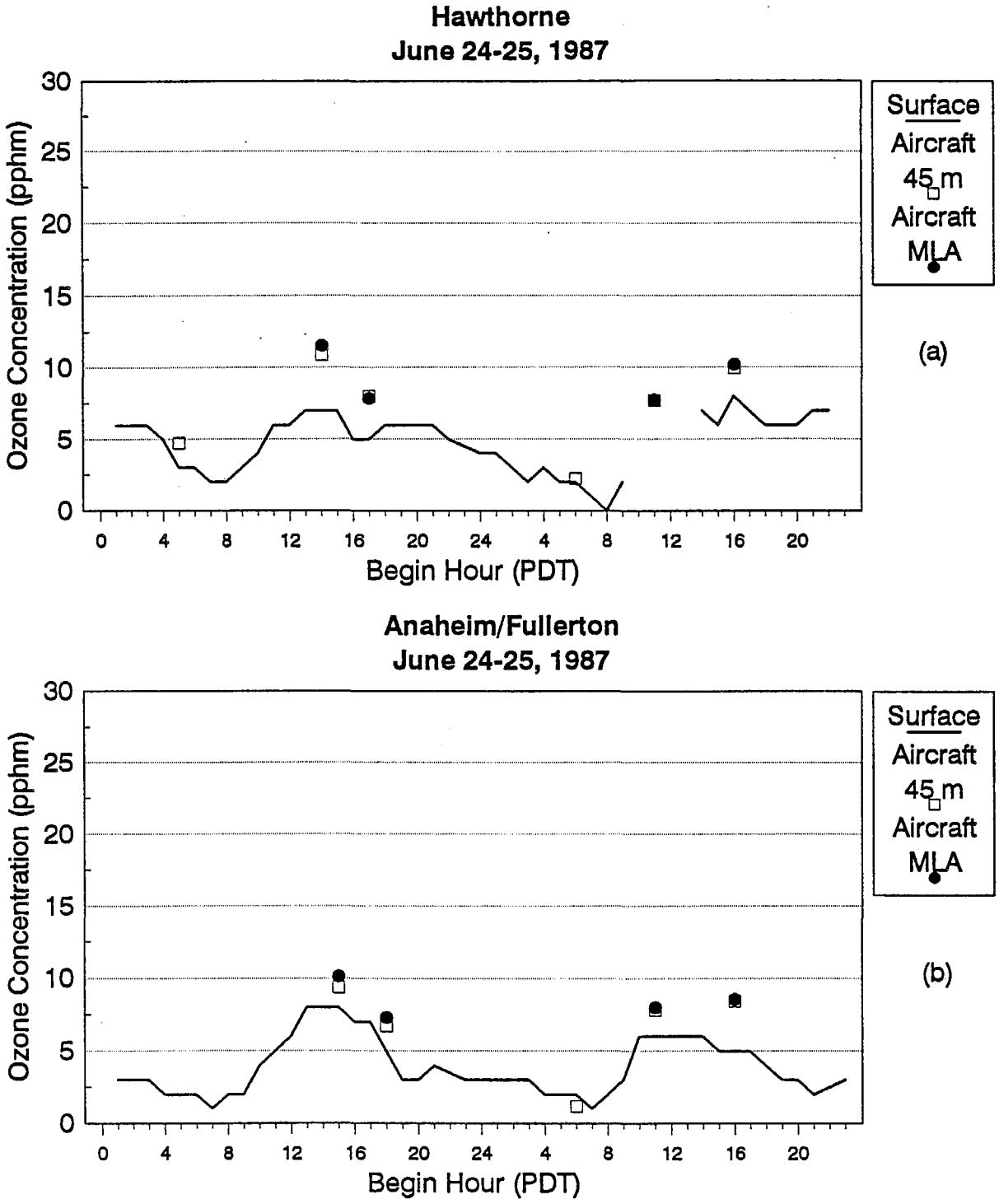

Figure 3-42. Comparison of Surface Ozone Concentrations With Mixed-Layer-Average (MLA) and the Lowest 45-Meter Average (45 m) Ozone at (a) Hawthorne and (b) Fullerton on June 24-25, 1987. The data compared to the Fullerton spiral are from the Anaheim surface monitor.

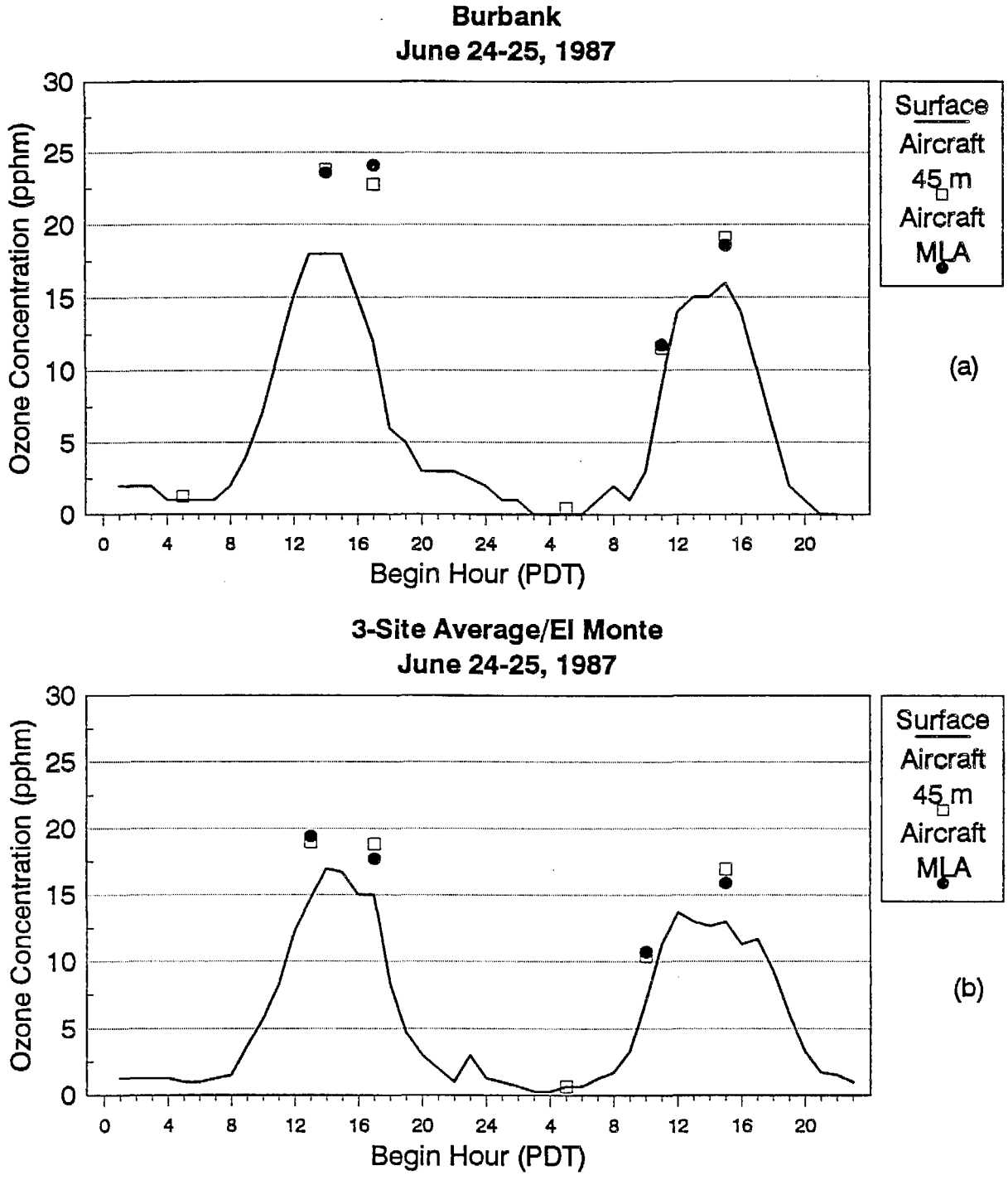

Figure 3-43. Comparison of Surface Ozone Concentrations With Mixed-Layer-Average (MLA) and the Lowest 45-Meter Average (45 m) Ozone at (a) Burbank and (b) El Monte on June 24-25, 1987. The data compared to the El Monte spiral are from the average of the Pico Rivera, Pasadena and Azusa surface monitors.